

# Geologic and Geophysical Maps of the Stockton 30' × 60' Quadrangle, California

Scale 1:100,000

Compiled by

M.P. Delattre<sup>1</sup>, R.W. Graymer<sup>2</sup>, V.E. Langenheim<sup>2</sup>, K.L. Knudsen<sup>2</sup>  
T.E. Dawson<sup>1</sup>, E.E. Brabb<sup>2</sup>, C.M. Wentworth<sup>2</sup>, and L.A. Raymond<sup>3</sup>

2023



*Prepared in cooperation with:*



---

1. Department of Conservation, California Geological Survey

2. U.S. Geological Survey

3. Coast Range Geological Mapping Institute



## CALIFORNIA GEOLOGICAL SURVEY

JEREMY T. LANCASTER  
ASSOCIATE STATE GEOLOGIST

The Department of Conservation makes no warranties as to the suitability of this product for any particular purpose.

## Table of Contents

INTRODUCTION .....	1
SOURCES OF GEOLOGIC MAPPING .....	2
ACQUISITION AND PROCESSING OF GEOPHYSICAL DATA.....	4
REGIONAL GEOLOGIC AND TECTONIC SETTING .....	7
BASEMENT COMPLEXES .....	13
Franciscan Complex .....	13
Great Valley complex .....	14
Coast Range ophiolite.....	14
Lower Great Valley sequence.....	15
Mesozoic granitic intrusive .....	16
Sierra Nevada Foothills metamorphic and plutonic complex.....	16
OVERLAP STRATA.....	16
Stratigraphic Assemblages.....	16
Upper Great Valley sequence.....	18
Cenozoic Rocks .....	21
Tertiary Strata .....	21
Intrusive Rocks.....	22
Quaternary Surficial Deposits.....	22
Landslides.....	24
GEOPHYSICAL EXPRESSION OF ROCK UNITS.....	25
Gravity Anomalies .....	25
Magnetic Anomalies .....	28
STRUCTURE .....	29
Mesozoic and Early Cenozoic Structure.....	29
Late Cenozoic Structure .....	32
GEOPHYSICAL EXPRESSION OF STRUCTURES .....	37
Gravity Anomalies .....	37
Magnetic Anomalies .....	38
DESCRIPTION OF MAP UNITS .....	40
Quaternary Surficial Deposits.....	40
Tertiary and Mesozoic Intrusive Rocks .....	45
Early Quaternary, Tertiary, and Mesozoic Stratigraphic Units .....	45
Great Valley Sequence Units by Assemblage.....	52
Mapped within Assemblage II: .....	52
Mapped within Assemblage V:.....	52
Mapped within Assemblage VI North:.....	53
Mapped within Assemblage VII:.....	54
Mapped within Assemblages VIII:.....	55
Mapped within Assemblages VI South and XI: .....	55
Coast Range Ophiolite.....	56
Franciscan Complex .....	56
Franciscan Units of Raymond (2014) (Cretaceous and/or Late Jurassic).....	58
REFERENCES CITED.....	60
AUTHORSHIP DOCUMENTATION AND PRODUCT LIMITATIONS .....	74

## Plates

Plate 1. Geologic and Geophysical Maps of the Stockton 30' × 60' Quadrangle, California

## List of Figures

Figure 1. Regional setting of the Stockton 30' × 60' quadrangle, California .....	2
Figure 2. Index map showing the 7.5' quadrangles within the Stockton 30' × 60' quadrangle.....	3
Figure 3. Isostatic gravity map of the Stockton quadrangle .....	5
Figure 4. Mosaic aeromagnetic map of the Stockton quadrangle.....	6
Figure 5a. Generalized map of northern California showing the distribution of Mesozoic and Cenozoic basement complexes and overlap sequences discussed in the text.....	8
Figure 5b. Generalized upper-crustal cross section of central California from the Hayward-Calaveras fault to the Sierra Nevada Foothills .....	9
Figure 6. Simplified model of the convergent plate boundary that existed in California during the late Mesozoic Era .....	9
Figure 7. Sequential cartoon upper-crustal cross sections of the western North American continental margin and adjacent oceanic crust between Middle Jurassic and Paleocene time .....	10
Figure 8. Map showing stratigraphic assemblages in structural blocks and depositional basins distinguished in the northern Diablo Range .....	17
Figure 9. Summary of Great Valley sequence units and correlations between stratigraphic assemblages in this compilation and selected source maps.....	19
Figure 10. Detailed correlation chart for the Tertiary units in the stratigraphic assemblages of the map area.....	23
Figure 11. Geophysical model (a) and geologic cross-section (b) across Stockton quadrangle.....	26
Figure 12. Simplified fault activity map of the Stockton 30' × 60' quadrangle.....	31
Figure 13. Detail of the geologic map at Mount Diablo illustrating the right releasing stepover between the Northern Calaveras and Concord faults and the left restraining stepover between the Greenville and Concord faults.....	34
Figure 14. Cross section for the northwest part of the map area through Mount Diablo, showing the relation of the Diablo fold and thrust belt and Diablo Anticline to the regional strike-slip faults (Northern Calaveras, Greenville, and Concord).....	35

# Geologic and Geophysical Maps of the Stockton 30' × 60' Quadrangle, California

Compiled by:

M.P. Delattre<sup>1</sup>, R.W. Graymer<sup>2</sup>, V.E. Langenheim<sup>2</sup>, K.L. Knudsen<sup>2</sup>, T.E. Dawson<sup>1</sup>,  
E.E. Brabb<sup>2</sup>, C.M. Wentworth<sup>2</sup>, and L.A. Raymond<sup>3</sup>

## INTRODUCTION

This pamphlet and accompanying geologic and geophysical maps are the products of cooperative efforts by the California Geological Survey (CGS) and United States Geological Survey (USGS) to compile a comprehensive, digital representation of the bedrock geology, Quaternary surficial deposits, and potential-field anomalies within the boundaries of the Stockton 30' × 60' quadrangle. The Stockton 30' × 60' quadrangle covers approximately 4,890 km<sup>2</sup> of Contra Costa, Alameda, San Joaquin, and Stanislaus Counties, California. From the rugged hillsides of the northern Diablo Range in the west to the San Joaquin Valley in the east, the map extends roughly 88 km across growing suburban communities of the eastern San Francisco Bay Area and Livermore Valley, grass-covered ranchlands along eastern slopes of the Diablo Range, and into the low farmlands of the San Joaquin Valley and Sacramento-San Joaquin River Delta (Figure 1). The elevation ranges from near sea level in the Delta to 1,173 meters on Mt. Diablo, the most prominent peak of the San Francisco Bay region.

The Stockton 30' × 60' geologic map compilation is intended to illustrate the distribution of the rocks and surficial deposits of the area and their structural and stratigraphic relations to one another. Many natural resources, from groundwater to natural gas, and natural hazards, from earthquake shaking to landslides, are constrained by the distribution and physical properties of the geologic units and the geometry of the geologic structures. The larger goal of the publication is to provide a regionally consistent picture of the geologic and geophysical framework to better understand the structural and stratigraphic relations across the region as an aid to natural resources management and evaluations of potential hazards from active earth processes.

The geologic map was compiled predominantly from 1:24,000- and 1:62,500-scale mapping. Although the map sheet was cartographically designed and formatted for display at 1:100,000-scale, details of the larger scale source maps were retained in the digital geodatabase. As a digital product, the map may be easily enlarged; however, the spatial accuracy of the data remains limited to that of the source maps. Similarly, the age and scale of topographic base maps used for the original mapping should be considered when overlying the digital compilation on newer base maps, which may produce apparent spatial discrepancies. Accordingly, it is important to recognize that neither the printed map sheet nor digital database is sufficiently detailed or spatially accurate to serve as a basis for site-specific evaluations.

---

1. Department of Conservation, California Geological Survey

2. U.S. Geological Survey

3. Coast Range Geological Mapping Institute

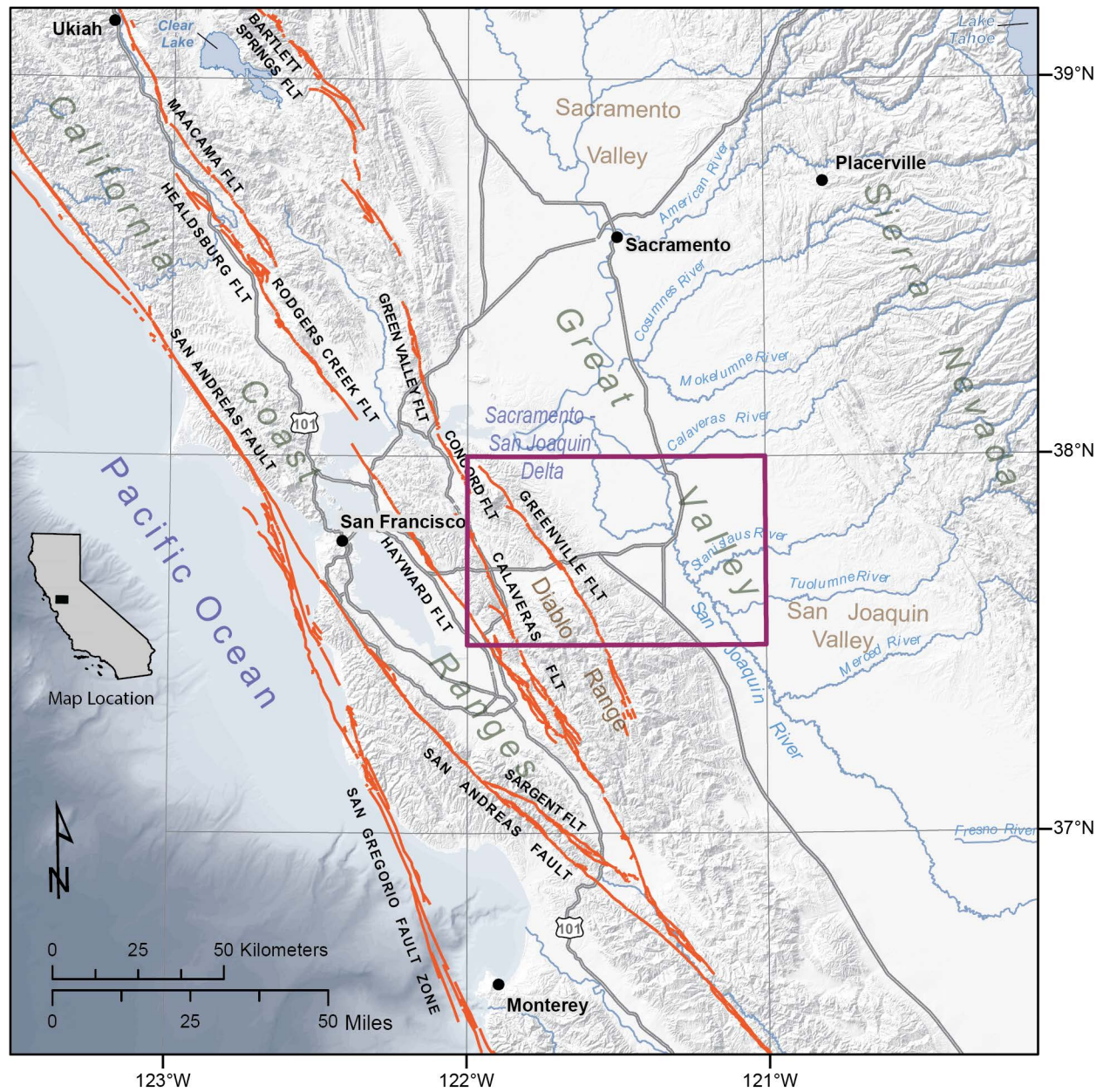


**Figure 1.** Regional setting of the Stockton 30' x 60' quadrangle (outline in purple) in relation to prominent physiographic features, and major strike-slip faults of the active San Andreas Fault System (in red).

## SOURCES OF GEOLOGIC MAPPING

The geologic map is an updated and significantly modified version of an unpublished USGS/CGS digital compilation of mapping covering the Stockton 30' × 60' quadrangle by Brabb, Graymer, Knudsen and Wentworth (2001). This earlier version of the compilation relied on 3 principal sources: 1) mapping in the northern Diablo Range with an emphasis on bedrock formations beginning with the work of Brabb, Sonneman, and Switzer (1971), which was updated and expanded with new work by Graymer and others covering Contra Costa County (1994) and Alameda County (1996); 2) mapping by Dibblee (1980 and 1981; reissued with edits by Dibblee and Minch, 2006 and 2007) for the portion of the Diablo Range in

San Joaquin and Stanislaus Counties; and 3) a synthesis of Quaternary mapping in the San Joaquin Valley and eastern flanks of the Diablo Range compiled by Knudsen and Lettis (1997).

The USGS continued intermittent work on the compilation, with CGS rejoining the effort in 2005 to incorporate more detailed mapping of Quaternary surficial deposits in the greater Bay Area by Knudsen and others (2000) and Witter and others (2006), and fault strands from the CGS Quaternary fault database (Bryant, 2005) and Alquist-Priolo Special Studies Zones fault maps (CDMG, 1980-1982). The bedrock mapping from Graymer and others (1994a and 1996) for Alameda and Contra Costa Counties was retained with only modest changes; however, for San Joaquin and Stanislaus Counties, Dibblee's somewhat generalized bedrock mapping was largely replaced by more detailed published and unpublished mapping by Raymond (1969, 1973a, 2014, 2015) and Throckmorton (1988). Also, the locations of the concealed Stockton, Vernalis, and West Tracy faults were updated based on the interpretation of borehole logs and other data from Harwood and Helley (1987), Sterling (1992), and Unruh and Hitchcock (2015). The sources used in compiling the final geologic map are listed below by 7.5' quadrangle (see Figure 2), in alphabetical order.

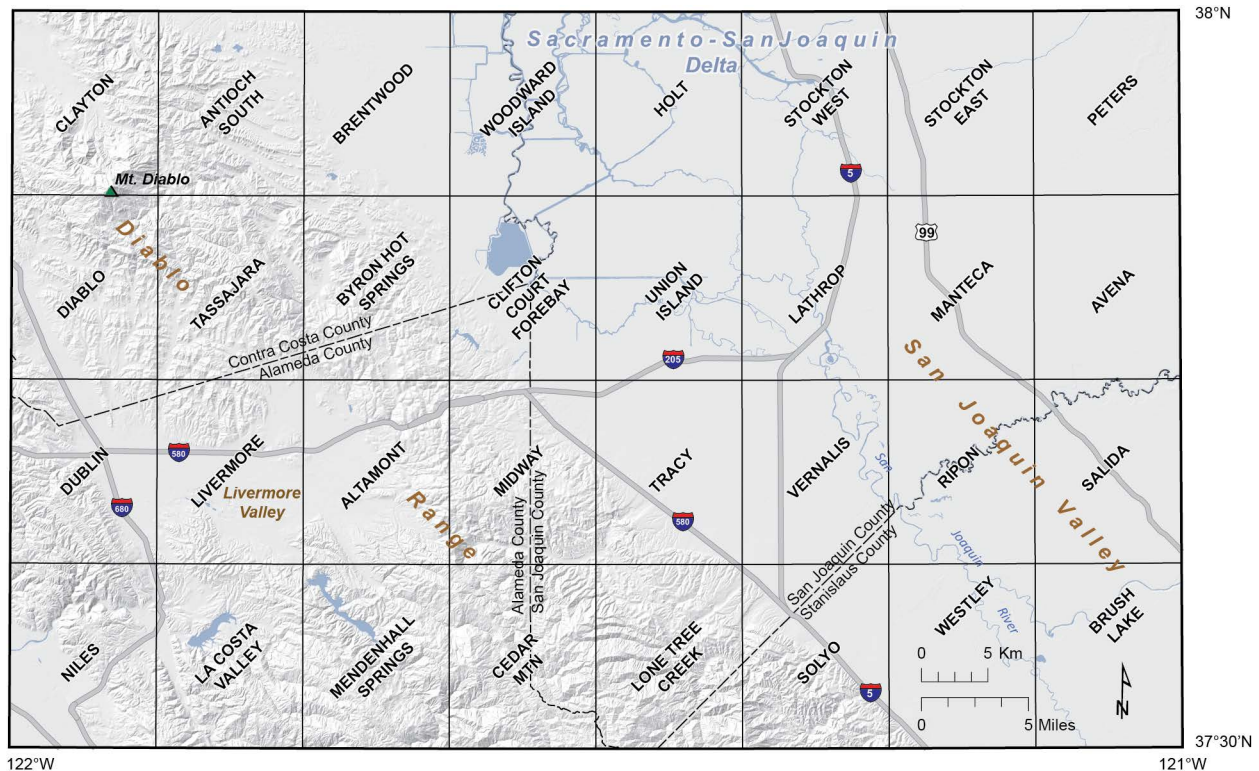


**Figure 2.** Index map showing the 7.5' quadrangles within the Stockton 30' x 60' quadrangle.

**Altamont:** Bryant, 2005; California Division of Mines and Geology, 1982b; Graymer and others, 1996; Knudsen and others, 2000.

**Antioch South:** Bryant, 2005; Graymer and others, 1994a; Knudsen and others, 2000.

**Avena:** Knudsen and Lettis, 1997.

**Brentwood:** Graymer and others, 1994a; Knudsen and others, 2000.

**Brush Lake:** Knudsen and Lettis, 1997.

**Byron Hot Springs:** Bryant, 2005; Graymer and others, 1994a; Graymer and others, 1996; Knudsen and others, 2000.

**Cedar Mountain:** Bryant, 2005; Graymer and others, 1996; Huey, 1948; Knudsen and Lettis, 1997; Knudsen and others, 2000; Dibblee, 1980; Throckmorton, 1988.

**Clayton:** Bryant, 2005; Graymer and others, 1994a; Witter and others, 2006.

**Clifton Court Forebay:** Graymer and others, 1994a; Graymer and others, 1996; Knudsen and Lettis, 1997; Knudsen and others, 2000, Unruh and Hitchcock, 2015.

**Diablo:** Bryant, 2005; Graymer and others, 1994a; Witter and others, 2006.

**Dublin:** Bryant, 2005; California Division of Mines and Geology, 1982c; Graymer and others, 1994a; Graymer and others, 1996; Witter and others, 2006.

**Holt:** Knudsen and Lettis, 1997.

**La Costa Valley:** Bryant, 2005; Graymer and others, 1996; Witter and others, 2006.

**Lathrop:** Bryant, 2005; Knudsen and Lettis, 1997.

**Livermore:** Bryant, 2005; California Division of Mines and Geology, 1982d; Graymer and others, 1994a; Graymer and others, 1996; Witter and others, 2006.

**Lone Tree Creek:** Bryant, 2005; Dibblee, 1981; Raymond, 1969, 1973a, 2015; Trask, 1950.

**Manteca:** Knudsen and Lettis, 1997.

**Mendenhall Springs:** Graymer and others, 1996; Knudsen and others, 2000.

**Midway:** Bryant, 2005; Dibblee, 1980; Graymer and others, 1996; Knudsen and Lettis, 1997; Knudsen and others, 2000; Sowers and others, 1993; Throckmorton, 1988.

**Niles:** Bryant, 2005; California Division of Mines and Geology, 1980; Graymer and others, 1996; Witter and others, 2006.

**Peters:** Harwood and Helley, 1987; Knudsen and Lettis, 1997; Marchand and others, 1981.

**Ripon:** Bryant, 2005; Knudsen and Lettis, 1997.

**Salida:** Knudsen and Lettis, 1997.

**Solyo:** Bartow and others, 1985; Bryant, 2005; Dibblee, 1981; Knudsen and Lettis, 1997; Raymond, 1973a, 2014; Trask, 1950.

**Stockton East:** Bryant, 2005; Harwood and Helley, 1987; Knudsen and Lettis, 1997.

**Stockton West:** Knudsen and Lettis, 1997.

**Tassajara:** Bryant, 2005; Graymer and others, 1994a; Knudsen and others, 2000.

**Tracy:** Bryant, 2005; Dibblee, 1981; Knudsen and Lettis, 1997; Raymond, 1969, 2015; Sowers and others, 1993; Sterling, 1992.

**Union Island:** Bryant, 2005; Knudsen and Lettis, 1997; Sterling, 1992.

**Vernalis:** Bryant, 2005; Knudsen and Lettis, 1997.

**Westley:** Bartow and others, 1985; Bryant, 2005; Knudsen and Lettis, 1997.

**Woodward Island:** Knudsen and Lettis, 1997; Knudsen and others, 2000.

## ACQUISITION AND PROCESSING OF GEOPHYSICAL DATA

Gravity and magnetic data are useful for projecting the surface geology into the subsurface. Gravity data are processed to reflect density variations within the upper and middle crust and are particularly well suited for determining the shape of Cenozoic basins, because of the significant density contrast between dense Mesozoic basement rocks and lighter Cenozoic rocks. However, variations in



the density within the basement complexes can cause gravity lows that mimic those related to Cenozoic basin deposits, complicating the gravity interpretation in some places. Magnetic data reflect magnetization variations within the crust and are well suited for mapping the distribution of rock types that contain magnetite. Both gravity and magnetic anomalies can be related to rock type, providing a means to map remotely some aspects of the geology.

2141 gravity measurements were used to produce an isostatic gravity map of the quadrangle (Figure 3). Sources of data include (1) Pan-American Center for Earth and Environmental Studies (2015), which incorporates data from Robbins and others (1974) and Griscom and others (1979), (2) Ponce (2001) and (3) data collected by the U.S. Geological Survey from 1993-2018 (Langenheim and others, 2022). Gravity measurements are non-uniformly distributed in the region, usually along roads, with an average density of 1 measurement per 4 km<sup>2</sup>.

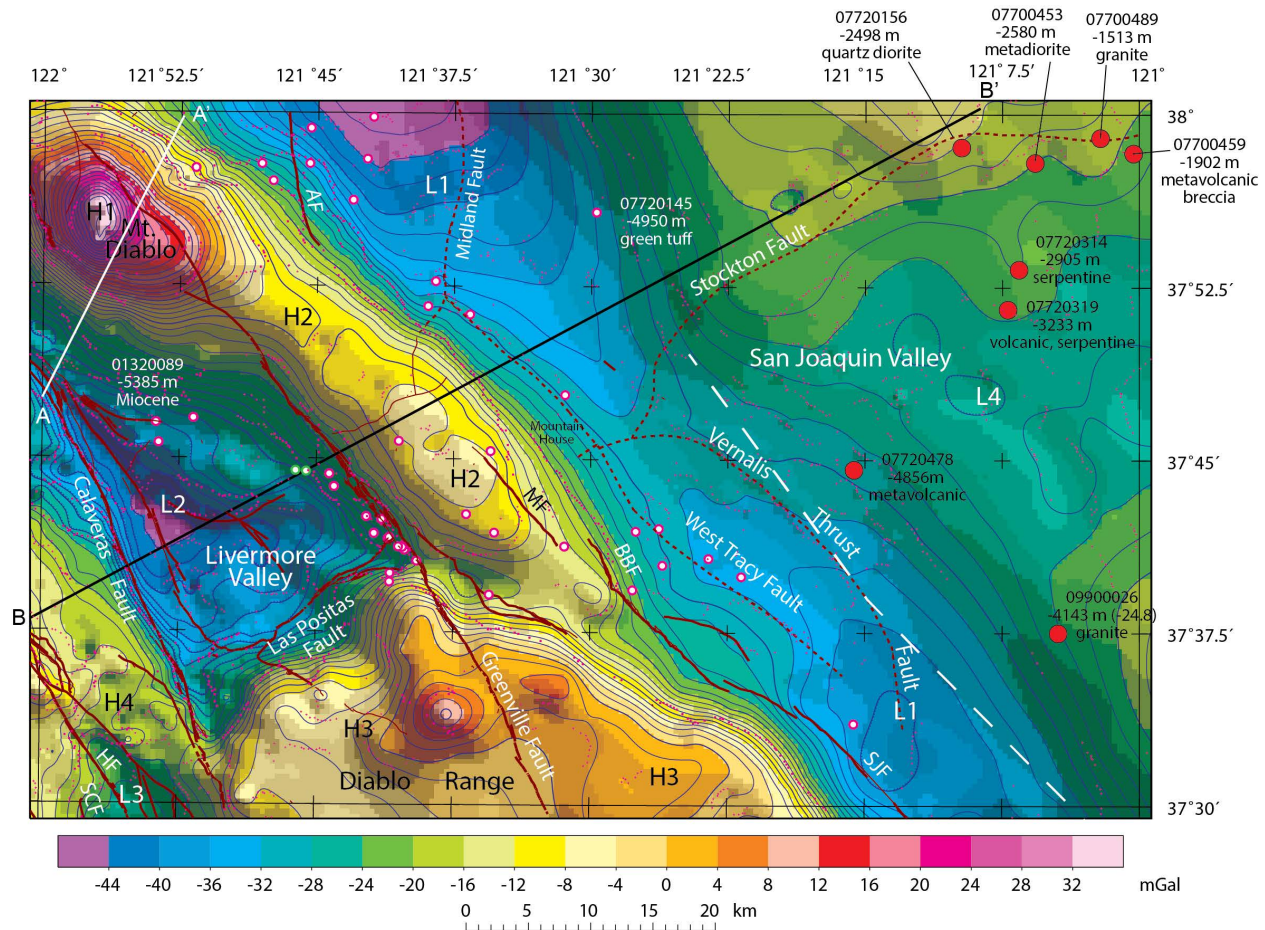


**Figure 3.** Isostatic gravity map of the Stockton quadrangle with faults (brown lines) modified from Figure 12, drillholes with sonic and/or density logs in Tiballi and Brocher (1998) and Brocher and others (1997; magenta-rimmed white circles), and wells that hit basement (Wentworth and others, 1995; solid red circles labeled by API number with elevation of basement in meters and rock type at bottom of well). White L# and black H# mark gravity lows and highs discussed in the text. Dashed white line, seismic refraction line (Colburn and Mooney, 1986). Magenta points are density boundaries from maximum horizontal gradient method. Dark blue lines, 2-mGal contours. Black line, location of model profile (Figure 11); white line, location of cross section shown in Figure 14. AF, Antioch Fault; BBF, Black Butte Fault; HF, Hayward Fault; MF, Midway Fault; SCF, Silver Creek Fault; SJF, San Joaquin Fault.

Gravity data were reduced to free-air anomalies using standard formulas (for example, Telford and others, 1976). Bouguer, curvature, and terrain adjustments to a radial distance of 166.7 km were applied to the free-air anomaly at each station to determine the complete Bouguer anomalies at a standard reduction density of 2,670 kg/m<sup>3</sup> (Plouff, 1977). An isostatic adjustment was then applied to remove the long-wavelength effect of deep crustal and (or) upper mantle masses that isostatically support regional topography. The isostatic adjustment assumes an Airy-Heiskanen model (Heiskanen and Vening-Meinesz, 1958) of isostatic compensation. Compensation is achieved by varying the depth of the model crust-mantle interface, using the following parameters: a sea-level crustal thickness of 25 km, a crust-mantle density contrast of 400 kg/m<sup>3</sup>, and a crustal density of 2,670 kg/m<sup>3</sup> for the topographic

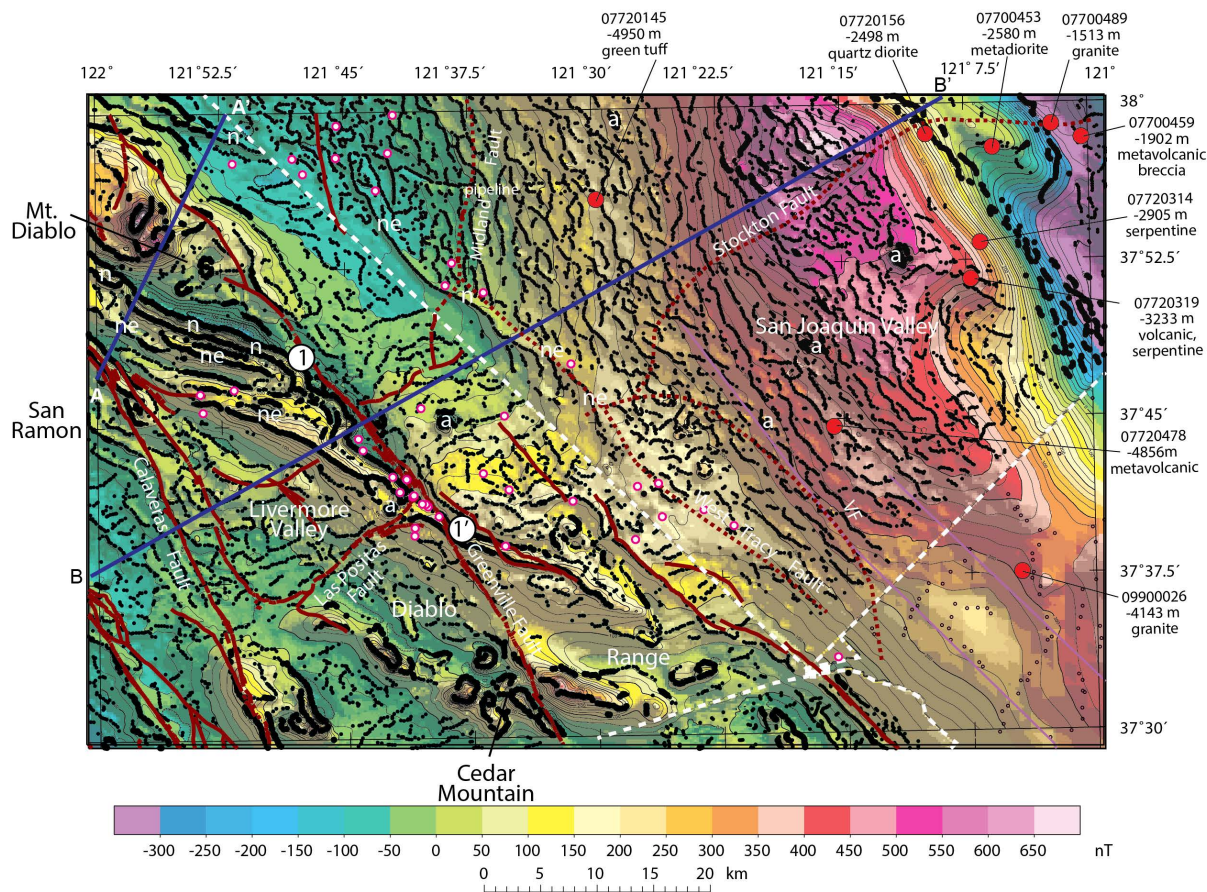


**Figure 4.** Mosaic aeromagnetic map of the Stockton quadrangle with faults (brown lines) modified from Figure 12, wells with sonic and/or density logs in Tiballi and Brocher (1998) and Brocher and others (1997; magenta-rimmed white circles), and wells that hit basement (Wentworth and others, 1995; solid red circles with elevation of basement in meters and rock type at bottom of well). Black circles are magnetization boundaries from maximum horizontal gradient method, with larger circles indicating gradients larger than the mean gradient. Contours, 25 nT. Thick dashed white lines, survey boundaries. Dark blue lines, model cross sections in Figures 11 and 14. “n”, magnetic anomalies attributed to outcrops of Neroly Formation and the lower part of unit PMgv, “ne” anomalies attributed to concealed Neroly and unit PMgv. “a”, magnetic anomalies caused by anthropogenic sources. Locations marked 1 and 1’ are correlated magnetic anomalies across the Greenville Fault. VF, Vernalis Fault.

load. These parameters were used because (1) they produce a model crustal geometry that agrees with seismically determined values of crustal thickness for central California, (2) they are consistent with model parameters used for isostatic corrections computed for the rest of California (Roberts and others, 1990), and (3) changing the model parameters does not significantly affect the resulting isostatic anomaly (Jachens and Griscom, 1985). The resulting isostatic residual gravity values should reflect lateral variations of density within the middle to upper crust. Accuracy of the data is estimated to be on the order of 0.1 to 0.5 mGal; this estimate is based on comparison of observed gravity values at the same location from the different sources of data and on the estimated error caused by the terrain corrections (assumed to 5-10% of the total terrain correction, which is on average 1.34 mGal).

The aeromagnetic map (Figure 4) is based on data from four surveys of varying resolution (table 1). The oldest survey (Meuschke and others, 1966) was flown close to the ground (150 m) relative to the spacing of the flight lines (1.6 km), predates modern, more precise positioning by GPS, and consists of analog data, making this dataset of low resolution. The other surveys (Abrams and others, 1991, U.S. Geological Survey, 1992; Langenheim, 2015) were collected digitally, were flown at better ratios of height above ground versus flightline spacing and located using GPS. Accuracy of these modern surveys is 1 nanotesla or better. Because of the variation in survey heights, the data were only adjusted to a common magnetic datum, without upward or downward continuation to a common height above ground, to preserve the original resolution of the surveys.

To help delineate structural trends and gradients expressed in the gravity and magnetic fields, a computer algorithm was used to locate the maximum horizontal gradient (Cordell and Grauch, 1985; Blakely and Simpson, 1986). Concealed basin faults beneath the valley areas were mapped using horizontal gradients (“density boundaries”) in the gravity field. We calculated magnetization boundaries on a filtered version of the magnetic field to enhance shallow sources. First, we subtracted a numerically derived regional field from the actual merged data. The regional field was computed by analytically continuing the merged aeromagnetic data to a surface 200 m higher than that on which the measurements were made, an operation that tends to smooth the data by attenuating short-wavelength anomalies (Blakely, 1995). Second, the resulting residual aeromagnetic field was mathematically transformed into magnetic potential anomalies (Baranov, 1957); this procedure effectively converts the magnetic field to the equivalent gravity field that would be produced if all magnetic material were replaced by proportionately dense material and accounts for the effect of the inclination of the Earth’s magnetic field (“reduction to the pole”). The horizontal gradient of the magnetic potential field was then calculated.

Gradient maxima occur approximately over steeply dipping contacts that separate rocks of contrasting densities or magnetizations. For moderate to steep dips (45° to vertical), the horizontal displacement of a gradient maximum from the top edge of an offset horizontal layer is always less than or equal to the depth to the top of the source (Grauch and Cordell, 1987).

## **REGIONAL GEOLOGIC AND TECTONIC SETTING**

The Stockton 30' × 60' quadrangle lies within both the California Coast Ranges and the Great Valley geomorphic provinces (Figure 1; Norris and Webb, 1976). The geology of these regions is made up of three distinctive basement complexes overlapped by Cretaceous and younger strata (Figure 5).

From east to west the basement complexes are made up of rocks related to the three main tectonic elements of a convergent margin: arc-related rocks of the Sierra Nevada Foothills metamorphic and igneous complex, forearc related rocks of the Great Valley complex, and subduction zone accretionary prism rocks of the Franciscan complex. However, the model usually shown to relate these three basement complexes (Figure 6) is too simple and does not take into account a more complex history of accretion,

Geologic and Geophysical Maps of the Stockton 30' × 60' Quadrangle, California

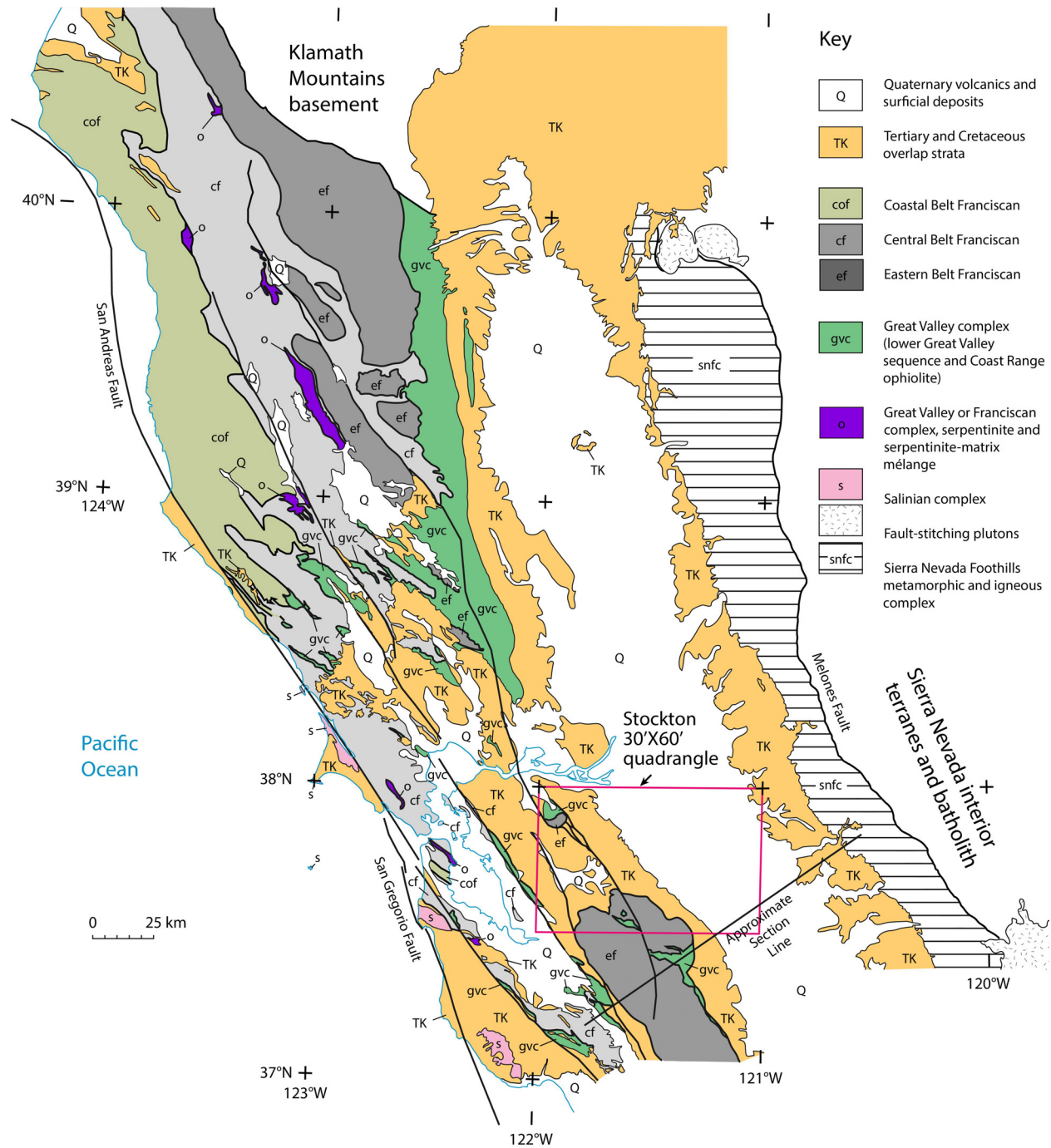


**Figure 5a.** Generalized map of northern California showing the distribution of Mesozoic and Cenozoic basement complexes and overlap sequences discussed in the text. Modified from Graymer (2005); Blake and others (1982); Jennings (1977). Line shows approximate location of cross section shown in Figure 5b).

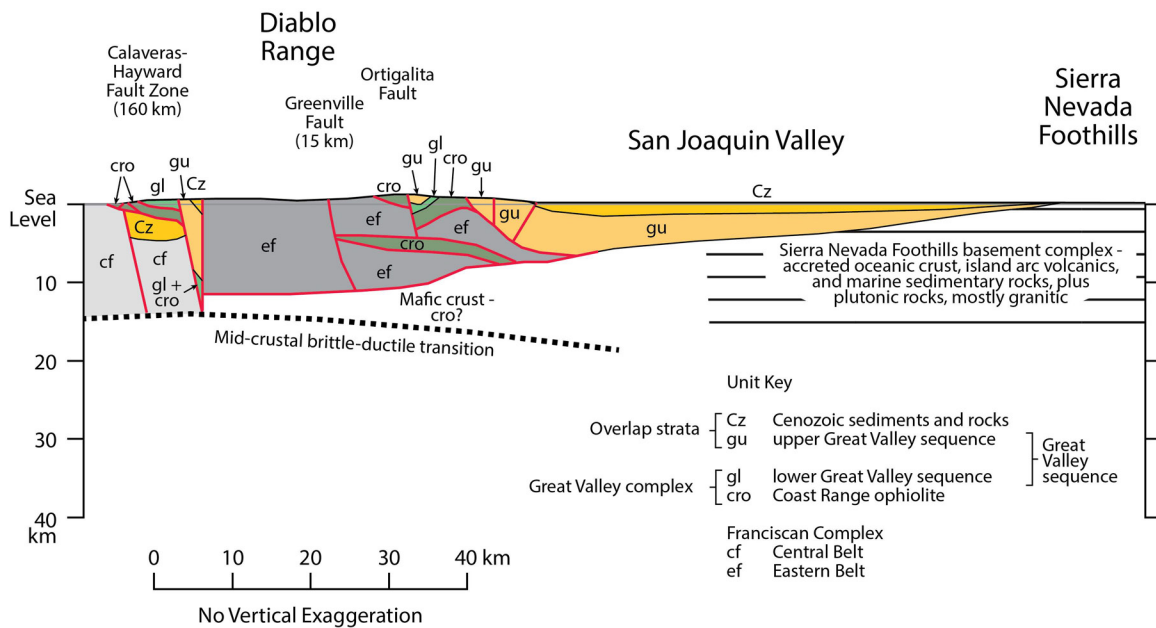


**Figure 5b.** Generalized upper-crustal cross section of central California from the Hayward-Calaveras fault to the Sierra Nevada Foothills, faults shown as red, depositional or intrusive contacts shown as black. Faults of the San Andreas System have the approximate amount of Neogene right-lateral offset indicated. Modified from Fuis and Mooney (1990). Approximate section line is shown in Figure 5a.

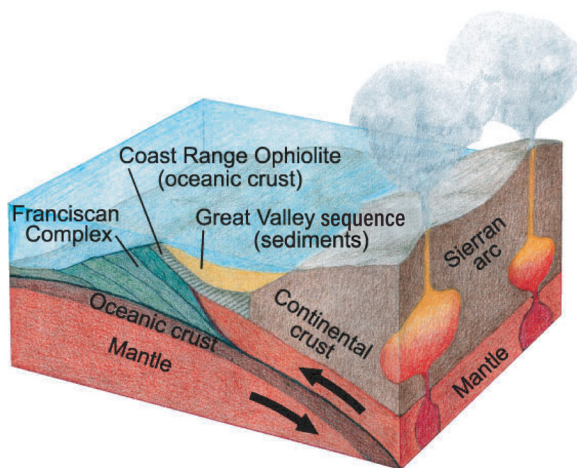


**Figure 6.** Simplified model of the convergent plate boundary that existed in California during the late Mesozoic Era (modified from Elder, n.d.).

unroofing, and deposition.

The regional story begins about 165 Ma in Middle Jurassic time (Figure 7-a). Rocks of that age in the Sierra Nevada Foothills complex are andesitic metavolcanic rocks derived from an island arc, as indicated by their geochemistry, the presence of pillow lavas, and the presence of marine fossils in volcanoclastic layers (Graymer and Jones, 1994). The 162-169 Ma radiometric age of high P/T (subduction zone) metamorphic minerals in the oldest Franciscan rocks (Ukar and others, 2012) show that at the same time there was a subduction zone to the west. Also, at this time, between the subduction zone and the island arc, ophiolite was being formed, the Coast Range ophiolite (Blake and others, 1992; Hagstrum, 1997; Hopson and others, 1997). The origin of this unit is somewhat controversial (e.g., Dickinson and others, 1996), but the geometry of the subduction zone on the west and an island arc on the east strongly argues that the ophiolite was formed in the forearc of an east-dipping ocean-ocean subduction system (Blake and others, 2002).

# Geologic and Geophysical Maps of the Stockton 30' × 60' Quadrangle, California

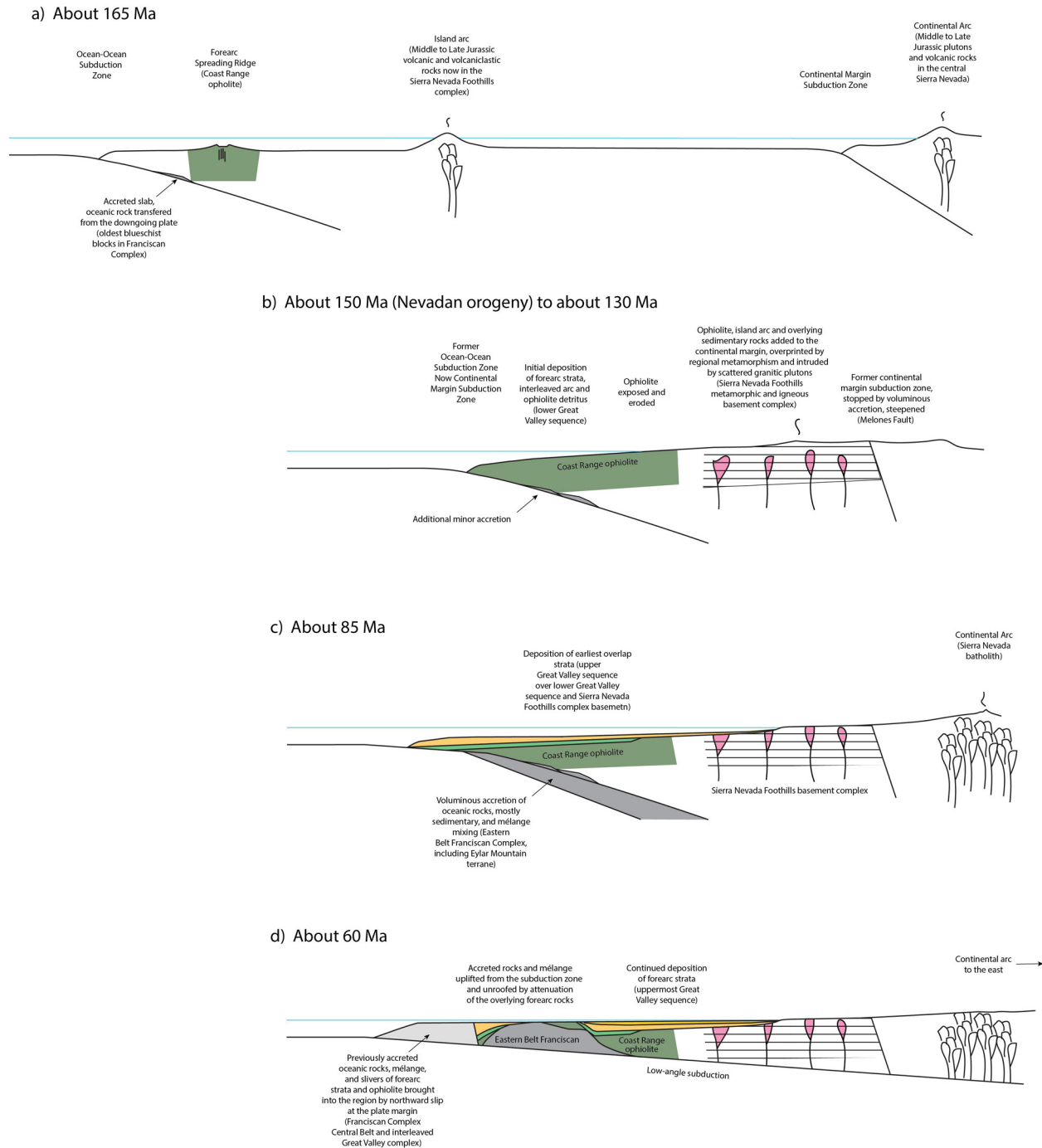


**Figure 7.** Sequential cartoon upper-crustal cross sections of the western North American continental margin and adjacent oceanic crust between Middle Jurassic and Paleocene time showing the tectonic setting of the formation and subsequent transport, accretion, juxtaposition, and deformation of the basement complexes and overlap strata discussed in the text. Colors match those in Figure 5b, late Jurassic and Early Cretaceous plutons in the Sierra Nevada Foothills basement complex are colored pink to emphasize Cretaceous uplift and unroofing, as well as their presence in the Great Valley subsurface.

To the east of the island arc was another subduction zone at the western margin of North America, as evidenced by Middle Jurassic plutons intruding continental margin rocks in the central Sierra Nevada (Irwin and Wooden, 2001). Regional deformation of the Middle and Late Jurassic arc volcanic and overlying sedimentary rocks and intrusion by ~150 Ma plutons mark the collision of the island arc with the continental margin (the Nevadan Orogeny of Hinds, 1934, see also Graymer, 2005). Subduction along the former continental margin ceased, and the former ocean-ocean subduction zone became the new continental margin (Figure 7-b). Scattered granitic plutons intruded the new continental margin made up of the accreted island arc and associated oceanic rocks, continuing until at least 138 Ma (Irwin and Wooden, 2001) to form the Sierra Nevada Foothills metamorphic and igneous complex.

At about the same time, during the Tithonian the ophiolite in the forearc was locally uplifted and eroded, with localized redeposition of ophiolitic detritus interfingering with sediments derived from the continental margin arc to the east (e.g. Ojakangas, 1968; Phipps, 1984; Bartow and Nilsen, 1990) to form the lower part of the continental forearc strata, or lower Great Valley sequence. Deposition of this strata continued into the Early Cretaceous (Berryessian and Valanginian). This initial forearc sequence is only found overlying Coast Range ophiolite, which has led some workers (e.g. Hall, 1991; Wright and Wyld, 2007) to propose large offset faults between them and the basement rocks of the Sierra Nevada and Klamath Mountain to the north and east. On the other hand, some workers (e.g. Godfrey and others, 1997; Dickinson, 2008) have correlated the forearc ophiolite with similar rocks in the Sierra Nevada Foothills and the eastern Great Valley subsurface, which would preclude such large offset. Subduction zone (high P/T) metamorphic rocks of this ~150-135 Ma age are known (Ukar and others, 2012), but are relatively rare, suggesting little accretion at the new continental margin in this period.

Late Valanginian time (~133-135 Ma) marks the first deposition of forearc strata on Klamath Mountain basement, and the start of deposition of the oldest overlap strata, the upper Great Valley sequence. Forearc deposition was still limited to the western part of the region, however. The age of the base of the upper Great Valley sequence gets progressively younger in a clockwise direction around the Great Valley, being late Late Cretaceous (Campanian; ~72-84 Ma) near Sacramento north of the map area. This indicates that forearc deposition progressively lapped onto the Sierra Nevada Foothills complex throughout the Cretaceous, accompanied by uplift and unroofing of plutonic rocks and metamorphic rocks of the Sierra Nevada Foothills complex (Figure 7-c). Arc volcanism and plutonic intrusion was farther east at this time. Note that Cretaceous forearc deposition was not limited to the present-day Great Valley, as shown by the presence of thick stacks of forearc strata as far west as the Hayward Fault (i.e. west of the Diablo Range; Figure 5).

Cretaceous time through the Campanian was also punctuated by the accretion of several large masses of oceanic rock (oceanic crust and seamounts plus overlying sedimentary rocks) to the continental margin by transfer of tectonic slabs from the down-going plate to the overlying plate in the subduction zone. These tectonic packages, or terranes, are made up of the coherent rocks of the Franciscan Complex. Each terrane is a suite of fault-bounded blocks that have a consistent internal depositional and metamorphic history that is distinct from other terranes, reflecting the distinctive pre- and post-accretion history of the several packages scraped off in the subduction zone. The slabs of coherent terranes are separated by sedimentary-matrix mélangé, volumes of structurally disrupted and sheared sandstone and shale that have incorporated blocks and lenses of rock derived from the surrounding terranes, serpentinite and other ophiolitic rocks from the forearc ophiolite scraped off the upper plate of the subduction megathrust, and “exotic” blocks not related to any known terrane, such as high-grade high pressure/temperature metamorphic blocks (including the previously accreted rocks mentioned above). Some sedimentary matrix mélangé is thought to derive from structural disruption of submarine landslide deposits (olistostromes; e.g., Page, 1978; Wakabayashi, 2011), explaining the presence of large blocks,

but some *mélange* is known to be formed by structural mixing during and after terrane accretion (Cloos, 1982; Blake and others, 2002). In the region around the map area the terranes and *mélange* make up the Eastern Belt of the Franciscan (Figure 5), characterized by widespread low-grade glaucophane schist facies metamorphism (Irwin, 1964; Blake and others, 1984).

Forearc deposition continued throughout the latest Cretaceous (Maastrichtian) and into the Paleocene (Figure 7-d). Water depth in the forearc was locally very shallow (Bartow and Nilsen, 1990) as evidenced by the presence of dinosaur fossils in the Maastrichtian Moreno Formation (Stock, 1941; Morris, 1971). Geologic processes at the subduction margin changed much more dramatically at this time, however. The dip of the subduction megathrust may have shallowed considerably (e.g., Coney, 1976; Coney and Reynolds, 1977), and no accretion is known to have taken place at this time. Instead, the presence of older and previously accreted rocks outboard (west) of the Eastern Belt suggest that tectonic transport along the continental margin brought additional accreted terranes into the region at this time, the Central Belt of the Franciscan Complex (Graymer, 2018). Paleontological and paleomagnetic evidence (Murchey and Jones, 1984; Hagstrum and Murchey, 1993) show that at least some of these rocks originally accreted far to the south, suggesting transport was northward, probably related to oblique subduction.

This period also saw the regional unroofing of the subduction accreted rocks of the Franciscan by attenuation of the overlying forearc rocks (Great Valley complex and overlap strata; Jayko and others, 1987; Unruh and others, 2007). In some places, including along the eastern margin of the Diablo Range in the map area, the attenuation of the Great Valley complex is complete, such that upper Great Valley sequence strata lie structurally on Franciscan rocks (Figure 5). The unroofing of Franciscan Complex rocks was at least locally complete in the region by Paleocene to Eocene time based on the presence of Franciscan detritus in strata of that age overlying the Great Valley sequence (Berkland, 1973; Dickinson and others, 1979) and the deposition of Eocene strata on Franciscan basement (Dibblee, 1974; Pampeyan, 1993). These Paleocene-Eocene strata mark the base of second set of overlap strata, lying on all three basement complexes in the region.

Late Eocene time saw renewed accretion of voluminous oceanic rocks, mostly sandstone and shale, at the continental margin subduction zone (the Franciscan Complex Coastal Belt), as well as continued marine deposition in the forearc. Subduction and accretion along the continental margin continued into the Oligocene, when major changes in the tectonic setting began, as expressed by significant differences in the geologic record. Far to the south, off Baja California, the spreading ridge between the Farallon and Pacific plates began to move into the continental margin subduction zone. Between about 30-25 Ma, the new plate boundary developed into a right-lateral transform fault between what is now known as the Mendocino triple junction (MTJ) on the north and the Rivera triple junction on the south. Around 25 Ma, the transform-transform-subduction junction of the present-day MTJ was formed and began migrating northward to its current position near Cape Mendocino, passing the latitude of the northern Diablo Range about 10 Ma (Atwater, 1970; Atwater and Molnar, 1973; Dickinson, 1996). In the wake of the newly formed transform boundary, crustal heating formed a series of generally northward migrating volcanic centers, starting about 26.5 Ma (Wilson and others, 2005) and continuing north to the Quaternary-active Clear Lake volcanic field. Between about 22-12 Ma, transform offset left the original continental margin plate boundary and jumped inland to form the San Andreas Fault System (Atwater and Stock, 1998), including the Calaveras Fault which lies along the western boundary of the Stockton quadrangle. The approach and eventual passage of the MTJ, along with a change in plate motions resulting in regional transpression (Atwater and Stock, 1998), initiated the ongoing uplift of the Diablo Range. Strike-slip on the faults of the San Andreas system (Figure 1) led to lateral displacement of depositional basins, including about 15 km of offset on the Greenville-Diablo-Concord Fault zone



since about 3.5 Ma (Graymer and others, 2002). In the ancestral forearc basin to the east, uplift of the Diablo Range led to progressive restriction of the basin, closing off of western outlets, and eventually to sedimentary infilling during latest Neogene and Quaternary time (Bartow, 1991).

## **BASEMENT COMPLEXES**

In the northern Diablo Range, Mesozoic basement rocks are divided between accreted subduction zone material of the Franciscan Complex and coeval, structurally overlying rocks of the Great Valley complex. In addition, basement rocks of the Sierra Nevada Foothills metamorphic and igneous complex are found in the subsurface of the San Joaquin Valley. Note that we do not use basement in the traditional sense, limited to crystalline rocks. Instead, our basement complexes denote tectonic packages of distinct provenance that are in turn overlain by sedimentary overlap strata. As such, our basement complexes include unmetamorphosed sedimentary rocks in both the Franciscan and Great Valley complexes.

### **Franciscan Complex**

Rocks of the Franciscan Complex represent the remnants of an accretionary wedge formed by subduction of the oceanic Farallon plate under the western margin of the North American plate that began in Mesozoic time (Figures 6 and 7). They include a wide range of variably deformed and metamorphosed material largely derived from accreted oceanic crust and pelagic deposits that were structurally interleaved with trench slope and basin deposits spanning from Late Jurassic to early Paleogene in age. In the Stockton quadrangle, Franciscan rocks are most widely exposed in the southern portion of the map area, between the Calaveras and Tesla-Ortogonal Faults (Figure 8), and on the heights of Mount Diablo. The Franciscan Complex is composed predominantly of weakly to moderately metamorphosed graywacke (sandstone), argillite, basalt, serpentinite, chert, and limestone, but also includes large zones and scattered pods of high-grade, blueschist-facies metamorphic rocks indicative of high-pressure alteration associated with subduction and accretion. The dynamic origins of the Franciscan Complex are reflected by the characteristically broken and dismembered strata, and the widespread presence of *mélange*, which is composed of coherent blocks within a pervasively sheared matrix. This structural complexity, combined with the puzzling association of rock types, incongruent metamorphic grades, and scarcity of age-diagnostic fossils inhibits the application of conventional stratigraphic divisions and geologic mapping methods. Consequently, geologists have long struggled to establish consistent methods for distinguishing mappable units in the Franciscan. Although the division, naming, and correlation of units remains somewhat unsettled, the Franciscan Complex in California, in broadly accepted terms, has been divided into tectonostratigraphic units consisting of fault-bounded blocks with internally consistent rock types and metamorphic grade distinguishable from those of adjoining structural blocks. The bounding faults between tectonostratigraphic units range from narrow shears to extensive zones of *mélange*. In the northern Coast Ranges, where the geology is less complicated by large lateral displacements across young strike-slip faults, the Franciscan Complex has been divided into three elongate belts that, in general, decrease in metamorphic grade and structural age of accretion from east to west (Ernst, 2011). The Eastern Belt is marked by high pressure/low temperature (blueschist facies) metamorphism. The Central Belt is dominated by lower-grade (prehnite-pumpellyite facies) metamorphism, although this belt characteristically includes extensive *mélange* units that may contain exotic pods of higher-grade metamorphic rocks within a weakly metamorphosed sedimentary matrix. The Coastal Belt typically displays very low-grade (zeolite facies) metamorphism, if any (Blake and Jones, 1981). These large 'belts' have been further subdivided into smaller fault-bounded units designated as 'terranes', which are sometimes further subdivided into 'blocks' or 'broken formations', and other unit designations. *Mélange*

is generally considered a tectonic mixture of rocks from multiple terranes (Blake and others, 2002), although locally it may also be a tectonically sheared and disrupted olistostrome (sedimentary mixture of rocks from multiple terranes; e.g. Wakabayashi, 2011; Erickson, 2011).

In the northern Diablo Range, the division and naming of Franciscan rocks have changed over time and among workers. Most Franciscan rocks in the map area share similarities in lithology, metamorphic grade and texture with those of the Eastern Belt and, to a more limited extent, the Central Belt; however, more specific correlations with Franciscan units in the northern Coast Ranges have not been confidently established. Early mapping of Franciscan rocks performed before the advent of plate tectonics treated them as a single unit, only locally distinguished by variations in lithology (Huey, 1948; Briggs, 1953) or units pertinent to mineral resource assessments (Trask, 1950). Beginning in the 1970s, recognition of the tectonic origins of the complex prompted efforts to distinguish variations in the metamorphic grade and structure as well as lithology. In the Mt. Oso area (latitude 37°30'N, longitude 121°22'30"W), Raymond (1973a, 2014) distinguished several different *mélange* units and broken formations through detailed field mapping and petrographic analysis. Farther west and just south of the Stockton quadrangle, in the vicinity of Eylar Mountain, Crawford (1976) assigned the name Eylar Mountain sequence to a suite of interlayered, blueschist-facies meta-sandstone, shale, chert, pillow basalt, and *mélanges* broadly similar to those described by Raymond. For the bedrock map of Alameda County, Graymer and others (1996) followed Crawford in assigning most Eastern Belt-type rocks to the Eylar Mountain terrane, together with several undifferentiated *mélange* and lithologic units. Blake and Wentworth (1999) looked at more regional correlations between Franciscan units and considered the Eylar Mountain terrane to be correlative with the blueschist facies metagraywacke- and metachert-rich units of the Yolla Bolly terrane mapped in the northeastern Coast Ranges. For the geologic map of the San Jose 30'x 60' quadrangle, Wentworth and others (1999a) dropped the Eylar Mountain name and reassigned the rocks to the Yolla Bolly terrane units and Eastern Belt *mélange*. Raymond (2014) presented a summary of the potential confusion associated with inconsistent naming conventions and uncertain correlations between mappable units in the Franciscan, highlighting dissimilarities in textural patterns, as well as detrital zircon maximum depositional age data that suggests the Diablo Range rocks are considerably younger than those in the Yolla Bolly type area. He considers the locally derived Eylar Mountain terrane name a more appropriate designation, at least tentatively, pending more complete analysis to indicate otherwise. Accordingly, the terrane name Eylar Mountain rather than Yolla Bolly has been used for this compilation of the Stockton quadrangle.

## **Great Valley complex**

The Great Valley complex consists of the Coast Range ophiolite, which represents a section of upper mantle and oceanic crust, and the lower, latest Jurassic and Early Cretaceous part of Great Valley sequence. The upper part of the Great Valley sequence, which also lies nonconformably on the metamorphic and igneous rocks of the Klamath/Sierra Nevada Foothills complex is the oldest overlap sequence in the region, and is described in the section “Overlap strata” below.

## **Coast Range ophiolite**

Rocks of the Coast Range ophiolite (CRO) consist predominantly of serpentinized ultramafic rocks, gabbro, diabase dikes and sills, and basaltic volcanic rocks, with minor keratophyre and quartz keratophyre (highly altered andesite and rhyolite). In the Stockton 30' × 60' quadrangle, units of the CRO are exposed along the Tesla-Ortigalita Fault near Lone Tree Creek, interleaved with Franciscan rocks west of the Greenville Fault in the vicinity of Cedar Mountain, and on the northwest side of Mount Diablo.

Serpentinite, presumably derived from the CRO, also occurs as slivers along many faults and as isolated pods within Franciscan mélangé units. Many of these rock types are magnetic and therefore coincide with magnetic anomalies, as discussed in the section below on “Geophysical Expression of Rock Units”.

High-precision U/Pb zircon dates indicate the CRO formed during the Middle Jurassic, between about 172 and 161 Ma (Shervais and others, 2004; Hopson and others, 2008). The Middle Jurassic ophiolite is locally overlain by Late Jurassic chert, tuff, and volcanoclastic sedimentary rocks (e.g. the Lotta Creek Formation in Assemblage VI south), which are in turn, locally intruded by mafic to felsic dikes and sills (Hopson and others, 2008). Emplacement of the ophiolite is thought to be induced by mantle upwelling linked to lithospheric extension, but the tectonic setting in which it originated is still under debate. Dickinson and others (1996) summarized three early models: backarc-interarc extension accreted to the continent; mid-ocean sea-floor spreading to form oceanic lithosphere then translated toward a subduction zone in front of the Sierran continental-margin arc; and forearc spreading within the Sierran forearc region. Blake and others (2002) proposed rifting in the forearc basin of an island arc that then accreted to the North American margin. Shervais and others (2006) describe petrologic, geochemical, stratigraphic, and radiometric age data that favors the CRO having formed to a large extent by rapid extension in the forearc region of a nascent subduction zone.

As mentioned in the section on regional setting above, we note the presence of accreted Middle Jurassic island arc volcanic rocks in the Sierra Nevada Foothills to the east of the quadrangle (e.g., Logtown Ridge Volcanics; Graymer and Jones, 1994), which combined with the coeval subduction zone Franciscan Complex rocks west of the CRO, and the forearc affinity of the CRO itself, form the classic subduction-forearc-island arc geometry of an east-dipping ocean-ocean subduction zone, which best fits the model of Blake and others (2002). However, Shervais and others (2006) also interpret that formation of the ophiolite was sufficiently complex to require several stages of formation, so our model (Figure 7) does not include or describe these details. Resolving the origins of the CRO remains an important component for understanding the tectonic evolution of the North America western margin during Mesozoic time.

### Lower Great Valley sequence

The Coast Range ophiolite is overlain in most places by the lower part of the Great Valley sequence. Although the contact is a fault everywhere in the map area, in other parts of the region the original nonconformable contact is preserved. As mentioned in the regional setting section, these rocks range in age from latest Jurassic (Tithonian) to Early Cretaceous (Valanginian), and only overlie the Coast Range ophiolite, as opposed to the remainder of the Great Valley sequence which also overlies basement of the Klamath Mountains and the Sierra Nevada Foothills complex. As such it is included in the Great Valley complex, even though it is sedimentary, to distinguish it from adjacent coeval rocks of different tectonic provenance (e.g., coeval plutons in the Sierra Nevada Foothills complex) and from the overlap strata of the upper Great Valley sequence.

In the map area the lower Great Valley sequence crops out in two areas. It is mapped at Mount Diablo as Knoxville Formation, predominantly thin-bedded sandstone and shale with *Buchia* and other fossils of Tithonian and Berriasian (early Cretaceous) age. It is also mapped as part of the unnamed unit KJs, a unit designated by previous workers for all strata below the Late Cretaceous Panoche Formation. These rocks contain both Late Jurassic to Early Cretaceous *Buchia* and other fossils characteristic of the lower Great Valley sequence in addition to late Early Cretaceous (Albian) and younger fossils characteristic of the lowest part of the upper Great Valley overlap strata in the map area (see the unit description below for details). Surpless and others (2006) used detrital zircon ages to document that some

*Buchia* localities actually represent redeposition of older fossils in younger units. However, the unit KJs in the map area is generally very fine-grained (clay to silt sized), so its depositional environment would seemingly have lacked the energy required to transport a large intact fossil such as a *Buchia*. Mapping out the contact between the two parts of unit KJs is beyond the scope of this compilation.

### Mesozoic granitic intrusive

A small stock of coarse-grained, quartz diorite intrudes the Coast Range ophiolite in the Cedar Mtn. quadrangle (unit KJqd). The stock intrudes the Middle Jurassic basalt unit of the ophiolite, so it probably postdates the formation of the main part of the ophiolite, but could very well be related to the Late Jurassic intermediate to silicic volcanic and volcanoclastic strata also included in the Coast Range ophiolite (units Jlc and Jvk). Alternatively, the stock could completely postdate the Coast Range ophiolite, and be perhaps related to continental margin subduction that occurred throughout the Cretaceous. Because this unit lies entirely within the Coast Range ophiolite in map view, we include it as part of the Great Valley complex.

### Sierra Nevada Foothills metamorphic and plutonic complex

Although nowhere exposed in the map area, much of the San Joaquin Valley is known to be underlain by basement rocks of the Sierra Nevada Foothills metamorphic and plutonic complex. These basement rocks have been penetrated by deep boreholes (Figure 3, see also Wentworth and others, 1995), and are manifest in the potential field geophysics as described below. These rocks are predominantly of three types. The first type is felsic and intermediate plutonic rocks, which are well represented and widely distributed in the basement penetrated by boreholes. Where exposed in the foothills to the east, these rocks form scattered plutons ranging in composition from granite to diorite, and in age from latest Jurassic (~150 Ma) to Early Cretaceous (~128 Ma; Bedrossian and Saucedo, 1981; Irwin and Wooden, 2001). The second type are gabbroic plutonic and related ophiolitic rocks of the Great Valley ophiolite (Godfrey and others, 1997; Dickinson, 2008). As discussed below, these are marked by a prominent gravity and aeromagnetic high that forms an elongate NNW-SSE trending belt in the eastern part of the Great Valley. The third type of basement rock is metamorphic rock, designated with terms such as slate, volcanic, metabasalt (greenschist), green tuff, and just “metamorphic” in the borehole data in and around the quadrangle. These rocks are probably related to accreted and regionally metamorphosed Middle to Late Jurassic island arc volcanics and overlying marine sediments that are exposed in the foothills to the east.

The interface between the Sierra Nevada Foothills complex and the Great Valley complex is not well understood. Some workers (e.g., Godfrey and others, 1997) have correlated the Great Valley ophiolite with the Coast Range ophiolite. If true, that would make the Great Valley complex just the westernmost extent of the Sierra Nevada Foothills complex. However, other workers (e.g., Hall, 1991) have postulated a major fault along the axis of the Great Valley, which would separate the two ophiolites. Resolution of the problem is beyond the scope of this effort.

## OVERLAP STRATA

### Stratigraphic Assemblages

The Cretaceous and younger stratigraphy exposed in the northern Diablo Range is complex, reflecting different depositional basins and rapid facies changes through time, together with large-scale offsets on numerous faults, many of which are still active. Late Early Cretaceous (Albian) and younger

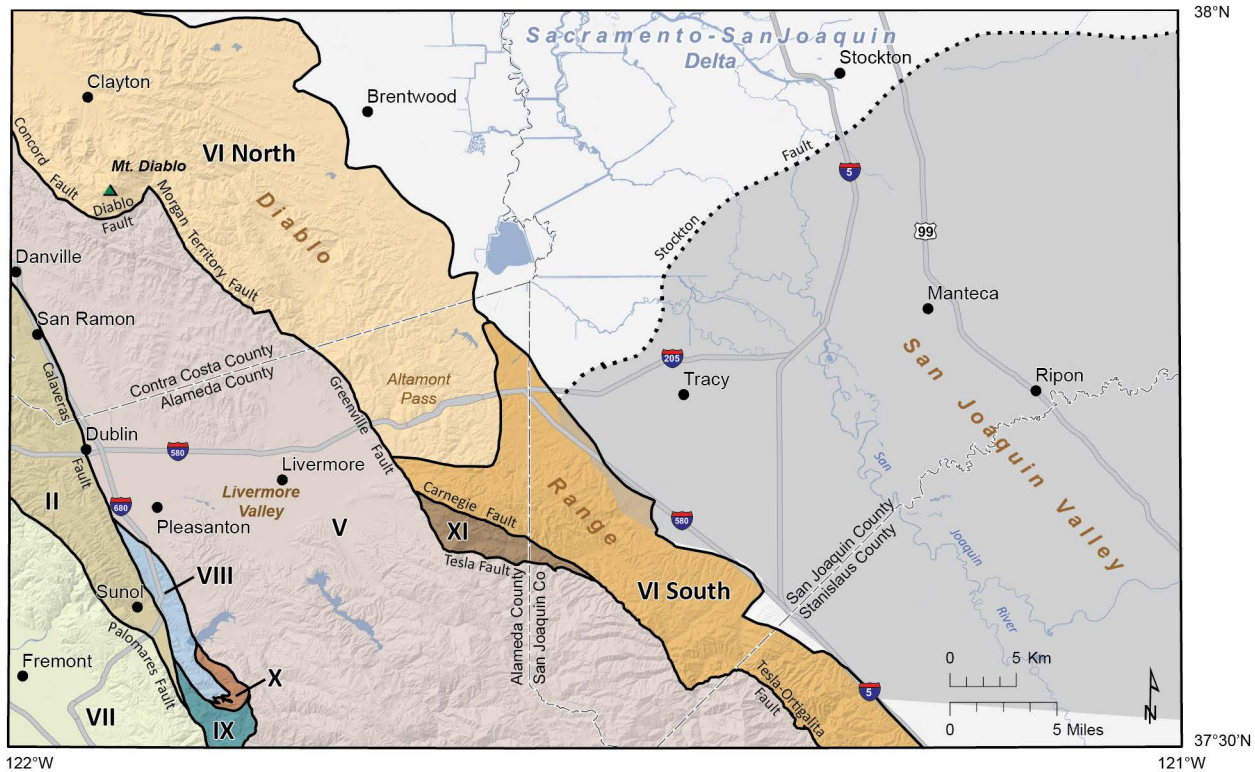


**Figure 8.** Map showing stratigraphic assemblages in structural blocks and depositional basins distinguished in the northern Diablo Range (modified from Graymer and others, 1994a and 1996), identified by roman numerals. Gray shading in the San Joaquin Valley marks the approximate extent of the concealed Stockton arch (modified from Bartow, 1991).

stratigraphic sequences in the Stockton 30' × 60' quadrangle are divided into eight distinctive stratigraphic assemblages (Figures 8 and 9) following the work of Graymer and others (1994a, 1996). As defined by Graymer, Jones, and Brabb (1994), the bedrock assemblages are large, fault-bounded blocks that contain a unique stratigraphic sequence representing changes in depositional conditions in one or more large depositional basins. The stratigraphic sequences vary among some assemblages by containing different rock units of the same age. For example, Assemblage VII includes the late Miocene nonmarine Orinda Formation and overlying volcanic rocks, whereas the adjacent Assemblage II includes coeval marine Neroly Formation and Cierbo Sandstone (Figure 10). In addition, some assemblages are distinguished by truncated sequences. For example, the Cierbo Sandstone directly overlies the Domengine Formation in Assemblage V, whereas in Assemblage VI North, the Nortonville Shale, Markley Formation, and Kirker Tuff totaling hundreds of meters of stratigraphic sequence lie between them. Although there is modest stratigraphic variation within assemblages, such as the lateral pinchout of Paleocene strata within Assemblage VI north, the contrast between assemblages is greater and more abrupt. As such, assemblage boundaries illuminate the position of tectonic deformation, and differences or similarities in adjacent stratigraphic sequences can constrain the timing of that deformation.

The current locations of the different assemblages in some cases reflect the juxtaposition of different basins or parts of basins by large strike-slip offsets along the faults that bound assemblages. For example, Assemblage VII is juxtaposed against Assemblage II by about 50 km of post-12 Ma right-lateral strike slip on the Calaveras and Palomares faults (Graymer and others, 2002). In other cases, differences between Assemblages reflect significant differences in tectonic uplift, such as the much thinner or missing Paleogene strata in Assemblages V and VI South as opposed to Assemblage VI north (discussed more

below).

The divisions and numbering assigned to assemblages by Graymer and others (1994; 1996) has been retained here for consistency with the source maps, which extend beyond the Stockton quadrangle boundaries. Note that Assemblages I, III, and IV are absent from this compilation, as they are confined to areas in northwestern Contra Costa County outside of the Stockton quadrangle (Graymer and others 1994a; Graymer, 2000). Assemblage VI along the eastern flanks of the Diablo Range was divided into separate VI North and VI South Assemblages. The division was made for this compilation as a means to resolve the substantial differences in unit names and age controls between the newer mapping for Alameda County and older mapping available for areas in San Joaquin and Stanislaus Counties. The location for the divide was selected to roughly coincide with a westward projection of the Stockton Fault that forms the northern boundary of the Stockton arch, a buried structural high (Figure 8) that separates the San Joaquin sedimentary basin from the Sacramento basin to the north (Bartow and Nilsen, 1990; Bartow, 1991). Latest Mesozoic and Paleogene uplift of the Stockton arch led to emergence and erosion of upper Cretaceous through Eocene strata, followed by some non-marine depositions on the arch, while marine deposition continued north of the Stockton Fault (Bartow, 1991). Although complicated by younger faulting, the change in depositional environments is reflected in the stratigraphic differences between Assemblages VI North and VI South. We have also changed the boundary between Assemblages V and VI North slightly, moving it east from the Riggs Canyon Fault to the Morgan Territory Fault (Figure 8). This change was made because the truncated Cretaceous section and the identity of the overlapping Eocene strata in the structural sliver between the two faults is more like that of Assemblage V than that of Assemblage VI North.

### **Upper Great Valley sequence**

The upper Great Valley sequence (GVS) consists of a thick accumulation of marine and lesser nonmarine clastic rocks of Valanginian (Albian in the map area) to Paleocene age that unconformably overlie the lower Great Valley sequence in the western portion of the ancestral forearc basin and Klamath and Sierran Foothills igneous and metamorphic basement rocks, including in the Sacramento Valley subsurface to the north and east (Blake and others, 1984), so that the upper GVS is considered to overlap on both the Great Valley and the Klamath/Sierran basement complexes. As mentioned above in the section on regional setting, the base of the upper Great Valley sequence gets younger in a clockwise manner around the Sacramento Valley, ranging from Early Cretaceous (Hauterivian) in the northwest part of the valley near Red Bluff (Blake and others, 1999), to Late Cretaceous (Coniacian) in the northeast part of the valley near Chico (Haggart, 1984), to late Late Cretaceous (Campanian) in the east-central part of the valley near Sacramento (Hilton and Antuzzi, 1997). Paleontologic data from deep boreholes suggest that the base of this unit may be a bit older (Santonian) closer to the center of the valley (e.g., Bishop and Davis, 1984; Brabb, 2011) as in the map area. This reflects a period of intrusion of Early Cretaceous plutons into the Sierra Nevada Foothills complex followed by a period of uplift and unroofing of the plutons along with the surrounding metamorphic rocks, followed by progressive onlap of the forearc strata, all while coeval forearc sedimentary rocks were being deposited to the north and west.

Deposition in the forearc was sporadic, marked by gaps in the stratigraphic record throughout the section. The pauses in deposition have been interpreted to indicate when sediments shed from the Sierran arc as well as from erosion of underlying plutonic and metamorphic rocks were able to pass through the forearc to deeper trench settings until tectonic uplift along the accretionary wedge caused sediment to pond within the forearc (Dickinson and Seely, 1979; Mitchell and others, 2010).

The lower part of upper GVS strata exposed in the Diablo Range were deposited in submarine-

Age	Stage	This compilation							Brabb and others, 1971 (Mt. Diablo - Byron area)	Huey, 1948 (Tesla 15' quad.)	Raymond, 1969/1970 (Lone Tree Creek & Sojyo 7.5' quads.)	Bartow and others, 1985 (Sojyo 7.5' quad. and south)	Throckmorton, 1988 (Corral Hollow area)					
		Assemblages																
		VI North	VII	V	II	VIII	VI South & XI											
		(From Graymer and others, 1994 & 1996)																
Cretaceous	Late	Maastrichtian	Deer Valley Sandstone		Undivided Great Valley	Unnamed local divisions: sandstone		VIII	Moreno Fm.	Deer Valley Sandstone	Moreno Fm.	Moreno Fm.	Moreno Fm.	Moreno Fm.				
		Unit E																
		Campanian	Unit D	Pinehurst Shale									Joaquin Ridge Sandstone				Panoche Fm., upper sandstone member	
		Santonian	Unit C	Redwood Canyon Fm.									Panoche Fm.				Panoche Fm.	Panoche Fm., siltstone member
		Coniacian		Unnamed sandstone & conglomerate									Marliff Shale	Panoche fm.				
		Turonian	Unit B	Oakland Sandstone					mudstone	Unnamed sedimentary rocks	Unnamed sandstone and shale			Unnamed sandstone & shale				
	Cenomanian											fault						
	Early	Albian	Unit A	Unnamed shale			sandstone & shale											
		Apian					shale with sandstone			Unnamed shale	Unnamed shale	Horsetown fm.	Hospital Formation/ Adobe Flat Shale	Unnamed shale	Panoche Fm., lower shale member			
		Barremian																
		Hauterivian																
		Valanginian																
		Berriasian																
Jurassic	Late	Tithonian	Knoxville Fm.	Knoxville Fm.														
		Kimmeridgian							Lotta Creek Formation	Knoxville Fm.	Lotta Creek Formation				Knoxville Fm.			

**Figure 9.** Summary of Great Valley sequence units and correlations between stratigraphic assemblages in this compilation and selected source maps.

fan, basin-plain, and slope depositional environments. Younger sections of the GVS, particularly in the subsurface of the San Joaquin Valley, also include some shelf and deltaic deposits (Bartow and Nilsen, 1990). Erosion of the Sierran arc was the principal source of sediment, as indicated by stratigraphic and spatial variations in composition that have been correlated with the timing and distribution of magmatic episodes in the Sierra Nevada region (Ingersoll, 1981). However, the recognition of Proterozoic and Archean zircon grains throughout the Great Valley sequence suggests that the basin also received sediment derived from the North American craton throughout its history (Surpless and others, 2006).

Rapid lateral facies changes are a common trait of depositional systems in an evolving tectonic trough, which makes the usefulness of lithostratigraphic subdivisions problematic for regional application. Consequently, stratigraphic divisions and nomenclature applied to the GVS has undergone considerable evolution and remains somewhat confused. Sequence stratigraphy based on seismically definable units, together with biostratigraphic controls and electric borehole logs for petroleum exploration have proved useful in distinguishing related depositional packets in the subsurface of the Great Valley, but these divisions are not readily correlated with outcrops in the Coast Ranges, nor are they recognized throughout the valley subsurface. Similarly, major outcrop units have not been systematically recognized in the subsurface. Consequently, stratigraphic nomenclature developed for the subsurface of the northern San Joaquin Valley has little in common with that developed from rocks that crop out in the Diablo Range (Bartow, 1991).

The stratigraphic nomenclature applied to exposures of the upper GVS in the Diablo Range evolved from the early work of Anderson and Pack (1915), who designated the names Panoche Formation and Moreno Formation for Cretaceous strata exposed at type localities in the Panoche Hills, some 130 km to the south of the Stockton quadrangle. Some later workers retained these formation names for Great Valley strata in the northern Diablo Range, whereas others assigned local names or unnamed lithologic unit designations, citing the lack of good age controls or other evidence to support correlation with strata of distant type localities. The Panoche and Moreno names remain widely applied to Late Cretaceous and older strata in some places.

Along the eastern margin of the northern Diablo Range in Contra Costa and Alameda Counties (Assemblage VI North), Graymer and others (1994a and 1996) substantially revised division of the GVS building on the detailed mapping by Brabb and others (1971). They found the Panoche/Moreno unit scheme for Late Cretaceous strata overly broad, encompassing multiple units in the map area, and did not fit well with their additional age controls and mapped lithologic variations. They also noted that while Brabb and others (1971) adapted names from the San Joaquin Valley margin to the south, other workers (e.g., Crane, 1995) applied names from the subsurface and western margin of the Sacramento Valley to the east and north, and that naming schemes brought from elsewhere did not fit uniformly well with the observed stratigraphy of the study area, probably because of lateral facies changes (see also Bartow and Nilsen, 1990). Instead, they subdivided the strata generally along the lines of Brabb and others (1971) but assigned generic unit labels (A to E) based principally on age. Their units Kb, Kc, and Kd are equivalent to the Panoche Formation, and their unit Ke and Kdv (Deer Valley sandstone) equivalent to the Moreno Formation in Assemblage VI South (Figure 9). Their unit Ka is equivalent to various Early Cretaceous shale units, sometimes included as part of the Panoche Formation. In other assemblages, previously designated unit names were retained, or unnamed lithologic divisions assigned.

For this compilation, division of the GVS and unit designations of Graymer and others (1994a, 1996) are followed for most areas of the map in Contra Costa and Alameda Counties. In Assemblages VI South and XI, where their more recent mapping and age data were not available, the Panoche and Moreno formation names used on most source maps were retained. However, because of disagreement between source maps and age uncertainties, the use of Knoxville and other names applied to pre-Panoche



strata mapped along the Tesla-Ortogonal Fault were grouped into a single unnamed shale unit of Early Cretaceous and possibly Late Jurassic age. Figure 9 presents a summary of GVS units used in this compilation and correlations with units from selected source maps.

## **Cenozoic Rocks**

### **Tertiary Strata**

Early in the Cenozoic Era, major changes in the tectonic regime along the continental margin begin to show up in the stratigraphic record. Regional uplift and deformation of the ancestral forearc basin during this time are reflected in the basin-wide unconformity that separates the GVS from late Paleocene and younger strata. Correlative unconformities identified from sequence stratigraphy elsewhere suggest a lowering of eustatic sea level contributed to this gap in the stratigraphic record; however, variations in angular discordance along the unconformity and changes in depositional systems point to a change in tectonic activity unevenly affecting the ancestral forearc basin (Bartow, 1991). The resumption of deposition preserved in Paleocene strata indicates more local variations in depositional environment and structural division of the ancestral forearc. Emergence of the Stockton arch (Figure 8) in the late Paleogene divided the depositional trough into the San Joaquin basin to the south and Sacramento basin to the north (Bartow and Nilsen, 1990; Imperato, 1992). The map area includes the northernmost part of the San Joaquin basin on the south side of the arch and the (equivalent?) folded and uplifted Late Cretaceous rocks in the Altamont Pass area, where the Paleogene Tesla Formation was deposited in a deltaic and shallow brackish environment that shoaled northward against the topographic high. Where exposed in the Corral Hollow area the Tesla Formation includes several transgressive/regressive phases extending through the middle or late Eocene (Throckmorton, 1988). This was followed by a period of erosion or non-deposition lasting through the Oligocene and into the Miocene on the Stockton arch and Altamont Pass area, while the Valley Springs Formation and overlying Miocene strata were being deposited farther south and east in the San Joaquin basin.

In contrast, on the north side of the Stockton Fault and arch, a much thicker and persistent record of marine deposition in the Sacramento basin is preserved in the Paleocene and Eocene succession of the unnamed Paleocene sandstone and shale, Meganos Formation, Domengine Formation, Nortonville Shale, and Markley Formation in Assemblage VI North (Figure 10). The Paleogene section in Assemblage V is much thinner than that of VI North, probably reflecting later northward offset by strike-slip along the Greenville Fault from an original depositional position closer to the uplifted basin bounding ridge in the Altamont Pass area, as well as possible earlier syndepositional down to the east normal faulting. We note the similarly thin Paleogene section in Assemblage XI would be roughly aligned with the Paleogene strata in Assemblage V after restoration of the 15 km right-lateral offset proposed by Graymer and others (2002). To the west of Assemblage V, a separate succession of Paleogene through Miocene deposition is represented by the Briones Sandstone and older units (much of this succession lies outside the map area), which have been variably displaced northward by late Neogene movement along the Calaveras and other dextral strike-slip faults. The western stratigraphic assemblages display an unconformity around the Oligocene-Miocene boundary similar to that recorded in stratigraphic gaps to the east, which suggest an extended area of emergence along what is now the Diablo Range during that time. The last evidence of widespread marine deposition in the map area is represented by the late Miocene shallow marine Neroly Formation, composed primarily of andesitic material derived from Miocene volcanic rocks in the Sierra Nevada (Isaacson and Andersen, 1992). The coeval nonmarine deposition of the Orinda Formation and overlying volcanic rocks in Assemblage VII on the west side of the map area indicate that Late Miocene marine deposition in the map area did not extend westward to the Pacific Ocean, but rather was a western

embayment of the northern part of a shallow inland sea connected to the ocean hundreds of kilometers to the south. Late Neogene uplift of the Diablo Range and unroofing of basement rocks are reflected in the younger terrestrial deposits of the area. In Assemblage V, fluvial deposits of the Green Valley and Tassajara Formations (map unit PMgv, informally referred to by some as the Sycamore formation) accumulated in the ancestral Livermore basin, a late Neogene depocenter located along the southwestern flank of the present Mt. Diablo massif (Isaacson and Andersen, 1992). Drill hole and seismic refraction data suggest that the thickness of the Livermore basin fill to the southwest of Mt. Diablo is more than 5,200 meters (Unruh, 2000), consistent with the prominent gravity low (L2 in Figure 3) discussed later in the pamphlet. This depth, as shown in Figure 11, reflects a faulted and folded section. The maximum stratigraphic thickness of unit PMgv is about 5 km, and the maximum stratigraphic thickness of the overlying Livermore gravels is about 3 km.

Like the GVS, unit correlations and names applied to Tertiary strata in the Stockton quadrangle have evolved over time and among workers as more data became available and a better understanding of the complex tectonic history of the region has emerged. Unit names and divisions used in this compilation for the most part follow those established by Graymer and others (1994a, 1996) for their bedrock maps of Alameda and Contra Costa Counties. Where unit names were chosen from conflicting source maps, some explanatory background is provided in the Description of Map Units section of this pamphlet.

## Intrusive Rocks

Cenozoic intrusive rocks of limited extent have been mapped in the Stockton 30'x 60' quadrangle. These rocks are not included in any assemblage because of their intrusive nature.

Small rhyolite plugs and other silicic intrusive rocks (Msv) are mapped in the Sunol (Figure 8) area and on the eastern flank of Mt. Diablo, and similar rhyolite intrusives (Tr) are mapped on Pleasanton Ridge north of Sunol. The rocks east of Mount Diablo have yielded a biotite Ar/Ar age of about 7.5 Ma (Ryan Fay, written commun.), which is roughly in line with the age expected for this latitude from the northward-younging suite of volcanics observed in the region when adjusted for post-volcanic offset on regional strike-slip faults (Fox and others, 1985; Graymer and others, 2002). However, these rocks lie well east of the other volcanic centers, so would represent an outlier. The rocks near Sunol and at Pleasanton Ridge are significantly farther south, even when accounting for slip on the intervening Greenville and northern Calaveras faults, and so are perhaps somewhat older.

## Quaternary Surficial Deposits

Quaternary surficial deposits cover nearly the entire northeastern portion of the map in the San Joaquin Valley and Delta and are widespread in valleys and larger drainages of the Diablo Range, including Clayton Valley in the north, San Ramon and Livermore Valley in the center, and Sunol Valley in the south. In addition, the map area includes a small part of the San Francisco Bay plain in the southwest corner.

Quaternary deposits in the San Joaquin Valley are largely made up of two suites of alluvial fans extending from the mountains to either side of the valley. San Joaquin Valley alluvial sediments can be broadly divided between those in the west derived principally from local sources along the Diablo Range, and those east of the San Joaquin River composed of material washed down from the foothills and glaciated heights of the Sierra Nevada mountains. The two suites of alluvial fan deposits are separated by fluvial deposits associated with the San Joaquin River. In addition, the eastern suite of fan deposits is further separated by fluvial deposits along the Tuolumne and Stanislaus Rivers. These fluvial deposits are primarily sets of terrace deposits preserved at different levels above the present channels, reflecting



downcutting of the channels due to regional uplift. About 10 km northwest of the confluence of the San Joaquin and Stanislaus rivers, the fluvial system spreads out along multiple interconnected channels into the Sacramento-San Joaquin River Delta. Surficial deposits in the Delta are predominantly fluvial flood plain deposits, which grade northward into paludal deposits along the north edge of the map area.

In addition to the four active depositional systems in the San Joaquin Valley, there are exposed deposits of an earlier eolian system. These are mostly located along the west side of the valley near the northern edge of the map area and in the southeast part of the map area. Thought to be wind-blown deposits of glacial till formed during and following the glacial period, about 10,000-40,000 years ago (Atwater, 1982), these dune sands are overlain by the distal part of the western alluvial fan system and the Delta deposits, and lie on Modesto Formation deposits of the eastern alluvial fan system.

Surficial deposits in San Joaquin Valley can be differentiated based on their sediment provenance as noted above. Further distinguishing mappable units in the young deposits of the San Joaquin Valley is based largely on subtle differences in soil composition documented in USDA Soil Survey maps and reports (Retzer and others, 1951; McLaughlin and Huntington, 1968; McElhiney, 1992) and geomorphic expression interpreted from topographic maps and aerial photographs (Marchand and Harden, 1978; Marchand and Allwardt, 1981; Knudsen and Lettis, 1997; Knudsen and others, 2000).

To the west of the San Joaquin Valley, surficial deposits are made up of alluvial fans extending from valley margins divided by fluvial systems. In the northwest corner of the map area, the fluvial deposits of Diablo Creek run through the alluvial deposits of Clayton Valley. Fluvial systems of several creeks that separate alluvial fan deposits in Livermore and San Ramon Valley merge into Arroyo de la Laguna, which has a narrow band of fluvial deposits reaching south along the Calaveras Fault to Sunol Valley. Alameda Creek forms a similarly narrow band of fluvial deposits through Sunol Valley. West of the confluence of Arroyo de la Laguna, Alameda Creek flows through the very narrow and steep walled Niles Canyon. There, Alameda Creek is probably an antecedent stream that cut down through the hills during a period of Quaternary uplift based on the meandering course of the steep canyon and the presence of correlated Pliocene to early Pleistocene alluvial deposits on either side of the ridge (Livermore and Irvington gravels, see Description of Map Units below), as well as measured uplift of late Pleistocene and Holocene terrace deposits in the canyon (Kelson and Simpson, 1995). West of Niles Canyon, Alameda Creek forms a band of fluvial deposits within the alluvial fan system that has developed on the broad plain extending down to San Francisco Bay west of the map area. In addition to these more extensive deposits, a large number of narrow canyons in the Diablo Range and East Bay Hills have fluvial and alluvial deposits.

## Landslides

The source maps for this compilation varied widely in their attention to landslides. The maps of Graymer and others (1994a, 1996) used for Alameda and Contra Costa Counties focus on bedrock and structure, including only some of the larger, more prominent landslides recognized in the area. Other sources present more detailed mapping of landslides, but with many landslides too small to be clearly displayed on a 100,000-scale geologic map. It is important to understand this compilation does not provide a thorough or uniform presentation of the distribution of landslides and is not representative of landslide hazards in the map area. For more information on landslides, the California Geological Survey information warehouse (<http://maps.conservation.ca.gov/cgs/informationwarehouse/index.html>) offers ready access to Landslide Inventory Maps and other resources focused on landslides and slope stability issues.

## GEOPHYSICAL EXPRESSION OF ROCK UNITS

### Gravity Anomalies

Gravity anomalies within the Stockton quadrangle (Figure 3; Gravity Map, see PDF) mostly reflect the density contrast between dense Mesozoic basement rocks and overlying, less dense Cretaceous and Cenozoic sedimentary rocks and deposits. Significant gravity lows are located along the western part of San Joaquin Valley (L1) and in Livermore Valley (L2). Two additional gravity lows are present in the map area in the southwest corner of the map area (L3) and in the east part of the map area south of the Stockton Fault (L4). Significant gravity highs are located at Mount Diablo (H1), the southeast flank of Mount Diablo (H2), the northern end of the main Diablo Range (H3), and the East Bay Hills in the southwest part of the map area (H4).

We modeled gravity and magnetic anomalies across the Stockton quadrangle along a cross-section that extends east-northeastward from the hills west of Pleasanton, across Livermore Valley, the Diablo Range into the Sacramento-San Joaquin Delta to the city of Stockton (Figure 11). The orientation was chosen to be perpendicular to the major strike-slip faults, such as the Calaveras and Greenville Faults. Our initial model was based on projection of geologic contacts and attitudes into the subsurface. Additional information was provided by stratigraphic picks encountered in nearby oil and gas wells that were projected onto the geologic section. Densities and magnetic susceptibilities were guided by available physical property information, such as density logs in deep drill holes in Livermore Valley and in the Delta (Brocher and others, 1997; Tiballi and Brocher, 1998; Langenheim and others, 2018) and densities and magnetic properties from hand samples of various rock types (Hagstrum and Jones, 1998; Ponce, 2001; Hillhouse and Jachens, 2005).

The low along the western San Joaquin Valley is a regional feature that extends to the north and south of the quadrangle and is attributed to Cenozoic and lower-density Cretaceous GVS sedimentary rocks. This package reaches a thickness of at least 5-5.5 km in the quadrangle, as indicated by drill holes and a northwest-oriented seismic-refraction profile (Colburn and Mooney, 1986; Wentworth and others, 1995). The low is not everywhere the same value and is marked by a saddle near the city of Tracy, west of the Stockton arch. Northwest of the Stockton arch, the gravity low becomes more pronounced, reaching the lowest values in the quadrangle along the northern margin of the map. This low extends another 80 km to the north and coincides roughly with the Rio Vista basin and with low P-wave velocities (< 5 km/s) to depths of 10-12 km (Thurber and others, 2009). Where our model profile intersects this gravity low, the basin depth is more than 7 km (Figure 11). South of the Stockton arch, the gravity low extends along the margin of the valley for nearly 300 km (Roberts and others, 1990). The saddle near Tracy coincides with the upthrown blocks of the Stockton and Vernalis Faults. As noted above, relationships across the Stockton Fault indicate a complex history so that the upthrown block, although missing the Paleogene sequence, has a thicker Cretaceous section and a depression of the basement surface, rather than a basement arch (Bartow, 1991).

The other prominent gravity low in the quadrangle is the roughly triangular low centered over Livermore Valley (L2 in Figure 3). The deepest drill hole in the basin (well 01320089 on Figure 3) bottomed in Miocene strata at a drilled depth of 5.3 km (true vertical depth of 5.2 km), consistent with a seismic refraction profile (Meltzer and others, 1987) that shows the basin locally reaches depths of 5.5 km. The drill hole is not located in the deepest part of the low, however, suggesting that the basin depth could easily exceed 6 km, perhaps as much as 8-9 km. Along our model profile, the basin depth is ~8 km (Figure 11).

The moderate gravity low in the southwest corner of the map area (L3) is the northern tip of a

Geologic and Geophysical Maps of the Stockton 30' × 60' Quadrangle, California

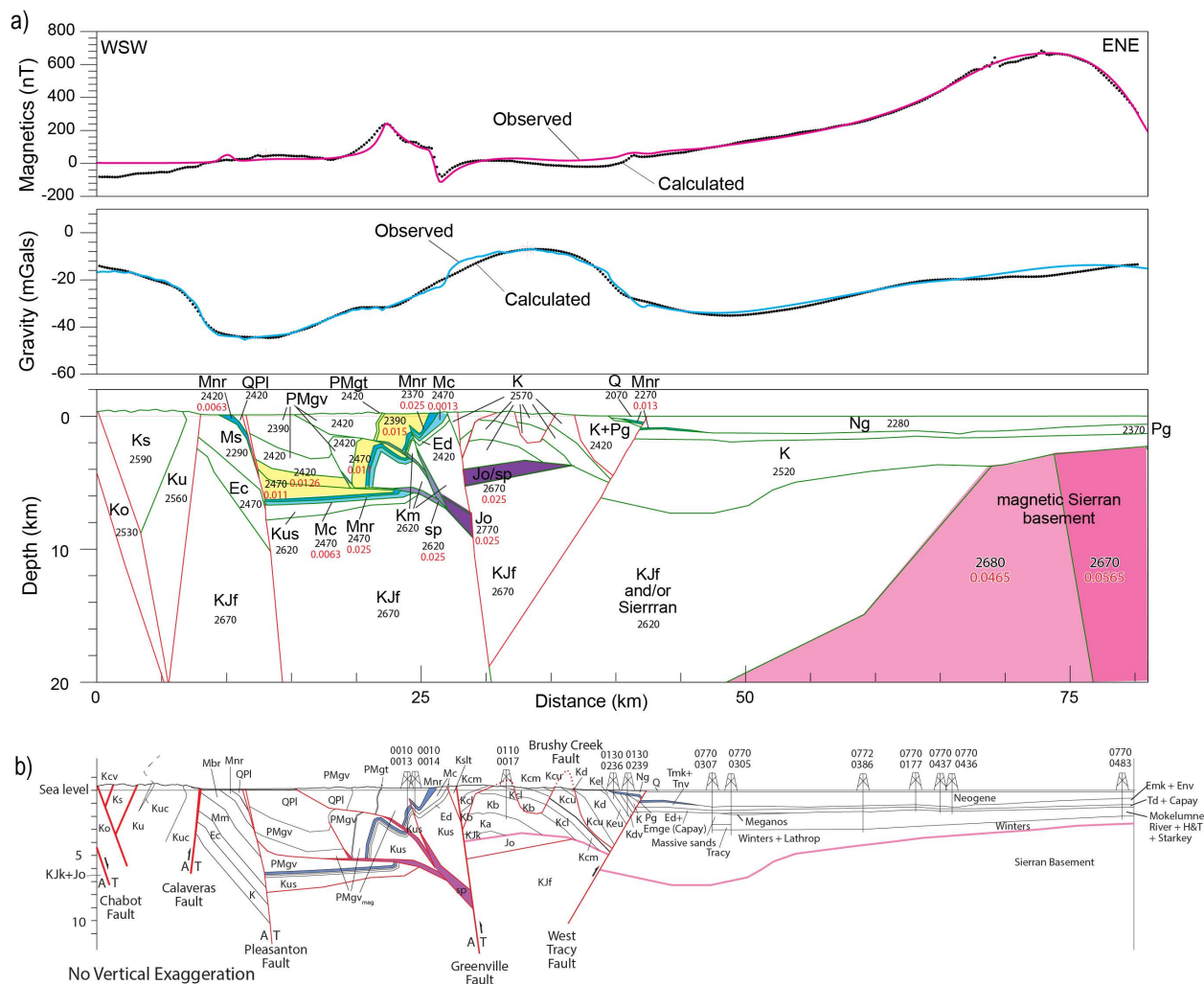


**Figure 11.** Geophysical model (a) and geologic cross-section (b) across Stockton quadrangle. Profile location shown in Figures 3, 4, and 12. Colored polygons in model are magnetic, with red numbers denoting magnetic susceptibility values in SI units. Black numbers are densities in kg/m<sup>3</sup>. All unit labels are the same as in the geologic map except: Q, undifferentiated Quaternary surficial deposits; Ng, undifferentiated Neogene strata; Pg, undifferentiated Paleogene strata; K, undifferentiated Cretaceous strata. Yellow areas in (A) reflect magnetic lower part of the unit PMgv. Subsurface units beneath the San Joaquin Valley are the same as in the DOGGR well files for the wells shown, which are labeled by their API number.

very large gravity low that lies mostly to the south of the map area, the Evergreen Basin (Jachens and others, 2017). This basin is about 5 km deep in its center and is thought to be made up of Neogene rocks deposited in a rhombochasm formed within a releasing right step between the Silver Creek Fault and the Hayward Fault between about 12-2.5 Ma (Graymer and others, 2015; Jachens and others, 2017). Note that the gravity low extends east beyond the Hayward Fault, reflecting the east dip of the fault and the presence of less dense material in the footwall. Higher gravity values in the southwesternmost corner reflect dense basement under relatively thin Quaternary cover west of the Silver Creek Fault.

Not all the gravity anomalies in the Stockton quadrangle reflect the geometry of Cenozoic basins,

but instead arise from density variations in the basement complex (Robbins and others, 1976). Drill-hole data indicate that the top of basement beneath the eastern two-thirds of the Central Valley slopes gently to the southwest (Wentworth and others, 1995); the broad low (L4) between relatively high gravity values in the northeast part of the map results in part from density contrasts within the basement rocks. The low roughly coincides with the Stockton arch, whose northern margin coincides with the south-dipping reverse Stockton Fault and whose southern margin is poorly constrained to lie along the southern margin of the Stockton quadrangle (Bartow, 1991). The combined effect of increasing the thickness of the Cretaceous sequence and thinning of the Cenozoic section over the Stockton arch would result in a gravity low of about 8 mGal. The southern edge of the gravity low, however, does not coincide with the southern edge of the Stockton arch, as defined by Bartow (1991) to extend roughly east-west at a latitude of 37°30'N, again suggesting that basement density variations are responsible for part of the gravity anomalies over the valley. Furthermore, the gravity field continues to climb another 30 mGal to the northwest and southeast of the boundaries of the quadrangle, perpendicular to the gentle southwest slope of the basement surface.

The highest gravity values correspond to outcrops of ultramafic and mafic rocks near Mount Diablo in the northwest part of the map (H1 in Figure 3). The Mount Diablo high is superposed on a northwest-trending ridge of gravity values that top out at values of -8 to -10 mGal (H2) and that coincide with exposures of Cretaceous marine sedimentary rocks of the GVS. The Mount Diablo high is roughly 10 km wide and 12 km long with a magnitude of 44 mGal relative to the gravity ridge, H2. The gradient marking its southwest edge is steeper than that along its northeast edge, suggesting some asymmetry to the source of the anomaly. Approximating the source of the dense body as a cylinder with a density contrast of 300 kg/m<sup>3</sup> between the ophiolite and the sedimentary rocks and a radius of 5 km, these dense rocks extend 7.5 km below the surface. This estimate, based on simplification of the exposed geology as a cylinder with a single density contrast, is supported by P-wave tomography, albeit of coarse resolution (horizontal node spacing of 10 km), that indicates higher velocities below Mount Diablo to 8 km and even deeper (Thurber and others, 2009). Wood (1964) also modeled the gravity high (using the simple Bouguer gravity anomaly) as a diabase body 4 km thick underlain by a dense vertical cylinder with a radius of 4 km (presumably diabase) that extends to 10-12 km depth.

The gravity ridge southeast of Mount Diablo (H2) is interpreted as a northwest trending antiform in the top of basement surface, with its apex about 3 km below the ground surface (Figure 11). Note that the gravity ridge does not directly underlie the crest of the Diablo Anticline as expressed by folded GVS, suggesting that, at least locally, the shape of the top of basement surface is not constrained by the shape of the overlying strata (Figure 11). This discordance could be because the contact is a fault, or because the contact is a high-angle buttress unconformity (Graymer and Langenheim, in press).

Another block of higher gravity values (H3) coincides with exposures of the Franciscan Complex and Coast Range ophiolite in the Diablo Range in the south-central part of the quadrangle. A simple calculation using the infinite slab approximation using the difference in gravity values between those in the Diablo Range and those northwest of Altamont Pass (10-22 mGal) and a density contrast of 130 kg/m<sup>3</sup> between the Franciscan Complex and the GVS suggests that the GVS is a minimum of 2-4 km thick north of Altamont Pass.

Relatively high gravity values (H4) separate the Livermore gravity low (L2) from the northernmost part of the Evergreen low (L3) and coincide with exposures of Late Cretaceous rocks. The moderate amplitude of this gravity high reflects the density contrast between upper GVS strata and less dense Cenozoic strata and surficial deposits, rather than the near-surface presence of basement rocks, which would result in higher anomaly values such as those along H2.

## Magnetic Anomalies

Sources of magnetic anomalies are those rock types that contain magnetite, usually mafic igneous and meta-igneous rocks. Exposed in the Stockton quadrangle, these rock types are serpentinite, gabbro, and diabase of the Coast Ranges ophiolite and serpentinite and basalt of the Franciscan Complex. Prominent magnetic highs coincide with outcrops of Jurassic diabase, pillow basalt, and serpentinite on Mount Diablo (Figure 4). Paleomagnetic studies of the diabase indicate that these rocks, although possessing remnant magnetizations of both normal and reversed directions, have in general larger induced magnetizations (Mankinen and others 1991; Hagstrum and Jones, 1998) and significant overprinting of the natural remanence by today's Earth field. This is borne out by the absence of magnetic lows and presence of magnetic highs with outcrops of the ophiolite. The highs associated with the exposed ophiolite at Mount Diablo are superposed on a broader magnetic high, indicating that these rocks extend concealed beneath younger sedimentary rocks, which is also consistent with the interpretation of the gravity anomaly and shown in Figure 11. Mafic volcanics in the Franciscan Complex at Mount Diablo, on the other hand, are not associated with a magnetic high; these rocks have been metamorphosed or hydrothermally altered such that any magnetic minerals (magnetite) have been destroyed.

In the Diablo Range, many of the anomalies are associated with serpentinite and can be used to infer the subsurface extent of serpentinite beyond small isolated slivers of serpentinite that crop out along northwest-trending fault zones along the northernmost part of the Diablo Range. East of the Greenville Fault southeast of Livermore Valley, a magnetic anomaly is present over outcrops of the Mélange of Blue Rock Springs (Franciscan Complex) and, to a lesser degree, adjacent Franciscan units. The gradients of the anomaly are broad, suggesting that the source is deep, not exposed, consistent with magnetic property measurements that show that the Franciscan Complex rocks (excluding serpentinite and basalt of the Marin Headlands terrane) are generally only weakly magnetic. The exact lithology of the source is unknown; the magnetic high has no corresponding gravity high so the source rock is of similar density to the exposed Franciscan mélange, sedimentary, and metasedimentary rocks. The shape of the anomaly suggests a steeply south-dipping, WNW trending tabular or lens shaped body about 10 km long.

Although in general sedimentary rocks do not produce pronounced aeromagnetic anomalies, the Miocene Neroly Formation and uppermost part of the Cierbo Sandstone are prominent exceptions. A study of the magnetic properties of these clastic rocks shows that the source of the magnetization in these rocks is detrital magnetite related to andesitic grains that are the dominant clast composition (Hillhouse and Jachens, 2005). Surface exposure of those units coincides with the northernmost, west-northwest-trending, 20-km-long, curvilinear magnetic high along the southwest flank of Mount Diablo ("n" in Figure 4). More subtle curvilinear anomalies west of the Calaveras Fault and east of Livermore Valley are also present over outcrops of Neroly Formation.

The gravity and magnetic model across the Stockton quadrangle (Figure 11) also suggests that the Neroly Formation may not be the only sedimentary unit that is magnetic. The magnetic high that strikes across the northeast margin of the Livermore basin cannot be solely sourced from the Neroly Formation unless there is significant duplication of the sequence that is not evident from the map relations at the surface. A plausible source may be the lower part of the undivided Green Valley and Tassajara Formations (unit PMgv). Although we do not have direct measurements of the magnetic properties of this unit, lithofacies analysis indicates that the lower part of the unit consists of reworked sand and gravel as well as well-lithified clasts from the Neroly Formation (Isaacson and Anderson, 1992). Thus, this unit could be as magnetic as the Neroly Formation and is modeled as a significant source of the magnetic high along the northeast margin of the basin (Figure 11).

The most prominent magnetic feature in the Stockton quadrangle is present over the eastern



part of the San Joaquin Valley, the source of which is not exposed. It is part of the Great Valley magnetic high that extends the length of the Central Valley (Cady, 1975; Jachens and others, 1995). Because the Great Valley magnetic high is in most places accompanied by gravity highs, the source of the anomalies has been attributed to ophiolite, either related to the Coast Ranges ophiolite (Cady, 1975; Jachens and others, 1995) or to ophiolitic rocks in the Sierran Foothills (Oliver and Hanna, 1970; Cady, 1972). Seismic tomography (Thurber and others, 2009) shows velocities of 7 km/s beneath much of the Great Valley, consistent with an ophiolitic source. However, the magnetic high over the Stockton Arch (area south of the Stockton Fault in Figure 4) does not correspond to an equivalent gravity high, indicating that the basement is more heterogeneous than uniformly dense ophiolite; this observation is furthermore supported by the presence of metavolcanic rocks and granite in two wells within the magnetic high near its southwest margin (07720478 and 09900026, respectively, in Figure 4). The magnetic anomaly is asymmetric, indicating a steep northeast edge. The southwest edge of the magnetic source dips more shallowly to the southwest (Figure 11) and probably does not coincide everywhere with the top of basement, supported by the presence of green tuff in drillhole 07720145. A bench in the magnetic gradient in the hanging wall of the north part of the Vernalis Fault, roughly in the same place as the saddle in the western San Joaquin Valley gravity low (L1 in Figure 3) mentioned above, suggests that magnetic basement is shallower in this region.

Not all magnetic anomalies are caused by geologic sources. Manmade features, such as oil and gas fields, landfills, and radio facilities, can produce very localized, sometimes high-amplitude anomalies. Anomalies known to coincide with such features are labeled as “a” in Figure 4. In addition, an east-west set of smaller-amplitude anomalies coincides with the Mokelumne aqueduct, where the pipeline lies on the ground surface. Very short-wavelength, low-amplitude anomalies over the city of Stockton are also due to urbanization (“a” in Figure 4).

## STRUCTURE

Detailed mapping of bedrock exposures in the Diablo Range, combined with deep borehole and seismic survey data from the San Joaquin Valley and Delta provide small windows into structural remnants of the early subduction margin, and a more detailed picture of the late Neogene deformation that accompanied transition to the dextral strike-slip tectonism that persists today. Additional findings from recent geophysical surveys in the quadrangle are incorporated into the structural descriptions and history described below.

### Mesozoic and Early Cenozoic Structure

The Stockton quadrangle includes the tectonic suture between the Franciscan Complex (generally to the west and below) and the Great Valley complex (generally to the east and above). Recognition of the overlapping age of these complexes and their very different origins led to the conclusion that the contact between accreted Franciscan rocks and those of the Great Valley complex on the overriding North American plate must be everywhere faulted. This tectonic boundary between the basement complexes was initially conceived as an east-dipping convergent suture zone referred to as the Coast Range thrust, along which the Franciscan accretionary wedge had been thrust eastward beneath the CRO and overlying GVS (Bailey and others, 1964, 1970). Jayko and others (1987) pointed out a variety of observed conditions that this simplified contractional model failed to satisfactorily explain, most notably the dramatic step in metamorphic grade across the fault. The high-pressure blueschist-facies terranes of the Franciscan Complex must have been metamorphosed during subduction deep within the lithosphere at depths on the order of 10 to 30 km, while the Coast Range ophiolite formed at much shallower crustal levels

experiencing metamorphic pressures corresponding to no greater than greenschist facies (Platt, 1986), and the overlying GVS remained unmetamorphosed. The juxtaposition of such incongruent metamorphic grades requires extensive exhumation of Franciscan rocks, which implies a normal sense of movement through attenuation rather than contractional thrust faulting (Jayko and others, 1987). Furthermore, in many places blueschist facies Franciscan rocks are separated from GVS sedimentary rocks by only a thin band of serpentinite above the Great Valley thrust, implying significant thinning of the hanging wall (Harms and others, 1992). Based on these observations and new interpretations, the name for the boundary between the two basement complexes was revised from Coast Range thrust to Coast Range fault (Jayko and others, 1987; Harms and others, 1992) to refer universally to all fault segments that constitute the tectonic contact between Franciscan rocks and those of the overriding ancestral North American plate, except where those rocks have been juxtaposed along younger faults such as the Neogene strike-slip faults of the San Andreas Fault System. Wakabayashi (1999) summarized a variety of early models put forth to explain observed metamorphic discrepancies across the Coast Range fault and mechanisms for exhumation of the high-grade Franciscan rocks. With the accumulation of additional data, models suggested to explain the structural relationship between the basement units continue to evolve and, not surprisingly, vary to fit with differing conditions found laterally along the ancestral plate boundary (Mitchell and others, 2010).

In the Stockton quadrangle, surface exposures of the contact between the Franciscan and Great Valley basement complexes are predominantly younger, steeply dipping faults that on close examination appear inconsistent with what would be expected for Coast Range fault segments that define the Late Cretaceous-early Tertiary paleo-subduction zone. For example, the Tesla-Ortogonal system of faults in the southern portion of the quadrangle (Figure 12) uplift the Franciscan Complex relative to the rocks to the east, suggestive of the Coast Range fault. However, exposures in the vicinity of Del Puerto Canyon just to the south of the Stockton quadrangle reveal high-angle Neogene segments of the Tesla-Ortogonal Fault truncating the older low-angle Coast Range fault (Raymond, 1973b). The best exposures of the Coast Range fault in the Stockton quadrangle are found near the summit of Mt. Diablo, where a band of pervasively sheared serpentinite along the fault separates Franciscan *mélange* from structurally overlying ophiolite and sedimentary rocks of the Great Valley complex. Consistent with the model of the Coast Range fault as an attenuational structure, Unruh and others (2007) interpret stratigraphic and structural relations around Mt. Diablo as evidence for upper crustal extension and graben formation in the ancestral Great Valley forearc basin synchronous with exhumation of deeply subducted Franciscan metamorphic rocks. Based on fission-track and detrital zircon age data from Franciscan metagraywacke, they inferred that these rocks were metamorphosed at a depth of roughly 20 km and began an episodic rise to the surface beginning sometime later than approximately 108 Ma (mid-Cretaceous time), with the final 3 to 4 km of exhumation occurring during the Pliocene to Holocene growth and erosion of Mt. Diablo.

Although not exposed at the surface, the map area also includes the boundary between the Great Valley complex and the Sierran Foothills basement complex beneath the Late Cretaceous and younger deposits of the San Joaquin Valley. The nature of this contact is not well understood, and even its location is not well constrained. Deep exploratory wells penetrate Sierran basement in the eastern part of the Stockton quadrangle (see discussion later in pamphlet), but no wells are deep enough to reach basement in the western part. Our preferred model for the origin of the Coast Range ophiolite suggests that the ophiolite formed by rifting of older oceanic crust in the forearc of an ocean island arc, and that the coeval arc volcanic rocks are now part of the Sierran Foothills basement complex. As such, the boundary would be the eastern side of the Jurassic forearc rift. On the other hand, there has been a long history of deformation since then, and the boundary may be significantly modified. For example, Wright and Wyld (2007) proposed that a strike-slip fault with several hundreds of kilometers of Late Jurassic to

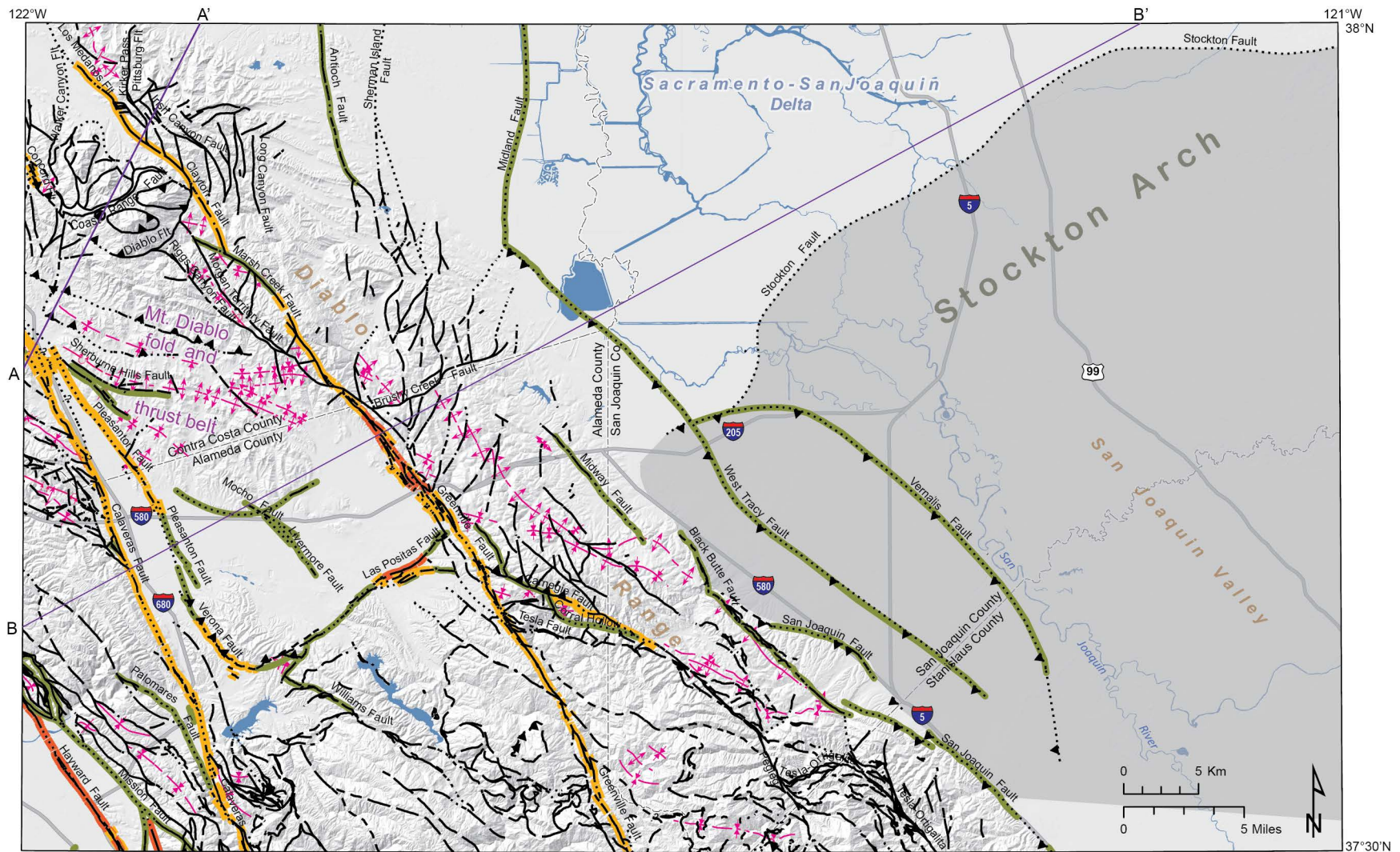


**Figure 12.** Simplified fault activity map of the map area (modified from Jennings and Bryant, 2010; Unruh and Krug, 2007). Fault traces are shown in black, dashed where approximately located, dotted where concealed by overlying sediments. Fold axes are shown in magenta. Quaternary faults are highlighted by age of most recent recognized displacement: red for historic (last 200 years); orange of Holocene (11,700 years), and green for Quaternary (2.6 Ma). Purple line A-A' shows location of geologic cross section in Figure 14, and B-B' the location of geologic cross section and geophysical model in Figure 11.

Early Cretaceous offset separates the Great Valley from Sierran Foothills basement, whereas Hall (1991) proposed a major Late Cretaceous thrust fault. Such modification could explain why the latest Jurassic and Early Cretaceous part of the GVS is only seen in areas underlain by Coast Range ophiolite and not found on Sierran Foothills basement.

As previously discussed, the ancestral forearc basin appears to have experienced north-south deformation during the latest Mesozoic and Paleogene, as implied by formation of the Stockton arch, a transverse structural high located between Stockton and Modesto that grew to divide the Great Valley forearc into the Sacramento basin on the north and San Joaquin basin to the south (Bartow and Nilsen, 1990). Paleogene and uppermost Cretaceous strata have been truncated by erosion on the arch, suggesting the structure was a low-relief positive feature through most of the Paleogene (Bartow, 1991). The northern side of the Stockton arch is bounded by the south-dipping Stockton Fault (Figure 6), while the southern flank is more poorly defined. The Stockton Fault appears to have a complex history extending back to the Late Cretaceous (Imperato, 1992), including ~500 m down-to-the-south normal and ~6 km left-lateral offset in Late Cretaceous time (Harwood and Helley, 1987), followed by down-to-the-north reverse-slip displacement of up to 1,100 meters, most of which occurred during the Oligocene and into the Miocene (Bartow, 1991). The Stockton Fault dies out to the east of the map area and is not seen in the Sierran Foothills basement or overlying GVS strata, although the Stockton Arch may be reflected by the southward pinch out of GVS strata there. Unruh and Hitchcock (2015) suggest a similar pattern of Paleogene north-south compression truncated on the east by the West Tracy Fault in the area around Altamont Pass and west of Clifton Court Forebay. They suggest that this deformation indicates an early period of activity on the West Tracy Fault, but it is also possible to achieve the relations they observe with later right-lateral reverse oblique offset (see below).

Also, in Late Cretaceous and Paleogene time, the area north of the Stockton Arch experienced extension that was oriented approximately east-west, which led to the formation of a graben system roughly bounded on the east by the Midland Fault and on the west by the Los Medanos-Clayton-Marsh Creek Fault system (Krug and others, 1992). The thickened Late Cretaceous and Paleogene section deposited in the structural trough is in part exposed on the northeast flank of Mount Diablo where the strata have been uplifted and tilted northeast by subsequent compressive deformation. Unruh and others (2007) relate the Paleogene extension to the attenuation at the Coast Range fault and associated uplift and unroofing of the Franciscan Complex. There is, however, no evidence that the Franciscan Complex rocks were entirely unroofed to the surface in the map area during the Paleogene (such as Franciscan clasts in Paleogene strata), although that did happen elsewhere (e.g. Berkland, 1973).

## Late Cenozoic Structure

The northward migration of the Mendocino triple junction through central California during the late Cenozoic marked the change from a convergent margin to a transform margin. Late Neogene and Quaternary (post-12 Ma in the East Bay) movement between the Pacific and North American tectonic plates has been largely accommodated by shearing distributed across the San Andreas Fault System, a complex system of northwest-trending, dextral strike-slip faults. In the Stockton quadrangle, the most prominent strike-slip faults of the San Andreas system are the Holocene-active Hayward, Calaveras, and Greenville Faults (Figure 12), all of which have generated historic earthquakes and/or display active creep. For example, a segment of the Greenville Fault was responsible for the January 1980 Livermore earthquake sequence (ML <5.8), which produced discontinuous right-lateral surface rupture from near the Alameda—Contra Costa county line southeastward to near I-580 (Sawyer and Unruh, 2012). Associated left-lateral displacement along the Las Positas Fault was also observed following the 1980 quake (Bonilla and others, 1980). The Hayward Fault generated a M6.8 earthquake in 1868, known as the “Great San

Francisco Earthquake” until eclipsed by the 1906 quake, with fault rupture from Oakland through the southwest corner of the map area and as far south as the Alameda/Santa Clara county line (Radbruch, 1967; Ellsworth, 1990). The northern Calaveras Fault generated a M5.6 earthquake near San Ramon in 1861 (Topozada and others, 1981).

Total right-lateral displacement on the strike-slip faults that transect the map area is about 175 km since 12 Ma (Jones and Curtis, 1991; McLaughlin and others, 1996). Graymer and others (2002) assign right-lateral slip of about 100 km on the Hayward, 10 km on the northern Calaveras (although Walker and Graymer (2003) suggest less than 5 km offset based on lack of offset of magnetic anomalies associated with the Neroly Formation, see below), and 15 km on the Greenville Fault, with the remaining 50 km assigned to the Palomares Fault which lacks evidence of Holocene offset. As discussed below, the continuity of a gravity high extending southeast from Mt. Diablo (H2 in Figure 3) suggests that long-term slip on the Greenville Fault passed west of Mount Diablo and onto the Concord Fault at the western margin of the map area.

GPS and paleoseismic data suggest that present-day right-lateral slip in the map area is concentrated on the northern Calaveras and Hayward Faults, with much less slip on the Greenville Fault (Dawson and Weldon, 2013; Parsons and others, 2013). The bulk of northern Calaveras slip continues onto the Concord Fault through a right step near the west edge of the map area southwest of Mount Diablo (Figure 13), although some slip also continues onto the Franklin Fault and related structures up to the West Napa Fault northwest of the map area. The right step connection between the northern Calaveras and Concord faults must be a very recent development because there is little right-lateral offset of Neogene and older strata on the southwest flank of Mount Diablo (Figure 13), and because there is no geomorphic evidence of the extensional deformation expected within a right step in a right-lateral fault zone.

Plate motion along the transform boundary has resulted in a predominantly transpressional regime in the northern Diablo Range characterized by the maximum horizontal stress axis oriented northeast-southwest. In addition to strike-slip, this stress field results in differential movements among the strike-slip faults that locally generate thrust faulting, folding, and related transpressional structures (Unruh and Lettis, 1998). The youngest folding must postdate the Pliocene and Pleistocene deposition of the Livermore gravels, as those strata are locally folded. Still younger late Pleistocene strata have been tilted and uplifted, reflecting the active tectonic forces affecting the region. Transpressional deformation mapped in the Stockton quadrangle can generally be divided into three structural domains separated by the major strike-slip faults. In the East Bay hills, contractional fault and fold features between the Hayward and Calaveras Faults are mostly oriented west-northwest, oblique to the more north-northwest trending strike-slip faults, and exhibit a right-stepping, en echelon geometry typical of a dextral shear setting (Unruh and Lettis, 1998). However, the fold axes are oriented more north-northwest near the bounding faults, and the bounding faults display a component of reverse slip, which suggests a component of fault-normal compression in addition to fault-parallel shear. A similar style prevails in the central core of the northern Diablo Range between the Calaveras and Greenville Faults, where a series of west-northwest striking contractional faults and associated folds have been mapped around Mt. Diablo and southward into the Livermore Valley. Compression there is enhanced by a component of fault-parallel compression related to the restraining left step between the Greenville and Concord Faults. Informally referred to as the Mt. Diablo fold-and-thrust belt, Unruh and Sawyer (1995) proposed the driving force for these contractional features to be solely the transfer of dextral shear across the restraining left stepover, but the compressional deformation extends well south of the stepover, so there must also be a component from regional fault-normal compression and/or dextral shear. Rising above this structural domain is the edifice of Mt. Diablo proper, formed by an asymmetric, doubly plunging, faulted anticline in the hanging

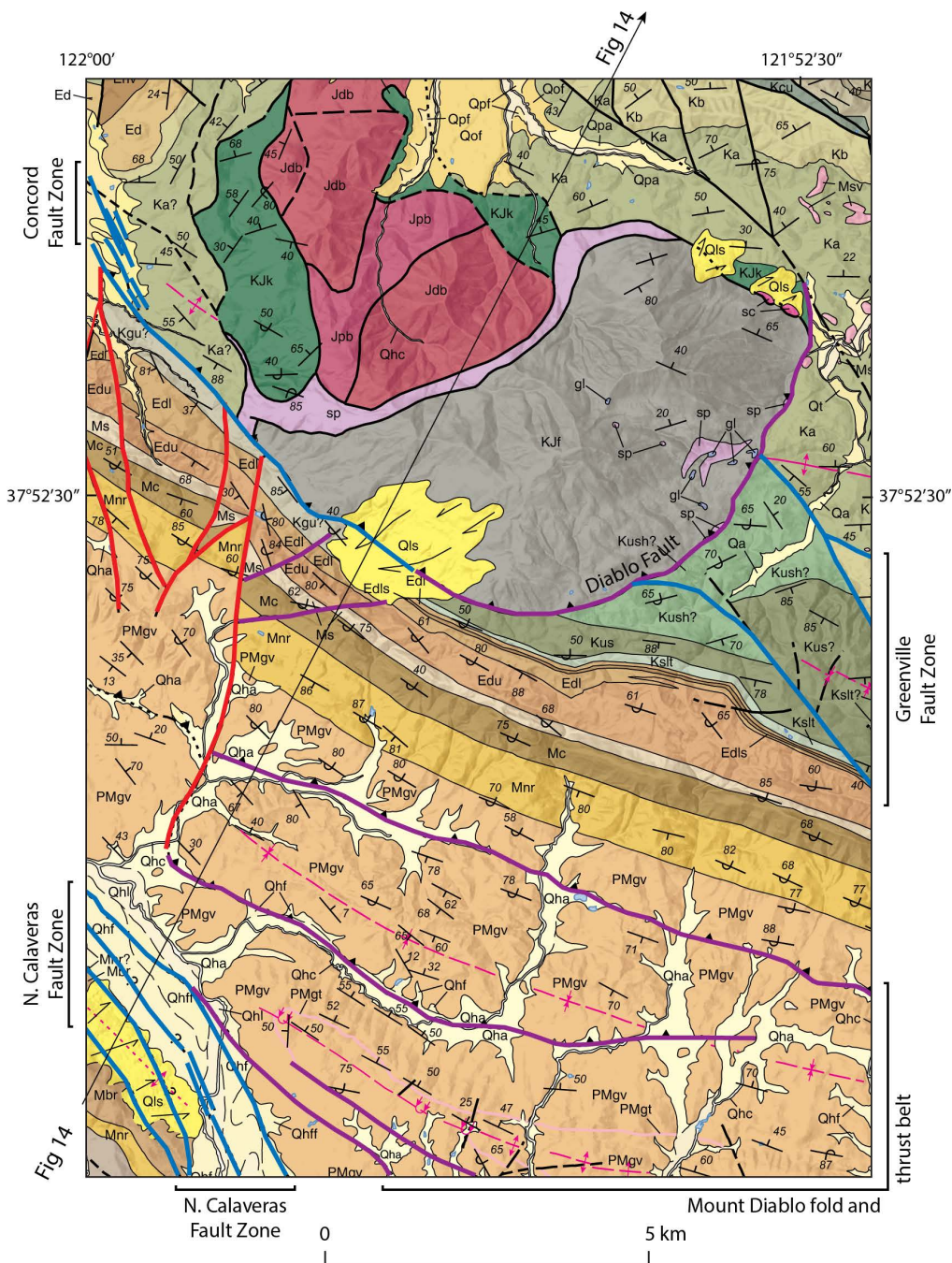


**Figure 13.** Detail of the geologic map at Mount Diablo illustrating the right releasing stepover between the Northern Calaveras and Concord faults and the left restraining stepover between the Greenville and Concord faults. Northern Calaveras-Concord connector faults are highlighted in red (some lie west of the map area), the small offset and multiple disconnected strands reflect the ongoing development of the connection. The Greenville-Concord stepover incorporates transpressional deformation in the Mount Diablo fold and thrust belt as well as right-lateral slip on northwestward extensions of Greenville Fault Zone strands under the basement flap in the hanging wall of the Diablo Fault, as shown in Figure 14 (section line shown as thin black line, extends northeast beyond detail area). Predominantly strike-slip faults are highlighted in blue, predominantly thrust/reverse faults of the fold and thrust belt and the Diablo Fault are highlighted in purple.

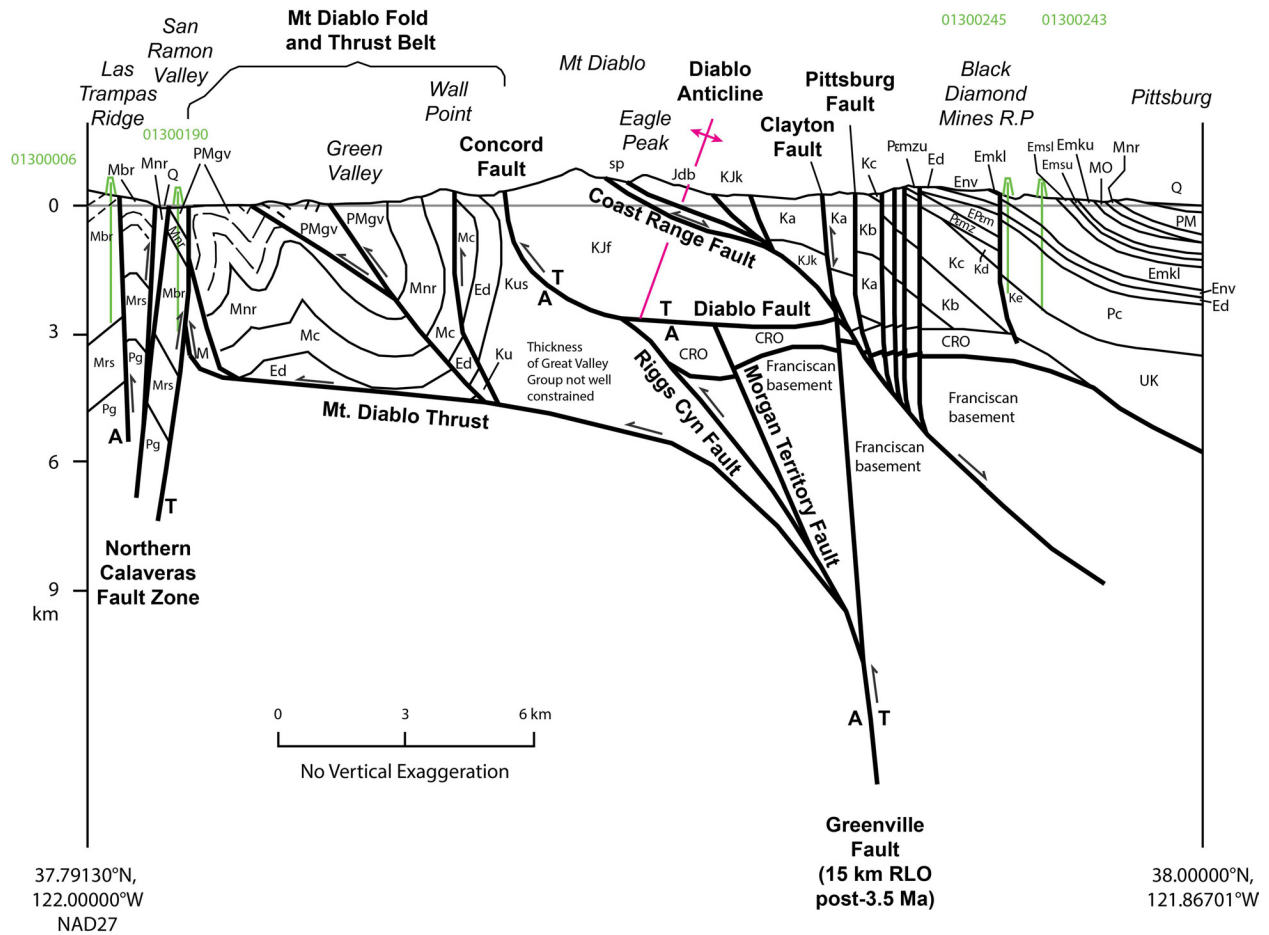


**Figure 14.** Cross section for the northwest part of the map area through Mount Diablo, showing the relation of the Diablo fold and thrust belt and Diablo Anticline to the regional strike-slip faults (Northern Calaveras, Greenville, and Concord). Units as shown on map, except some generalized units where too thin to show at scale or where subdivision is uncertain (PM-Pliocene and Miocene; Mrs-Rodeo to Sobrante (Miocene); M-Miocene; MO-Miocene and Oligocene; Pc=Paleocene; Pg=Paleogene; UK-Upper Cretaceous); CRO-Coast Range ophiolite. Green symbols indicate well data projected into the line of the cross section, labeled with API number. Note the 15 km out of plane right-lateral offset (RLO; A=away; T=toward) on the Greenville-Concord faults.

wall of the northeast-dipping Greenville-Concord and connecting stepover faults. Like earlier workers, Unruh and others (2007) included the structural domains both east and west of the Greenville Fault in the anticline, and based on the asymmetry of the folds and analysis of a seismic reflection profile southwest of the fault, they interpreted the Mount Diablo anticline to be a fault-propagation fold above a northeast dipping blind thrust fault termed the Mount Diablo thrust fault. However, their analysis does not account for the significant post 3.5 Ma right-lateral offset of 15 km on the Greenville-Concord Faults. Their analysis was based on retrodeformation of Pliocene and older strata on either side of the mountain, but strata correlative to those northeast of Mount Diablo are actually now located northwest of the map area near Martinez, not those southwest of Mount Diablo that were used. Given the large strike-slip offset, it seems more likely that the thrust fault imaged in the seismic reflection profile southwest of the Greenville Fault does not project under the mountain to the subsurface of the San Joaquin Valley, but instead roots into or is truncated by the steeply dipping Greenville-Concord faults (Figure 14). The configuration of

thrust faults rooting back into steeply dipping mostly strike slip faults is reflected in the sandbox models of restraining stepovers of McClay and Bonora (2001). Deformation of late Neogene strata in the fold and thrust belt point to Mount Diablo being a relatively young geomorphic feature, with most of its rise above the surrounding landscape taking place since about 4 Ma. More recent studies by Sawyer (2015) support the restraining stepover model for development of the fold-and-thrust belt and suggest the Mt. Diablo blind thrust fault has the highest slip rate of any contractional structure in the San Francisco Bay area and thus presents a significant seismic hazard to the region.

East of the Greenville Fault, the style of deformation is more complex, including older compressional and extensional faults reactivated and deformed by late Cenozoic transpressional deformation. In the broad sense, Late Cenozoic deformation was expressed by uplift of the northern Diablo Range, together with broad warping of the San Joaquin basin into an asymmetrical fold so that the ancestral forearc basin deposits of the GVS and younger strata are now prominently exposed along the eastern range front as a northeast-dipping homocline (Bartow, 1991). In the northern part of the map area, the homocline itself has been warped, resulting in a more westerly strike overall, as well as a pair of broad shallowly dipping roughly north trending folds in the Neogene strata. The Neogene strata there are also slightly offset in an apparent right-lateral sense by several roughly north-south trending faults including the Kirker Pass–Pittsburg, Antioch, and Sherman Island Faults. These faults are part of the upturned Late Cretaceous and early Cenozoic extensional regime west of the Midland Fault described above, so offset of Neogene strata shows that either extensional slip continued in a modest way into the early Pliocene, or that these faults were reactivated in Neogene time to accommodate some dextral shear. The Kirker Pass–Pittsburg Fault runs into the Clayton Fault north of Mount Diablo, but other north-trending faults are truncated north of Altamont Pass by the ENE-trending Brushy Creek Fault. This fault exhibits apparent left-lateral offset in the Cretaceous strata (which could be related to the Stockton Fault, as mentioned above).

South of the Brushy Creek Fault, late Miocene strata, which are deposited unconformably on Late Cretaceous GVS strata, are folded in a suite of roughly east-west trending broad synclines and anticlines, bounded on the south by the north-dipping panel above the Tesla Fault. The axes of the southern syncline/anticline pair change to a southeast trend east of Corral Hollow. These fold axes truncate against the Black Butte Fault such that only the southernmost northeast dipping limb remains, extending southward to become the broad northeast dipping homocline mentioned above. These folds are cut and slightly offset by numerous north to northwest trending, steeply dipping reverse faults, along with some northwest trending folds. The reverse faults root southward into the Carnegie and Corral Hollow Faults, steeply dipping WNW trending oblique right-lateral reverse faults that extend from the Greenville Fault on the west to the Pegleg Fault on the east.

All these structures are bounded on the east by the northwest-striking faults that exhibit evidence for both strike-slip and reverse separation of late Neogene and Quaternary strata (Unruh and Krug, 2007), including the Midway and Black Butte faults, and, farther east in the San Joaquin Valley, the West Tracy, Vernalis, and San Joaquin faults. As previously noted, some of these may be relatively old features that have been reactivated to accommodate late Cenozoic transpressional deformation (Unruh and Hitchcock, 2015), but may also be Neogene right-lateral oblique faults. About 10 km late Cenozoic right-lateral offset on the West Tracy Fault accounts for the apparent offset from the southern pinchout of Paleogene strata northwest of Clifton Court Forebay to the southern margin of Paleogene strata in the subsurface north of the Stockton Arch and roughly aligns the Stockton Fault with the Brushy Creek Fault. These right-lateral reverse oblique faults may have the potential to generate significant earthquakes (Unruh and Hitchcock, 2015). Although mostly concealed by young surficial deposits, the location and Quaternary activity of these faults is reflected in subtle geomorphic changes locally or, in the case of the San Joaquin thrust fault,



more pronounced expression as the physiographic divide between the San Joaquin Valley and Diablo Range (Unruh and Hitchcock, 2015). The compressive (and possibly right-lateral) deformation appears to extend northward onto the Midland Fault, reactivating the older normal fault north of the intersection with the West Tracy Fault (Unruh and Hitchcock, 2009).

## **GEOPHYSICAL EXPRESSION OF STRUCTURES**

The potential-field anomalies can provide additional insight into the continuity and geometry of faults in the Stockton quadrangle. Gradients in these fields indicate where the faults juxtapose rocks of different density or magnetic properties with significant horizontal or vertical offset and the location of the maximum horizontal gradient (slope) with respect to the fault can provide information on the fault dip. On the other hand, continuity of anomalies across faults preclude significant offset. Below we describe some of the geophysical features and their relation to structures in the quadrangle.

### **Gravity Anomalies**

Some of the most prominent gravity gradients in the quadrangle mark the east side of the Diablo Range. In the southern part of the quadrangle, the gradient approximately follows the fault contact of Mesozoic basement with structurally overlying Cretaceous and younger rocks. Here the Tesla-Ortogonalita fault coincides with the northeast margin of the Diablo Range gravity high (H3 in figure 3) as defined by this gradient. The southern extent of the San Joaquin fault in the quadrangle is roughly parallel to this gradient but located some 4-5 km to the northeast, consistent with a southwest dip, perhaps rooting into structures associated with the Tesla-Ortogonalita fault. This steep gradient wraps to the west around the north end of the main part of the Diablo Range, and extends west-southwest as far as the Calaveras Fault. Where the steep gradient bends west, a lesser gradient marking the southeast margin of gravity H2 (Figure 3) continues NNW about 12 km to the vicinity of Mountain House, roughly marking the right-lateral reverse oblique faults east of Altamont Pass (Black Butte, Midway, West Tracy). The location of the gradient parallel to but southwest of the trace of the West Tracy fault is consistent with a southwest fault dip. The gradient continues north-northwest along the valley margin for another 15 km, gaining amplitude between the Rio Vista Basin low (L1 north in Figure 3) and the high associated with the Diablo Anticline (H2 in Figure 3, see below). The maximum slope (density boundary) of this gradient bifurcates near its intersection with the Midland Fault, with one steep inflection that continues nearly parallel to the strike of the Cretaceous sequence, and the other trending more northerly, roughly parallel to north-striking faults, including the Sherman Island Fault, that offset the Neogene and older section. The more westerly steep inflection bends to the north along the Antioch Fault near Brentwood, and both bend to the west to follow the strike of the Paleogene and younger section near Antioch. The absence of a gradient along the Midland fault suggests little appreciable offset of the basement.

The continuity of the gravity high (H1 and H2) from Mount Diablo southeast to the area around Altamont Pass reflects that significant long-term right-lateral slip on the Greenville Fault must continue northwestward onto the Concord Fault (rather than onto the Clayton Fault) or else there would be an observable offset in the gravity high. Restoration of the proposed ~15 km post-3.5 Ma offset aligns the CRO and Franciscan basement exposed at Mount Diablo with CRO and minor Franciscan basement, as well as gravity and magnetic highs, now north of the map area near Benicia. The Benicia area also includes relatively thick Eocene strata (Domengine through Markley) overlying Late Cretaceous strata, like that in the northwest corner of the map area, northeast of the Concord Fault, consistent with the proposed offset.

Other prominent gradients marking the pronounced gravity low of the Livermore basin (L2

in Figure 3) provide information on basin and fault structure. The position of the pronounced gravity gradient along the southwest margin of the low L2 with respect to the Calaveras Fault indicates a near-vertical dip of the Calaveras perhaps with a steep dip to the southwest near the western edge of the quadrangle, whereas the southeast, northeast and northwest basin margins, as defined by steep gravity gradients, have a less obvious relationship to mapped faults. The Las Positas Fault marks the southeast margin of the valley and is a northeast-striking reverse fault (Herd, 1977a). The southeastern margin of the sedimentary basin based on gravity gradients, however, only locally coincides with the mapped trace of the Las Positas Fault and lies as much as 6 km to the southeast of the fault trace. The Las Positas Fault lies well within the surface outcrops of Neogene deposits and thus does not mark a large density contrast, at least at the surface. This suggests that the southeast basin margin consists of more than one fault and could be interpreted as the result of structural superposition as has been documented in other Miocene basins nearby in the Santa Clara Valley to the west of the Stockton quadrangle (Graymer and others, 2015).

The northeast margin of the Livermore basin is similarly complex. Although the Greenville Fault is an important strike-slip fault within the San Andreas system with significant right-lateral displacement (15-20 km; Graymer and others, 2002), the fault is not associated with major density boundaries, except for the roughly 15-km-long stretch east of the city of Livermore. Here the fault is modeled as the steep northeast-dipping boundary of the Livermore basin (Figure 11). Along that stretch, there are two sets of density boundaries, one along or slightly to the northeast of the Greenville Fault and the other parallel but 2-3 km southwest of the fault. The northern termination of the set of density boundaries along the Greenville Fault also coincides with the northern end of the aftershock sequence of the 1980 Livermore earthquake (Ellsworth and Marks, 1980), roughly where the Greenville Fault splits up into the multiple faults of the restraining step to the Concord Fault and joins with the Marsh Creek Fault. The latter set of density boundaries may be related to the velocity contrast imaged by seismic refraction data, interpreted as an ancestral Greenville Fault by Meltzer and others (1987), presumed to have been active during the Pliocene by Sweeney (1982). Using the density boundaries as a guide, this structure appears to deviate from the strike of the mapped Greenville Fault at the latitude of drillhole 01320089, changing to a more westerly strike that is parallel to fold axes and thrust faults mapped south of Mt. Diablo. The more westerly density boundary may be related to an ancestral Greenville Fault, but there is no evidence of Miocene or younger strike slip in the mapped geology there. Alternatively, the orientation of the density boundary is parallel to the fold and thrust structures mapped on the southwest flank of Mt Diablo, suggesting the density boundary could be related to east-side uplift on one of those structures (Figure 11). Other gradients to the south between gravity high H1 and gravity low L2 coincide locally with Quaternary-active faults, suggesting locally steeper fault dips in the fold and thrust belt.

## **Magnetic Anomalies**

Magnetic gradients outline the extent of Coast Range ophiolite in the quadrangle, providing information on the dip of the Coast Range fault and offset along the Greenville Fault. The magnetic gradients that coincide with the southeast edge of the magnetic high at Mt. Diablo are slightly offset to the northwest, indicative of a steep northwest dip for the Coast Range Fault. Along the southern margin of the Stockton quadrangle, a prominent anomaly associated with serpentinite and gabbro of the Coast Range ophiolite at Cedar Mountain is truncated by the Greenville Fault. The correlation of this ophiolite body and its associated magnetic anomaly with a similar ophiolite and anomaly on the other side of the fault at Red Mountain south of the quadrangle provides an estimate of 9 km of right-lateral displacement (Sweeney, 1982). This estimate was revised to  $15 \pm 2$  km by Graymer and others (2002), which accounts for offset across all the strands of the Greenville Fault. Further supporting this estimate of 15 km are offset

magnetic anomalies associated with the Neroly Sandstone.

The magnetic anomalies associated with the Neroly Sandstone are valuable for delineating structure, both exposed and concealed. The long, curvilinear magnetic anomalies associated with the Neroly south of Mt. Diablo (“n” and “ne” anomalies in Figure 4) reflect duplication and folding of the Cenozoic sequence in the Mt. Diablo fold and thrust belt. The continuity of the anomalies beyond the exposures of the Neroly and Cierbo rocks allows one to map their concealed extents. Examples of anomalies interpreted to result from concealed Neroly (“ne” in Figure 4) are those south of the west-northwest-striking exposures of Neroly south of Mount Diablo, which appear to be truncated and smeared along the Greenville Fault, and the short-wavelength anomaly that hugs the western margin of the San Joaquin Valley. Note that horizontal magnetic layers do not produce magnetic anomalies unless they are truncated. One can estimate the approximate dip of a tabular layer, such as a stratigraphic unit, by examining the asymmetry of the magnetic anomaly that has been reduced to the pole (Langenheim and others, 2012). For the anomaly along the western margin of the San Joaquin Valley, the asymmetry of the anomaly indicates a low to moderate dip to the northeast.

In other places, the continuity of these Neroly anomalies places constraints on the amount of post-Miocene offset. One short wavelength anomaly associated with Neroly Sandstone near San Ramon, and possibly another near Dublin, is significant because it is bisected but not appreciably offset by the presently active strands of the Northern Calaveras Fault, suggesting that the fault has little long-term offset (Walker and Graymer, 2003). Continuity of the magnetic anomaly across the southern extent of the Midland Fault also suggests little long-term offset whereas a small jog in the anomaly at the Sherman Island fault suggests some apparent right-lateral offset (Graymer and Langenheim, in press).

Lastly, the continuity of the magnetic high in the northeast part of the map across the Stockton Fault argues for little left-lateral offset across the fault, in contrast to ~6 km proposed by Harwood and Helley (1987). Certainly, the geologic relations along the eastern projection of the fault into the Sierra Foothills geology do not support a large amount of left-lateral or vertical offset.

## DESCRIPTION OF MAP UNITS

The arrangement of the Abbreviated Explanation on the map plate is designed as a simplified correlation of map units to illustrate the variation in stratigraphic sequences and unit names between assemblages in different structural blocks and areas of the map. The descriptions of map units below generally progress from youngest to oldest, but are organized similarly to the map explanation, with divisions between Quaternary surficial deposits, intrusive rocks, deformed bedrock assemblages, and basement rocks. Based on differences in the style of mapping among source maps, as well as the sources of sediment, surficial units are subdivided between those mapped west of the San Joaquin River/Delta and those to the east. In the case of bedrock units, the description of a given unit may differ substantially among the assemblages. Lithologic variations limited to a specific assemblage(s) are noted in the unit descriptions. Because of the many differences in nomenclature associated with the Great Valley sequence, unit descriptions are grouped by stratigraphic assemblages (II, V, VI North, VI South, VII, VIII, IX, X, and XI). Map labels are abbreviations that indicate the age and origin of surficial deposits, or age and name of bedrock units. Where unit assignment is tentative, a query (?) is added to the label.

### Quaternary Surficial Deposits

Descriptions of surficial deposits are modified from Witter and others (2006), Knudsen and others (2000), and Knudsen and Lettis (1997) for units mapped west of the San Joaquin River and Delta, and from Knudsen and Lettis (1997) for units to the east. Where informal subunits are represented by subscripted numbers, numbers increase with increasing age (i.e., of subunits 1-4, 1 is the youngest and 4 is the oldest).

- af**        **Artificial fill (historical)**—Undifferentiated constructed deposit of various materials and ages. Locally includes some dredge spoils, levee fill, and fill over Bay mud, as well as road embankments, earthen dams, and railroad grades. Mapping of this unit is largely based on topographic expression on the most recent USGS 7.5' quadrangles of the area.
- afbm**     **Artificial fill placed over bay mud (historical)**—Artificial fill placed in the estuarine environment to create new land. May be engineered and/or non-engineered.
- alf**        **Artificial levee fill (historical)**—Man-made deposit of various materials and ages, forming artificial levees as much as 6.5 meters in height. Some are compacted and quite firm, but most fills made before 1965 consist simply of dumped materials. Levees bordering waterways of the Sacramento/San Joaquin Delta, mudflats, and large streams were first emplaced as much as 150 years ago.
- ads**        **Artificial fill, dredge spoils (historical)**—Fill located adjacent to channels dredged for navigation.
- ac**        **Artificial stream channel (historical)**—Modified stream channels including straightened channels, flood control channels, and concrete canals. Deposits in artificial channels range from concrete in lined channels to sand and gravel similar to natural stream channel deposits (Qhc).
- gq**        **Gravel quarries and percolation ponds (historical)**—Excavations, spoil piles, and disturbed ground in areas being used for the extraction of sand and gravel.
- Qhc**        **Stream channel deposits (late Holocene to modern <150 years)**—Loose sand, gravel, and cobbles with minor clay and silt deposited within active, natural stream channels.

- Qhay **Alluvial deposits, undivided (latest Holocene, <1,000 years)**—Loose sand, gravel, silt, and clay deposited in active depositional environments and judged to be less than 1000 years old based on geomorphic expression or historic records of inundation by sediment-bearing waters.
- Qhty **Stream terrace deposits (latest Holocene, <1,000 years)**—Stream deposits found on terraces above the present stream level, judged to be latest Holocene (<1,000 years) in age based on records of historical inundation, the identification of youthful meander scars and braid bars on aerial photographs and/or geomorphic position (elevation) very close to the stream channel. Consists of moderately to well-sorted and moderately to well bedded sand, gravel, silt, and minor clay deposited in point bar and overbank settings.
- Qhfy **Alluvial fan deposits (latest Holocene, <1,000 years)**—Alluvial fan sediment judged to be latest Holocene (<1,000 years) in age based on records of historical inundation or the presence of youthful braid bars and distributary channels. Consist of loose sediments, mostly lacking cohesion, deposited by streams emanating from mountain canyons onto alluvial valley floors or alluvial plains. Typically mapped where the stream channel is incised into older fan deposits near the fan apex, then gradually is less incised down-fan, until the stream becomes unconfined and distributes young sediment across the toe of the fan.
- Qhly **Alluvial fan levee deposits (latest Holocene, <1,000 years)**—Natural levee deposits of alluvial fans judged to be latest Holocene (<1,000 years) in age based on records of historical inundation. Identified as long, low, sinuous ridges oriented down-fan, levee deposits are typically composed of overbank material coarser than adjoining interlevee areas.
- Qhfp **Alluvial floodplain deposits, undivided (late Holocene)**—This unit lies along the San Joaquin River and within the Delta. Most, if not all of this area has been inundated historically during large floods. Part of this area was historically covered with tidal-wetland peat but has since been exhumed and is now protected by levees and farmed (Atwater, 1982). These deposits are younger than, and lap onto, the Antioch-Oakley dune field, which may be coeval with the upper member of the late Pleistocene Modesto Formation (Atwater, 1982). This unit includes abandoned oxbows, channels and interdistributary basins, flood basins and basin rims, distal alluvial fans, and low natural levees adjacent to the San Joaquin River.
- Qhdm **Delta mud (late Holocene)**—Sediment deposited at or near sea level in the Sacramento-San Joaquin Delta that is presently or was once tidal marsh. Delta peat and mud typically have low bulk density and include silt, clay, and peat with minor sand (Atwater, 1982). This unit generally occupies historical lowlands (tidal wetlands and waterways) that are now dry because of the construction of dikes and levees. Also included within this unit are small areas of artificial fill too small to differentiate at map scale.
- Qhb **Basin deposit (late Holocene)**—Sediment of late Holocene age deposited in topographic lows, at the distal margin of alluvial fans, and between floodplain and bay/Delta mud deposits, predominantly clay and silty clay. These areas have a high-water table and are subject to flooding. This sediment is finer grained than fan sediment or floodplain deposits because clays and silts settle out of standing water collected in these basins or areas of very slow-moving water.
- Qhbm **Bay mud (Holocene)**—Estuarine silt, clay, peat, and fine sand deposited at, or near sea level in the San Francisco Bay estuary. Limited to a small area at the southwest corner of the map area.

- Qha**      **Alluvium, undivided (Holocene)**—Alluvium deposited on fans, terraces, or in basins. Sand, gravel, and silt that are poorly to moderately sorted. Mapped where separate types of alluvial deposits are not delineated.
- Qht**      **Stream terrace deposits (Holocene)**—Moderately well-sorted sand, silt, gravel, and minor clay deposited in point bar and overbank settings. These deposits are as much as 10 meters above the historic flood plain, but mostly undissected by later erosion. Along the Stanislaus River and upstream San Joaquin River, Holocene terrace deposits include meander scars and abandoned oxbows that may have filled with finer sediment than is typical of terrace deposits. Holocene terrace deposits along the lower San Joaquin River are finer grained than those mapped elsewhere in the study area. Locally, subdivided based on topographic positions and inferred age:
- Qht1**      **Unit 1**—Lowest/youngest
- Qht2**      **Unit 2**—Higher/older
- Qhf**      **Alluvial fan deposits (Holocene)**—Alluvial fan sediment deposited by streams emanating from the mountains as debris flows, hyper-concentrated mudflows, or braided stream flows. Sediments include sand, gravel, silt and clay, that are moderately to poorly sorted, and moderately to poorly bedded. Locally subdivided by geomorphic relationships and inferred age:
- Qhf1**      **Unit 1**—Youngest
- Qhf2**      **Unit 2**
- Qhf3**      **Unit 3**—Older
- Qhff**      **Alluvial fan, fine-grained facies (Holocene)**—Fine-grained sand, silt, and clay deposited mostly as overbank deposits on alluvial fan surfaces between fan levees and at the distal part of fan deposits.
- Qhl**      **Fan levee deposits (Holocene)**—Natural levees formed on alluvial fans where streams overtop their banks and deposit sediment adjacent to the channel; typically identified by their topographic expression of long, low ridges oriented down fan. The deposits contain coarser material than the adjoining interlevee areas.
- Qa**      **Alluvium, undivided (latest Pleistocene to Holocene)**—Undivided alluvium consisting of flat, relatively undissected fan, terrace, basin deposits, and small active streams.
- Qds**      **Dune sand (latest Pleistocene to Holocene)**—Very well-sorted fine- to medium-grained eolian sand. In addition to the Antioch-Oakley (Brentwood) dune field, there are dunes over much of the area east of the San Joaquin River south of Stockton, including a dune field around Manteca and large deposits in the southeast corner of the map area.
- Qf**      **Alluvial fan deposits (latest Pleistocene to Holocene)**—Sand, gravel, silt, and clay mapped on gently sloping, fan-shaped, relatively undissected alluvial surfaces. Moderately to poorly sorted, and poorly to moderately bedded.
- Qt**      **Stream terrace deposits (latest Pleistocene to Holocene)**—Sand, gravel, silt, minor clay on relatively flat surfaces above the present stream level. Moderately to well sorted, and moderately to well bedded.
- Qls**      **Landslide deposits (Pleistocene to Holocene)**—Chaotic deposits of sand, silt, clay, boulders, and blocks of bedrock. In general, only larger landslides depicted on earlier geologic maps have been included in this compilation. Accordingly, this map does not present a thorough

or uniform presentation of the distribution of landslides and is not representative of landslide hazards in the map area.

- Qpf**      **Alluvial fan deposits (latest Pleistocene)**—Sand, gravel, silt, and clay that is moderately to poorly sorted and bedded. Similar to Holocene fans (Qhf), but they are more dissected and generally topographically higher. Locally subdivided by subtle topographic variations into:
- Qpf1**      **Unit 1**—Youngest/lowest
- Qpf2**      **Unit 2**
- Qpf3**      **Unit 3**
- Qpf4**      **Unit 4**—Older/higher
- Qpt**      **Stream terrace deposits (latest Pleistocene)**—Includes sand, gravel, silt, with minor clay, and is moderately to well sorted, and moderately to well bedded. Typically deposited in point bar and overbank settings, since elevated above the creek bottom by incision of the streambed.
- Qpa**      **Alluvium, undifferentiated (latest Pleistocene)**—Intercalated sand, silt, and gravel that are poorly to moderately sorted. Mapped on gently sloping to level alluvial fan or terrace surfaces where latest Pleistocene age is indicated by depth of stream incision, development of alfisols, and lack of historical flooding.
- Qoa**      **Old alluvial deposits, undivided (early to late Pleistocene)**—Alluvial fan, stream terrace, basin, and channel deposits. Topography is gently rolling, with little or no original alluvial surfaces preserved; moderately to deeply dissected. Locally subdivided based on geomorphic position and soil development into:
- Qoa1**      **Unit 1**—Youngest
- Qoa2**      **Unit 2**—Older
- Qof**      **Old alluvial fan deposits (early to late Pleistocene)**—Sand, gravel, silt, and clay, deeply dissected. Topography is moderately rolling with little or no original alluvial surfaces preserved.
- Qot**      **Old stream terrace deposits (early to late Pleistocene)**—Moderately to deeply dissected alluvial terrace deposits capped by alfisols, ultisols, or soils containing a silicic or calcic hardpan. Terrace sediment includes sand, gravel, and silt, with minor clay, and is moderately to well sorted, and moderately to well bedded. Terrace sediment typically was deposited in point bar and overbank settings and has since been elevated above the creek bottom by incision of the streambed. This unit differs from Qoa in that some terrace surface morphology is preserved.
- Qop**      **Old pediment deposits (early to late Pleistocene)**—Alluvial deposits that veneer broad, planar erosional surfaces cut on bedrock or older sediment along the eastern margin of the Diablo Range. These pediments typically occur tens to hundreds of meters above the present stream channel and are extremely dissected. Soils formed on these deposits are typically well developed and include alfisols and ultisols. Locally subdivided based on geomorphic position, soil development, and estimated age into:
- Qop1**      **Unit 1**—Youngest
- Qop2**      **Unit 2**
- Qop3**      **Unit 3**—Older

- Qm Modesto Formation, undivided (late Pleistocene)**—Alluvium derived either from the interior of the Sierra Nevada along major west-flowing streams (commonly arkosic material), or contemporaneously, locally from small foothill watersheds (commonly from andesitic or metamorphic source material), deposited in fan, interdistributary area, and basin settings. Modesto Formation alluvium occurs in a wide band east of the San Joaquin River and west of the Riverbank Formation and older fan remnants. Marchand and Harden (1978) and Marchand and Allwardt (1981) distinguished numerous subunits based on geomorphic relationships, soil development, and/or composition, which have been simplified for this compilation into the following:
- Qmu Modesto Formation, upper member, undivided alluvium (late Pleistocene)**—Alluvium associated with lower (younger) terraces and younger fans. Moderate to slight erosional modification and soil profile development differentiate it from older deposits. Soils formed on these deposits are typically Hanford, Oakdale and Tujunga series.
- Qmub Modesto Formation, upper member, fine-grained (late Pleistocene)**—Commonly stratified alluvium of flood basins, lower fans and interdistributary fan areas. Soils formed on these deposits are typically Dinuba, Landlow and Stockton series.
- Qml Modesto Formation, lower member, undivided alluvium (late Pleistocene)**—Arkosic alluvium derived either from the interior of the Sierra Nevada or andesitic and metamorphic material derived from the lower foothills, associated with terraces slightly above (older) than the highest level associated with the upper member. Soils formed on these deposits are typically Greenfield and Chualar series.
- Qmlb Modesto Formation, lower member, fine-grained (late Pleistocene)**—Commonly stratified alluvium of very low gradient flood basins, lower fans and interdistributary fan areas. Groundwater typically occurs near the surface. Soil hardpans and “hog-wallow microrelief” also are typical of these deposits. The microrelief is expressed on early 20th century topographic maps as irregularly spaced and shaped closed-depressions. It is possible the soil development and topographic criteria used to define this unit are a function of topographic position, or “subtle differences in soil drainage or in soil parent material due to contrasts in depositional environment” (Marchand and Harden, 1978), rather than deposit age.
- Qr Riverbank Formation (late to middle Pleistocene)**—Of Marchand and Harden (1978) and Marchand and Allwardt (1981). Arkosic alluvium, derived both from the interior of the Sierra Nevada (probably glacial outwash) and contemporaneously from foothill watersheds. Riverbank Formation terraces and fans truncate Turlock Lake alluvium or fill post-Turlock Lake gullies and ravines, and, in turn, are cut and filled by terraces and fans of the Modesto Formation. As such, Riverbank alluvium is identified by its relative degree of erosional modification, by superpositional relationships, and by the relative degree of soil profile development. Soils formed on these deposits are typically Montpelier, Peters, and Redding series.
- Qtl Turlock Lake Formation (middle Pleistocene)**—Alluvium derived from the interior of the Sierra Nevada, and contemporaneously, from foothill watersheds. The highly dissected nature of the Turlock Lake geomorphic surfaces distinguishes it from younger deposits. Turlock Lake deposits stand topographically above younger fans and terraces near the northeastern margin of the map area.



## Tertiary and Mesozoic Intrusive Rocks

Descriptions are from Graymer and others (1994a and 1996).

- Msv**      **Silicic volcanic rocks (Miocene or younger)**—Rhyolite to andesite porphyry stocks, dikes, and sills. Crops out around Marsh Creek Springs east of Mount Diablo and very small outcrops east of Alameda Creek south of Sunol. Rhyolite from this unit east of Mount Diablo has yielded a biotite Ar/Ar age of about 7.5 Ma (Ryan Fay, written commun.).
- Tr**        **Rhyolite dikes (Tertiary?)**—Small lenses of resistant, light gray, quartz and feldspar porphyry rhyolite. Intrudes Early Cretaceous (Hall, 1958) Great Valley sequence strata on Pleasanton Ridge north of Sunol. Uncertain age based on intrusive relation and similarity to unit Msv (Graymer and others, 1994b).
- KJqd**     **Quartz diorite stock (Jurassic or younger)**—Coarse-grained, crystalline-granular quartz diorite. Feldspars are more or less altered. Outcrop is limited to one small stock (several hundred meters in diameter) near Cedar Mountain in the Diablo Range.

## Early Quaternary, Tertiary, and Mesozoic Stratigraphic Units

Descriptions of units modified from Graymer and others (1994a and 1996), Raymond (1969 and 1973a), Throckmorton (1988), and Bartow and others (1985).

- QP<sub>i</sub>**      **Irvington Gravels of Savage (1951) (Pleistocene and Pliocene?)**—Mapped within Assemblage VII. Poorly to well consolidated, distinctly bedded pebbles and cobbles, gray pebbly sand, and gray, coarse-grained, cross-bedded sand. Cobbles and pebbles are well- to sub-rounded, as much as 25 cm in diameter, and consist of about 60 percent micaceous sandstone, 35 percent metamorphic and volcanic rocks and chert probably derived from the Franciscan Complex, and 5 percent black laminated chert and cherty shale derived from the Claremont Shale. A large suite of early Pleistocene vertebrate fossils from this unit was described by Savage (1951).
- QP<sub>i</sub>**      **Livermore gravels (Pleistocene and Pliocene)**—Mapped within Assemblages II, V, VII, and VIII. Poorly to moderately consolidated, indistinctly bedded, cobble conglomerate, gray conglomeratic sandstone, and gray coarse-grained sandstone. Also includes some siltstone and claystone. Clasts contain mostly graywacke, chert, and metamorphic rocks probably derived from the Franciscan Complex. This unit is similar to the Irvington Gravels, but lacks clasts derived from the Claremont Shale. Differentiated from the underlying nonmarine units by color and clast composition (Barlock, 1989). The basal contact is locally unconformable and locally gradational.
- QP<sub>u</sub>**     **Unnamed sandstone, siltstone, and gravel (early Pleistocene and late Pliocene)**—Mapped within Assemblage VI North. Semi-consolidated to unconsolidated poorly sorted gravel, sand, silt and clay. Modestly erosion resistant, forms minor topographic highs above younger fan deposits (Q<sub>pf</sub> and Q<sub>hf</sub>).
- P<sub>b</sub>**        **Basaltic rocks (Pliocene)**—Generally flat lying remnants of basalt flow rock. Crops out mostly over Markley Sandstone east of Concord, but also in two very small (not shown due to scale) patches overlying Neroly Sandstone and Pliocene Lawlor Tuff southwest of Pittsburg (Graymer and Langenheim, in press). Generally flat orientation suggests deposition after tilting of the Pliocene Tehama Formation. Topographic position above and greater dissection by erosion suggest that this unit is older than unit QP<sub>u</sub>.

- Pl** **Laguna Formation (Pliocene)**—Pebble to cobble conglomerate, arkosic sandstone, and siltstone mapped in the low foothills near the northeastern edge of the Stockton quadrangle. Includes some andesitic detritus reworked from the underlying Mehrten Formation in the lower part. Lithologically similar to younger alluvial deposits (**Qr** and **Qtl**), thus usually distinguished by its relative topographic position and soil development. Soils formed on these deposits are typically Redding series, with a well-cemented “duripan” pedogenic horizon developed on pediment surfaces.
- Pth** **Tehama Formation (Pliocene)**—Mapped within Assemblage VI North. Poorly consolidated, gray to maroon, nonmarine siltstone, quartz arenite sandstone, tuff, and pebble to cobble conglomerate. Probably laterally equivalent to the upper part of the Carbona Formation (**PMc**). Includes a tuff bed correlated with the ~4.7 Ma tuff of Napa (Sarna-Wojcicki and others, 2011). Constrained to Pliocene age by stratigraphic position above the Lawlor Tuff.
- Plt** **Lawlor Tuff (Pliocene)**—Mapped within Assemblage VI North. Nonmarine, pumiceous, andesitic ash-flow tuff produced by Plinian eruptions and ash flows derived from the Sonoma Volcanics northwest of the map area. Ar/Ar age of  $4.83 \pm 0.04$  Ma (Sarna-Wojcicki and others, 2011).
- Plp** **Unnamed freshwater limestone (Pliocene(?))**—Mapped within Assemblage VIII, one small body south of San Antonio Reservoir, underlain by Briones Sandstone and bounded by fault above.
- PMss** **Unnamed sandstone (Pliocene and/or late Miocene)**—Mapped within Assemblage VIII. Distinctly to indistinctly bedded, poorly consolidated, white, fine-grained sandstone and siltstone, interbedded with diatomite, gray diatomaceous chert, and tan, freshwater limestone. Limited to two small mapped bodies west of Arroyo Laguna northeast of Sunol.
- PMm** **Mehrten Formation (early Pliocene to Miocene)**—Includes brown, pale reddish-brown tan, white, and grayish-pink andesitic sandstone, pinkish-gray and gray or pale yellowish-brown siltstone, waterlain tuff and conglomerate. Volcanic mudflow deposits interbedded with sandstone and conglomerate. Mapped in the northeast corner of the quadrangle where exposed on eroded slopes beneath younger alluvial deposits. Clasts are compositionally distinct, dominated by andesite. Lahar beds laden with andesite cobbles are particularly resistant and often form a cap and corresponding cliff faces.
- PMgv** **Green Valley and Tassajara Formations of Conduit (1938), undivided (Pliocene and Miocene)**—Mapped within Assemblage V. Non-marine sandstone, siltstone, and conglomerate. The lower part of the unit has been informally referred to by some as the Sycamore formation (Isaacson and Andersen, 1992) and joint geophysical and geological modeling shows that this unit is responsible in part for magnetic highs along the southwest margin of Mt. Diablo (Graymer and Langenheim, in press). Structural complexity, poor exposure, and lithologic similarity prevents the confident mapping of the Green Valley and Tassajara units separately across the map area. This unit also includes the unit mapped as Lower Livermore Gravel by Barlock (1989) and as unit Tps by Dibblee (1980a; 1981b) south of Livermore Valley. We incorporate those units based on similar nonmarine fossils and lithology, as well as the presence of Lawlor and Huichica tuff in both (Sarna-Wojcicki and others, 2011). The age of the base of the unit is about 9.7 Ma, based on magnetostratigraphy and mammal fossils (Prothero and Tedford, 2000). The lower part of this unit is correlative with the unnamed unit Mus west of the Calaveras Fault, based on similar age, stratigraphic position, lithology, and the presence of at least some of the same tuff layers, although the base of that unit is slightly older. Tuff in this unit is correlated with the  $4.834 \pm 0.011$  Ma Lawlor

- Tuff and the informally named  $4.76 \pm 0.05$  Ma Huichica tuff (Sarna-Wojcicki and others, 2011), while a tuff layer lower in the unit has been correlated with the Roblar tuff in Sonoma County (Sarna-Wojcicki, 1976) which has Ar/Ar age  $6.26 \pm 0.03$  Ma (Wagner and others, 2011). Also includes, mapped locally where thick enough to be visible at map scale:
- PMgt**      **Tuff marker bed**—North of Livermore Valley approximately 5 meters thick, correlated with the Pinole Tuff that has a K/Ar age of  $5.2 \pm 0.1$  Ma (Sarna-Wojcicki, 1976). South of Livermore Valley the marker bed is a composite of two tuffs separated by roughly 8 meters of tuffaceous sandstone, the lower 3 m thick tuff correlated with the Lawlor Tuff and the upper 3 m thick tuff correlated with the Huichica tuff (Sarna-Wojcicki, 1976; Sarna-Wojcicki and others, 2011).
- PMc**      **Carbona Formation of Pelletier (1951) (early Pliocene(?) to late Miocene)**—Mapped within Assemblage VI South and XI. Predominantly poorly to moderately consolidated and moderately well-bedded conglomerate, sandstone, and siltstone. Locally includes lacustrine clay, silt, diatomite, and freshwater limestone. The unit is folded concordantly with the underlying bedrock series and unconformably overlain by Pleistocene alluvium. Franciscan-dominated clasts indicate central Diablo Range origins and lithologies suggest deposition in alluvial fan and floodplain settings along the eastern flanks of the range. A confusing variety of unit designations have been applied to these and similar strata along the west side of the San Joaquin Valley. Anderson and Pack (1915) originally mapped these rocks as part of the Tulare Formation. In work west of Tracy, Pelletier (1951) found late Miocene vertebrate fossils near the locally conformable contact with the underlying Neroly Formation and recognized the structural discordance with younger deposits. His mapping distinguished these older strata from the Tulare Formation and assigned them the name Carbona Formation. Raymond (1969) followed Pelletier in use of the name Carbona Formation for his mapping in the Tracy and Lone Tree Creek 7.5' quadrangles. Lettis (1982) described a late Miocene or early Pliocene(?) diatom assemblage found near the top of the Carbona Formation in the Tracy 7.5' quadrangle. Dibblee (1981) mapped the same strata as “unnamed nonmarine sedimentary rocks.” Bartow and others (1985) referred to the unit as “unnamed fanglomerate”, while Throckmorton (1988) described exposures in the Midway and Tracy 7.5' quadrangles as an upper, finer-grained member of the Neroly Formation. Briggs (1953) considered Pelletier's Carbona Formation correlative with strata in the Laguna Seca Hills to the south that he named the Oro Loma Formation. Graymer and others (1994a) followed Briggs, as did some updated versions of Dibblee's mapping (Dibblee and Minch, 2006d, 2006e) that revised his “unnamed nonmarine sedimentary rocks” to Oro Loma Formation. Similarities in age, lithology, and structure suggest the strata mapped as Carbona Formation by Pelletier and Raymond are at least in part equivalent to strata of the Oro Loma Formation to the south, and perhaps portions of the Tehama Formation mapped north of the Stockton Arch. However, because of variations in sediment provenance, uncertain ranges in age, and gaps in distribution of these strata along the range, the more locally applied name Carbona Formation is used for this compilation. South of Lone Tree Creek, a finer grained sequence within the formation is distinguished:
- PMcl**      **Lower member**—Greenish-gray claystone, sandstone, and pebble conglomerate.
- Mus**      **Unnamed sedimentary and volcanic rocks (late Miocene)**—Mapped within Assemblage II. Marine and nonmarine conglomerate, sandstone, and siltstone. Outside the map area to the west, includes basalt. Just west of the map area in Bolinger Canyon, includes a mammal fossil fauna about 10 million years old near the base of the unit (Edwards, 1982). This unit is

correlative with the lower part of unit PMgt to the east, though the base of this unit may be a bit older. In Assemblage II, includes:

- Musl**        **Limestone**—One very small lens west of San Ramon Village.
- Mv**        **Unnamed volcanic rocks (late Miocene)**—Mapped within Assemblage VII north of Alameda Creek. White to gray rhyolite, dacite, and andesite tuff, breccia, and volcanoclastic conglomerate, and massive, black and red, plagioclase, pyroxene, and olivine porphyry basalt. Three samples from this unit yielded Ar/Ar ages of 10.913±0.012, 10.478±0.053, and 10.86±0.11 Ma (Fay and Fleck, 2014; recalculated with current decay constants, R. Fleck, USGS, written commun.). Possibly correlative with late Miocene Moraga Basalt (also overlies Orinda Formation) in the Berkeley Hills, west of the map area, though Ar/Ar dates from this unit are older. Possibly correlative with late Miocene Quien Sabe-Northbrae-Burdell Mountain volcanics of the same age (Ford, 2007), which are distributed by fault offset both northwest and south of the map area (Jones and Curtis, 1991; Murphy and others, 2002), although those have a different stratigraphic association.
- Mor**        **Orinda Formation (late Miocene)**—Mapped within Assemblage VII. Nonmarine pebble to boulder conglomerate, conglomeratic sandstone, coarse- to medium-grained lithic sandstone, and minor siltstone. Conglomerate clasts predominantly from Franciscan Complex, include red, green, and black chert, quartzite, greenstone, diorite, lithic sandstone, and minor andesite. No fossils are known from the map area, age based on stratigraphic position above the Briones Sandstone, and age of interbedded and overlying volcanics. Correlated with the Orinda Formation of similar age and lithology in the Berkeley Hills, west of the map area. Mapped locally, the formation contains:
- Morv**        **Interlayered plagioclase porphyry dacite**—One very small lens near Warm Springs west of Mission Peak.
- Mnr**        **Neroly Formation (late Miocene)**—Mapped within Assemblages II, V, VI North, VI South, X, and XI. Blue to blue-gray, fine to coarse-grained, volcanic-rich, shallow marine sandstone, with minor siltstone, shale, tuff and andesite-pebble conglomerate. The abundant volcanic clasts make this unit a source of magnetic anomalies (Hillhouse and Jachens, 2005). In Assemblage VI North, contains tuffs with K/Ar ages of about 9.7 Ma (Black Diamond Park Tuff) and 10-12 Ma (Alves Tuff) (Graymer and others, 1994a). Locally mapped separately, includes:
- Mns**        **Upper shale member**—Siltstone and shale at the top of the unit in Assemblage VI North.
- Mnu**        **Upper sandstone member**—Light-gray quartz-lithic sandstone in Assemblage II. Erroneously mapped as Cierbo Sandstone overlying Neroly Formation by Graymer and others (1994a).
- Mnc**        **Upper conglomerate and sandstone member**—Green, glauconite-bearing, pebble conglomerate layers and overlying sandstone within Assemblage X. Conglomerate includes clasts up to 5 cm diameter of chert and siliceous shale.
- Mc**        **Cierbo Sandstone (late Miocene)**—Mapped within Assemblages V, VI North, VI South, and XI. Light-gray, light-blue, and white, massive to thick-bedded, fine- to coarse-grained, moderately consolidated, quartzitic, marine sandstone with minor lithic and biotite grains. Locally, the unit contains beds of highly fossiliferous, coarse-grained sandstone, minor pebble conglomerate, siltstone, and tuff. In Assemblages VI North and VI South in the Altamont Pass area, the fossils are predominantly of the genus *Ostrea*.

- Mbr**      **Briones Sandstone (Miocene)**—Mapped within Assemblages II, VII, VIII, IX, and X. Distinctly to indistinctly bedded, gray and white, fine- to coarse-grained, shallow marine quartz-lithic sandstone and shell breccia. Pebble and cobble conglomerate lenses are present in a few places. Conglomerate clasts include black and red chert, quartzite, andesite, argillite, siltstone, basalt, felsic tuff, and quartz. Shell breccia beds form erosion resistant ridges and peaks. This unit unconformably overlies Franciscan greenstone (KJfg) and mélange (KJfm) in the east part of Assemblage X. In Assemblage II, this unit includes a tuffaceous layer with a K/Ar age of  $14.5 \pm 0.4$  Ma (Lindquist and Morganthaler, 1991), and is divided locally after Wagner (1978) into:
- Mbri**      **I member**—Massive feldspathic sandstone.
- Mbrg**      **G member**—Massive sandstone, pebble conglomerate, and shell breccia.
- Mbre**      **E member**—Medium-grained sandstone with abundant shell breccia beds.
- Mbrd**      **D member**—Massive, medium-grained sandstone with local conglomerate layers.
- Mr**      **Rodeo Shale (middle Miocene)**—Mapped within Assemblage II. Brown and brownish gray marine siliceous shale, calcareous shale, and silty to sandy shale with yellow carbonate concretions.
- Mt**      **Tice Shale (late or middle Miocene)**—Mapped within Assemblages II, VII, VIII, and IX. Distinctly bedded, dark brown, gray, and tan marine sandy siltstone, siltstone, mudstone, siliceous shale, porcellanite and chert. In Assemblage VII, the shale contains numerous fish scales and poorly preserved foraminifers in places, also bright orange weathering lenses of tan dolomite locally.
- Mo**      **Oursan Sandstone (late or middle Miocene)**—Mapped within Assemblages II, VII, VIII, and IX, with considerable lithologic variations between Assemblages. The unit mostly consists of indistinctly bedded, fine- to medium-grained, olive marine sandstone, with lesser siltstone and claystone. In Assemblage II, the sandstone includes calcareous concretions. In Assemblage IX, pebble and shell fragment conglomerate is present near the base. In Assemblage VII, the unit occupies the same stratigraphic position as the type Oursan Sandstone in Contra Costa County, but differs from the type in color, presence of dolomite lenses, and absence of invertebrate fossils. There it is described as distinctly bedded black mudstone, foraminifer-bearing, brown to tan siltstone, and fine-grained sandstone with large (as much as 2 meters long) lenses of bright orange weathering, tan dolomite, similar to those found in the overlying Tice Shale in Assemblage VII.
- Mro**      **Rodeo Shale, Hambre Sandstone, Tice Shale, and Oursan Sandstone, undivided (middle Miocene)**—Mapped within Assemblage II.
- Mcs**      **Claremont Shale (middle Miocene)**—Mapped within Assemblages II, VII, and IX. Brown siliceous marine shale with yellow carbonate concretions and interbedded gray to black, laminated chert. Some of the shale contains poorly preserved fish scales and foraminifers. Bright orange weathering lenses of tan dolomite, light colored, calcareous sandstone, and 0.3- to 2-meter-thick beds of limestone occur locally. The unit is distinguished from the overlying Tice Shale by the presence of chert beds and lack of non-siliceous mudstone. Mapped locally in Assemblages II and VII, includes:
- Mcss**      **Interbeds of light brown, gray and white, fine-grained quartz sandstone and siltstone**

- Ms**        **Sobrante Sandstone (middle and/or early Miocene)**—Mapped within Assemblages II, V, and VII. Massive, white, fine- to medium-grained calcareous, quartz sandstone, marine. In Assemblage V, previously mapped as part of the Cierbo Sandstone (Graymer and others, 1994a) and in part as Monterey Formation (Dibblee and Minch, 2005), but includes early to middle Miocene (Temblor stage) invertebrate fossils (Stewart, 1949).
- Mtem**      **Temblor Sandstone (middle and/or early Miocene)**—Mapped within Assemblage IX. Thickly and indistinctly bedded, olive, fine- to coarse-grained marine sandstone and pebble conglomerate. Vertebrate and invertebrate fossils are common in many parts of this unit, including a very large collection from the Calaveras Dam site on Alameda Creek just south of the map area. Unconformably lies on the Franciscan mélange.
- Msh**        **Unnamed shale, sandstone, chert and dolomite (early Miocene)**—Mapped within Assemblage VII. Massive, orange weathering, marine medium-grained quartz sandstone, interbedded, laminated gray chert and dolomite, dark gray, concretionary siltstone and mudstone, and conglomerate. Conglomerate contains pebbles of varicolored chert, andesite, and quartzite in a dolomite matrix.
- MOvs**      **Valley Springs Formation (early Miocene and late Oligocene)**—Mapped within Assemblage VI South. Yellowish-gray and tan fluvial and paludal clayey sandstone, sandy tuffaceous claystone, and light-gray vitric tuff. Locally shows crude irregular bedding. Correlation with the type locality in the Sierra Foothills is based on similar lithology, equivalent stratigraphic position, and trace- and minor-element chemistry of the glass in vitric tuff interbeds, reinforced by its subsurface occurrence throughout much of the northern San Joaquin Valley; base is unconformable (Bartow and others, 1985).
- Kirker Tuff (Oligocene)**—Mapped within Assemblage VI North.
- Okt**        **Tuff member**—Pumiceous, white rhyolite tuff with minor tuffaceous sandstone. Ar/Ar age of  $29.197 \pm 0.065$  Ma (Sullivan and others, in press).
- Oks**        **Light-gray marine tuffaceous sandstone, conglomerate and siltstone**
- Emk**        **Markley Formation (late? and middle Eocene)**—Mapped within Assemblage VI North. Marine and estuarine sandstone and shale, predominantly white-weathering brown and light gray quartz-muscovite arkose and mostly brown carbonaceous shale. Locally, divided into:
- Emku**        **Upper member**—Thin-bedded micaceous sandstone, siltstone, and claystone.  
              **Sidney Flat Shale Member**—Divided into:
- Emsu**        **Upper part**—Black shale with minor siltstone and sandstone.
- Emsl**        **Lower part**—Interbedded shale and sandstone.
- Emkl**        **Lower member**—Thin-bedded to massive, gray, medium to coarse grained micaceous sandstone with minor siltstone and mudstone. Sandstone in many places includes large (0.5 cm across) flakes of white mica. Locally, includes:
- Emlu**        **Upper siltstone bed**
- Emll**        **Lower siltstone bed**
- Env**        **Nortonville Shale (middle and early? Eocene)**—Mapped within Assemblage VI North. Brown to grayish-green marine mudstone and claystone with minor siltstone and sandstone.

- Ed Domengine Formation (middle? and early Eocene)**—Mapped within Assemblages V and VI North. White marine quartz sandstone and light-brown siltstone. Locally includes conglomerate and thin beds of gray shale. Divided into:
- Edu Upper member**—Massive, pebbly, white sandstone.
- Edl Lower member**—Gray shale and minor sandstone. Distinguished locally in Assemblage V, includes:
- Edls Sandstone marker bed**—Fine-grained, white, quartz sandstone.
- Ets Tolman Formation of Hall (1958) (Eocene?)**—Mapped within Assemblage VII, one small lens east of the Chabot Fault north of Niles. Gray, algal limestone interbedded with carbonate-matrix pebble conglomerate and medium-to coarse-grained arkose with carbonate cement. Dark gray to dark greenish-gray, indistinctly bedded, glauconite bearing, medium-to coarse-grained lithic sandstone, locally interbedded with minor amounts of fine-grained sandstone and siltstone. The Tolman Formation is bounded above by a fault and overlies Redwood Creek Formation sandstone and Pinehurst shale along an obscured contact, shown on the map as a fault to avoid implying a depositional relationship without evidence.
- EFt Tesla Formation (middle Eocene to Paleocene)**—Mapped within Assemblages VI South and XI. Interbedded white and buff, arkosic, quartzose sandstone, siltstone, brown mudstone, and carbonaceous shale, with minor pebble conglomerate and lignite. Brackish and shallow marine faunas occur in the sandstones and siltstones. Originally described by Huey (1948), Throckmorton (1988) distinguished an informal upper sandstone member in the Corral Hollow area:
- Etu Upper sandstone member (late? Eocene to late early Eocene)**—Predominantly fine- to medium-grained, brown, gray, and white sandstone containing shallow-marine faunas. Throckmorton (1988) states that mollusks indicate a late early Eocene through early middle Eocene age for most of the member, but that uppermost part may possibly be as young as late Eocene.
- Meganos Formation (Eocene and Paleocene)**—Mapped within Assemblage VI North. Divided into:
- Eme Upper member (Eocene)**—Greenish-gray to light gray, biotite-rich siltstone and silty mudstone, with abundant plant debris in places. Division E of Meganos Formation of Clark (1921). Lateral equivalent to the unit identified as Capay Formation in the subsurface to the north and east based on stratigraphic position, fossils, and lithology (Stewart, 1949).
- Emd Sandstone member (Eocene)**—Medium-grained, light gray to bluish-gray sandstone with carbonaceous laminations; pebble conglomerate present locally at base. Division D of Meganos Formation of Clark (1921). Lateral equivalent to the unit identified as (Margaret) Hamilton sand in the subsurface to the north and east based on stratigraphic position and lithology (Stewart, 1949).
- Emc Shale member (Eocene)**—Bluish-gray shale with sandstone interbeds. Division C of Meganos Formation of Clark (1921). In part equivalent to Meganos (paleo-submarine) Canyon fill (Fischer, 1984; Almgren, 1984). Locally includes:
- Emcs Sandstone interbeds**

- EP<sub>1</sub>ma**      **Lower member (Eocene and(or) Paleocene?)**—Sandstone with basal conglomerate. Medium- to coarse-grained, clean, white, distinctly cross bedded, biotite bearing arkosic sandstone. Equivalent to Divisions A and B of Meganos Formation of Clark (1921). Equivalent to the Meganos (paleo-submarine) fan facies of Fischer (1984). Almgren (1984) and McDougall and Block (2014) interpret this unit as Eocene, although McDougall and Block don't include age-diagnostic foraminifera for this unit in their report. On the other hand, Fischer (1984) interprets this unit as Paleocene, though also without citing specific fossil evidence. Given that the overlying member Emc is late early Eocene (Penutian benthic foraminiferal stage), there would be an unconformity between that member and this member if this member is Paleocene, which does not fit for the depositional history proposed for the Meganos Formation. It seems likely, but not proven, that this member is early early Eocene (Bulitian benthic foraminiferal stage).
- EP<sub>2</sub>mz**      **Unnamed sandstone and shale (Paleocene)**—Mapped within Assemblage VI North. Originally mapped as Martinez Formation (Brabb and others, 1971), that name was abandoned by Graymer and others (1994) because the rocks in the map area are distinct from those exposed at Martinez. Marine sandstone, siltstone, and shale. Locally, divided into:
- EP<sub>2</sub>mzu**      **Upper member**—Siltstone and shale.
- EP<sub>2</sub>mzl**      **Lower member**—Glaucconitic sandstone, silty sandstone, and gritstone. Thin limey shale at the base.
- EP<sub>3</sub>ps**      **Unnamed siltstone and sandstone (Paleocene)**—Mapped within Assemblage VII, a thin layer overlying unit Ks north of Alameda Creek at the mouth of Niles Canyon. Dark gray, indistinctly to distinctly bedded siltstone, claystone, and shale, in places containing abundant, poorly preserved foraminifers. Grades downward into indistinctly bedded, dark brown to green, coarse-grained, glauconite bearing lithic sandstone.

## Great Valley Sequence Units by Assemblage

### *Mapped within Assemblage II:*

- Ku**      **Unnamed sedimentary rocks (Late Cretaceous (Cenomanian and Turonian))**—Massive to distinctly bedded, biotite-bearing, brown weathering, coarse- to fine-grained marine lithic wacke, siltstone, and mudstone. Also includes, locally:
- Kuc**      **Lenses of pebble to boulder conglomerate**

### *Mapped within Assemblage V:*

- Kgu**      **Undivided marine sandstone, siltstone, and shale (Cretaceous)**—Locally divided into unnamed units:
- Kss**      **Sandstone (Late Cretaceous (Maastrichtian and Campanian))**—Massive to distinctly bedded, coarse- to fine-grained, biotite- and quartz-bearing lithic wacke and siltstone. Also includes lenses of pebble to cobble conglomerate and minor amounts of mudstone.
- Kslt**      **Siltstone (Late Cretaceous (Campanian))**—Siltstone interbedded with minor shale, claystone, and sandstone.
- Kmd**      **Mudstone (Late Cretaceous (Turonian and Cenomanian))**—Massive to distinctly bedded, gray mudstone and fine siltstone. Also includes minor amounts of biotite- and quartz-bearing lithic wacke, mapped locally:



- Kmds            **Sandstone member**—Fault-bounded below, lens of ridge-forming sandstone at the base of unit Kmd in Arroyo Valle southeast of Lake del Valle.
- Kus            **Sandstone and shale (Early Cretaceous (Albian))**
- Kush           **Shale with minor sandstone (Early Cretaceous (Albian))**
- KJk            **Knoxville Formation (Early Cretaceous and Late Jurassic)**—Mainly dark, greenish-gray marine siltstone or clay shale with thin sandstone interbeds.

*Mapped within Assemblage VI North:*

- RkDv           **Deer Valley Sandstone of Colburn (1964) (Paleocene and(or) Late Cretaceous (Maastrichtian))**—Fine- to medium-grained, gray, distinctly bedded to massive, biotite-bearing marine arkosic sandstone and minor conglomerate. McDougall and Block (2014) report middle to late Paleocene foraminifers from the base of this unit southwest of Deer Valley, southeast of Somersville.

**Unit E – Marine siltstone and mudstone (Late Cretaceous (Maastrichtian and Campanian?))**—Consists of:

- Keu            **Upper member**—Light gray siltstone, interbedded with medium to coarse grained, clean, white and orange, lithic sandstone with many large (as much as 50 cm diameter) iron concretions. Weathers to light orange.

- Kel            **Lower member**—Light gray to gray brown, foraminifer bearing siltstone and mudstone. Reddish-brown weathering and iron concretions are conspicuous. Locally includes (mapped in part):

- Kels            **Sandstone interbeds**—Coarse-grained, clean white, fossiliferous, lithic sandstone. Grains include quartz, feldspar, and black lithic grains. Mica is rare; iron concretions common.

- Kd            **Unit D – Marine sandstone (Late Cretaceous (Campanian))**—Medium- to coarse-grained, light gray, clean sandstone. Grains include quartz, feldspar, and biotite. Spherical weathering is common. In places, the clean sandstone is interbedded with fine to medium grained, biotite and muscovite bearing wacke with mudstone rip-up clasts. Sandstone beds form packages up to 10 meters thick with 1 to 2 meters of interbedded siltstone and mudstone. The unit also locally includes:

- Kds            **Shale member**—Brown to gray, micaceous mudstone and brown micaceous siltstone. One layer is dark gray-brown to dark gray, massive, foraminifer rich, siliceous mudstone.

**Unit C – Marine sandstone and shale (Late Cretaceous (Campanian, Santonian, and Coniacian?))**—Consists of:

- Kcu            **Upper member**—Shale and siltstone. Also includes:

- Kcus           **Sandstone interbeds**—Mapped locally.

- Kcm            **Middle member**—Medium-grained, brown to gray, biotite-rich wacke with some mudstone rip-up clasts. Contains interbeds of siltstone, shale, and conglomerate.

- Kcl            **Lower member**—Shale and siltstone with minor sandstone. Also includes:

- Kcls           **Sandstone interbeds**—Mapped locally.

- Kb**      **Unit B – Marine sandstone and shale (early Late Cretaceous (Santonian?, Coniacian, Turonian, and – Cenomanian?))**—Base marked by 1 m thick bed of cobble conglomerate overlain by 10 meters of conglomeratic sandstone. Includes at least one layer, 10 meters thick, of white rhyolite tuff. Locally, includes (mapped in part):
- Kbsh**      **Shale member**—Olive-gray mudstone and micaceous siltstone. Forms reddish soil. Contains sandstone interbeds.
- Kbs**      **Sandstone member**—Medium-grained, olive-brown wacke with large biotite grains and many small (3 mm long) mudstone rip-up clasts. Interbedded with thin beds of siltstone and mudstone.
- Ka**      **Unit A – Marine shale with minor sandstone (Late and Early Cretaceous (Turonian?, Cenomanian, and Albian))**—Olive-brown to dark gray siltstone and mudstone. Spherical concretions common. Locally, includes (mapped in part):
- Kas**      **Sandstone member**—Fine- to medium-grained, brown to olive, biotite-rich wacke with micaceous siltstone interbeds. In places grades into coarse-grained, bluish-gray wacke with large (up to 3 cm long) mudstone rip-up clasts and phosphate nodules.
- KJk**      **Knoxville Formation (Early Cretaceous to Late Jurassic)**—Mainly dark, greenish-gray marine shale with sandstone interbeds; also, locally includes conglomeratic sandstone in its lower part. Locally contains abundant specimens of bivalve fossil *Buchia*.

*Mapped within Assemblage VII:*

- Kph**      **Pinehurst Shale (Late Cretaceous (Campanian))**—Marine siliceous shale with interbedded sandstone and siltstone. This unit also includes maroon, concretionary shale at base. This formation was originally considered to be Paleocene but contains foraminifers and radiolarians of Campanian age in its type area and throughout its outcrop extent.
- Kr**      **Redwood Canyon Formation (Late Cretaceous (Campanian))**—Distinctly bedded, cross-bedded to massive, thick beds of fine- to coarse grained, marine biotite and quartz rich wacke and thin interbeds of mica rich siltstone. This formation is conformably overlain by the Pinehurst Shale.
- Kcv**      **Unnamed sandstone, conglomerate, and shale of the Castro Valley area (Late Cretaceous (Turonian and younger?))**—The lower part of the unit is composed of distinctly bedded, mica bearing marine siltstone, fine-grained mica bearing wacke, shale, and, locally, one thin pebble conglomerate layer. The middle part of the unit is composed of distinct, thick beds of medium- to coarse-grained, mica-rich wacke and pebble to cobble conglomerate. The middle part grades upward into the upper part, which is composed of distinctly to indistinctly bedded, medium- to fine-grained, mica-rich wacke and siltstone. This unit is bounded above and below by faults.
- Ko**      **Oakland Conglomerate (Late Cretaceous (Cenomanian and/or Turonian))**—Massive, medium- to coarse-grained, marine biotite and quartz-rich wacke and prominent interbedded lenses of pebble to cobble conglomerate. Conglomerate clasts are distinguished by a large amount of silicic volcanic detritus, including quartz porphyry rhyolite. Conglomerate composes as much as fifty percent of the unit in the Oakland hills, but it becomes a progressively smaller portion of the unit to the south.
- Ks**      **Unnamed marine sandstone and shale (Cretaceous)**—Distinctly bedded, gray to white, hard, in places cross-bedded, mica bearing, coarse- to fine grained sandstone, siltstone,

and shale. Sandstone is granitic (quartz, feldspar, and biotite grains) or lithic, and forms discontinuous outcrops on ridges and uplands. Siltstone and shale crop out only in canyons.

**KJk**      **Knoxville Formation (Early Cretaceous to Late Jurassic)**—Mainly dark greenish-gray marine siltstone and clay shale with thin sandstone interbeds. Elder and Miller (1992) report Tithonian and Berriasian *Buchia* and other fossils from four localities in this unit. Includes locally in lower part:

**KJkc**      **Conglomerate**—Thick pebble to cobble conglomerate beds.

*Mapped within Assemblages VIII:*

**Ks**      **Unnamed marine sandstone and shale (Cretaceous)**—Distinctly bedded marine biotite-lithic wacke and biotite arkose.

*Mapped within Assemblages VI South and XI:*

**RkM**      **Moreno Formation (Paleocene and latest Cretaceous (Maastrichtian))**—Dark gray to dark brown, vaguely bedded, micaceous, crumbly, marine, silty shale and claystone with calcareous concretions. Locally, includes:

**Kms**      **Interbedded sandstone, light gray to tan, fine to medium grained, arkosic**

**Panoche Formation (Late Cretaceous)**—Marine sandstone and shale mapped separately as:

**Kp**      **Shale member**—Gray to dark gray, micaceous, shale and claystone, with occasional thin layers of arkosic sandstone.

**Kps**      **Sandstone member**—Light gray to light brown, hard, bedded, fine- to medium-grained, arkosic sandstone. Locally contains large (up to 1/2 m) dark brown concretions, and thin interbeds of gray claystone.

**KJs**      **Unnamed shale (Early Cretaceous (Albian and older?) and Late Jurassic (Tithonian))**—Dark greenish gray to nearly black shaley mudstone and siltstone, with minor sandstone, lenticular pebble conglomerate, and calcareous concretions. The unit includes Early Cretaceous and possibly older strata mapped discontinuously along the Tesla-Ortogonal Fault Zone and are usually bounded by faults on top as well. Differentiating these basal shales without the help of age-diagnostic fossils is problematic. The structural dismemberment between faults adds to the uncertainty, as is reflected in the confusing differences between source maps reviewed for this compilation. Huey (1948) first distinguished an older unit below the Panoche Formation in his mapping south of Corral Hollow, which he named the Horsetown formation based on the presence of Horsetown age (Early Cretaceous, Hauterivian to Albian [Murphy, 1956]) fossils. On Dibblee's 1980 map of the Midway Quadrangle, Huey's Horsetown strata are referred to as an unnamed Cretaceous and/or Jurassic shale unit. Throckmorton (1988) collected Tithonian (Late Jurassic) *Buchia* as well as Early Cretaceous fossils from the same area and, based on his new fossil evidence, divided Huey's Horsetown formation and other basal shales along the Tesla Fault between the Late Jurassic Knoxville Formation and an Early Cretaceous informal shale member of the Panoche Formation. Graymer and others (1996) reverted to the Early Cretaceous Horsetown formation designation, while the updated Dibblee map (edited by Minch, 2006) indicated an Early Cretaceous and Late Jurassic Knoxville Shale designation. In Assemblage VI South, this unit is distinguished from younger Great Valley strata by abundant Albian Stage fossil content. Although no fossils older than Albian are known from the basal Great Valley sequence in Assemblage VI South, older strata may be present, as recognized by the identification of Late

Jurassic (Tithonian) fossils near the base of the unit in Assemblage XI (Throckmorton, 1988).  
Locally includes:

**KJss**            **Thin-bedded, fine-grained sandstone**

### Coast Range Ophiolite

**Jlc**            **Lotta Creek Formation (Late Jurassic)**—Mapped within Assemblage VI South. Tuffaceous sandstone, white crystal-lithic tuff, and interbedded dark green siliceous shale. The unit is everywhere bounded by faults within the map area but reported to be conformably overlain by Knoxville Formation farther south in the Mount Boardman quadrangle (Maddock, 1964), and to depositionally overlie volcanics of the Coast Range ophiolite in the Del Puerto Canyon area (Wentworth and others, 1999b). Included as part of the CRO because it predates the final stage of Late Jurassic dikes and sills.

**Jvk**            **Keratophyre and quartz keratophyre (Late Jurassic)**—Mapped in the eastern Diablo Range in the southern part of the map area. Highly altered intermediate and silicic volcanic and hypabyssal rocks. Feldspars are almost all replaced by albite. In some places, closely associated with (intruded into?) basalt. Includes rocks previously mapped as the Del Puerto Keratophyre Member of the Franciscan Formation by Maddock (1964), and the Del Puerto Formation by Raymond (1969). Biostratigraphic and isotopic analyses have revealed the Jurassic age of these rocks (Jones and Curtis, 1991), including a hornblende Ar/Ar age of  $150 \pm 2$  Ma from rock collected just south of the map area (Evarts and others, 1992).

**Jo**            **Undifferentiated ultramafic and related rocks (Jurassic)**—Mapped at Mount Diablo and in the Diablo Range in the southern part of map area. Distinguished locally, includes:

**Jb**            **Massive basalt and diabase**

**Jgb**           **Gabbro and diabase**

**Jpb**           **Pillow basalt, basalt breccia, and minor diabase**—Mapped in Assemblage VI South.

**Jdb**           **Diabase**—Mainly sills and dikes; also includes screens of pillow basalt.

**sp**           **Serpentinite**—Mainly sheared serpentinite, but also includes massive harzburgite. In places, pervasively altered to silica carbonate rock (**sc**).

### Franciscan Complex

Jurassic and Cretaceous age basement rocks exposed at Mount Diablo and in the Diablo Range; presumed to underlie all assemblages in the map area west of the San Joaquin Valley at depth.

**KJf**           **Undivided Franciscan rocks (Cretaceous and Jurassic)**—Mapped at Mount Diablo, includes both mélangé and large coherent slabs of Eylar Mountain terrane sandstone, chert, and greenstone, as described below. Recent reconnaissance mapping (Graymer and Langenheim, in press) showed the previously mapped extent of the coherent rocks to be unreliable, and remapping the area is beyond the scope of this effort, so we revert to this more generalized unit. Mélangé at Mount Diablo includes blocks of graywacke, chert, and basalt presumably from the Eylar Mountain terrane, as well as high-grade metamorphic blocks and slabs and lenses of serpentinite, mapped locally. Coherent graywacke ranges from massive, coarse-grained and conglomeratic sandstone to distinctly bedded, medium- and coarse-grained sandstone. The graywacke at Mount Diablo has yielded a suite of detrital zircons with a youngest zircon population (YZP, which equals maximum depositional age) of  $108 \pm 2$  Ma (Unruh et al., 2007), although Dumitru et al. (2018) suggest the YZP is “slightly younger”.

- Chert at Mount Diablo is mostly thin-bedded, red and green, more or less recrystallized, containing a few well-preserved radiolarians locally. In some places chert has been altered to white metachert. The depositional contact between graywacke and chert is preserved locally. Basalt on Mount Diablo is in many places distinctly pillowed basalt, elsewhere basalt breccia. In many locations the basalt has been converted to bright green metabasalt (greenstone). This alteration likely accounts for the absence of magnetic anomalies associated with the km-scale slabs of basalt.
- KJfm**      **Franciscan mélangé, undivided (Cretaceous and Late Jurassic)**—Highly sheared dark gray to black argillite and graywacke, which form a matrix enclosing blocks and lenses of many rock types. Matrix may display textures and metamorphic mineral assemblages indicating high P/T metamorphism. Enclosed blocks include:
- fc**              **Chert and metachert**—Typically with shale partings and interbeds.
- fg**              **Greenstone (metabasite)**
- fgg**             **Glaucophane metabasite**
- gl**              **Glaucophane blueschist**
- spu**             **Serpentinite of uncertain affiliation**—Serpentinite bodies in Franciscan mélangé may be tectonically incorporated fragments of Coast Range ophiolite or serpentinite formed as part of the accreted oceanic crust (e.g., serpentinite diapirs emplaced near spreading ridges). The detailed geochemical studies required to potentially differentiate serpentinite affiliation have not been done in the map area.
- sc**              **Silica carbonate rock**
- KJfe**      **Eylar Mountain terrane of Crawford (1976) undivided (Cretaceous and Late Jurassic)**—More or less sheared and metamorphosed mudstone, siltstone, graywacke, conglomerate, chert, and minor pillow basalt. Mudstone is almost everywhere metamorphosed to slate or chlorite phyllite. Sedimentary structures are well preserved locally. Graywacke ranges from massive, coarse-grained and conglomeratic sandstone to distinctly bedded, medium- and coarse-grained sandstone. Although most Eylar Mountain terrane graywacke in the Stockton quadrangle is little foliated, locally it displays foliation as pronounced as textural zone 2A. The depositional contact of clastic sedimentary rocks on chert is preserved in several locations. Chert is mostly thin-bedded, red and green, more or less recrystallized, containing a few well-preserved radiolarians locally. In some places chert has been altered to white metachert. The estimated age of the Eylar Mountain terrane was previously based on Tithonian to Valanginian (151-136 Ma) macrofossils, but relatively recent detrital zircon and other dating methods indicate significantly younger Late Cretaceous ages of deposition for portions, suggesting some Eylar Mountain terrane rocks may represent transported and redeposited materials (Snow and others, 2010). Detrital zircons in graywackes of the Eylar Mountain terrane in the Diablo Range have yielded YZPs ranging from ~85-114 Ma (Joesten et al., 2004; Tripathy et al., 2005; Ernst et al., 2009; Dumitru et al., 2018). Because Franciscan Complex graywackes are thought to have been deposited in an active subduction zone, the proximity to an active volcanic arc means that it is likely that the availability of recently erupted volcanic zircons means the YZP is probably close to the actual depositional age. The Eylar Mountain terrane also includes widely dispersed, small outcrops of basalt that are distinctly pillowed, amygdaloidal, and lacking phenocrysts. In many locations the basalt is converted to bright green metabasalt (greenstone). Larger blocks of greenstone mapped separately as:

**KJfg**            **Franciscan greenstone**—More or less metamorphosed basalt, generally pervasively altered. Pillow structure is well preserved locally. In places, the basalt is amygdaloidal.

*Franciscan Units of Raymond (2014) (Cretaceous and/or Late Jurassic)*

Mapped south of the Tesla–Ortogonal Fault and east of the Greenville Fault. Franciscan rocks exposed here widely display blueschist facies metamorphic mineralogy and are tentatively considered part of the Eylar Mountain terrane, together with structurally interleaved mélanges. Raymond (2014) distinguished several broken units and mélange units based on variations in associated rock types, metamorphic texture, and structure:

**Kfbm**            **Mélange of Blue Rock Springs**—A diverse array of rock types, including blocks of coarse-grained glaucophane schists and gneisses in a sheared shale matrix. The apparent tabular nature of the mélange of Blue Rock Springs could indicate an olistostromal origin. At least four large masses of metagraywacke-metashale turbidites occur as fault-bounded slabs, possibly originally interlayered within the olistostrome protolith of the mélange:

**Kfss**            **Metagraywacke of Sperry Springs**—Detrital zircons from this unit indicate a maximum depositional age of roughly 85 Ma (Joesten and others, 2004).

**Kfwf**            **Broken formation of West Fork**

**Kfhc**            **Broken formation of Hellsinger Canyon**

**Kfmf**            **Metagraywacke of Middle Fork Headwaters**

**Kfpr**            **Broken to Dismembered Formation of Pegleg Ridge**—Metagraywacke turbidites with metashale that locally includes isolated blocks of metachert (**fc**) and basic metavolcanic rock (**fg**), as well as rare high-grade blocks in the western part of the unit.

**Kfim**            **Mélange of Ingram Canyon**—Containing all the typical rocks of the Franciscan Complex mélanges, including metagraywacke, metashale, metaconglomerates, metacherts (mapped locally as **fc**), low to high SiO<sub>2</sub> metavolcanic rocks (mapped locally as **fg**); fine- to coarse-grained glaucophane schist (mapped locally as **fgg**), altered eclogite, actinolite schist, serpentinite, and aragonite marble. Detrital zircons from this unit indicate a maximum depositional age of roughly 98 Ma (Joesten and others, 2004).

**KJfrm**            **Mélange of Gerber Ranch**—Typical mélange rocks, but no serpentinite or coarse-grained ('high-grade') schists and gneisses. Rock types include glaucophane metabasites (mapped locally as **fgg**), glaucophane-poor metabasites ('greenstones', mapped locally as **fg**), metagraywackes, metashales, metaconglomerates, and metacherts (mapped locally as **fc**), minor aragonite marble, and rare actinolite schist.

**KJfgc**            **Dismembered formation of Grummett Creek**—Composed of folded metachert blocks (mapped locally as **fc**) with sheared metagraywacke, metashales, greenstone (mapped locally as **fg**) and manganese ores (e.g. rhodochrosite marble).

**KJfsg**            **Metagraywacke of Sulphur Gulch**—Predominantly metagraywacke and metashale turbidites. Includes small lenses of metachert, mapped locally as **fc**.

**KJfgm**            **Garzas mélange**—Matrix of scaly metagraywacke and metashale enclosing metaconglomerates, metacherts, and metavolcanic rocks of blueschist facies. Also includes blocks of serpentinite, glaucophane schist, actinolite schist, and aragonite

marble. In the map area limited to one small area along the southern map boundary south of Cedar Knob.

Jsch

**Schist (Jurassic)**—Coarse-grained rocks such as hornblende schist, glaucophane schist, and glaucophane-quartz-white mica schist; mapped locally in slivers along the Tesla-Ortogonalita Fault zone.

## REFERENCES CITED

- Abrams, G.A., Kucks, R.P., and Bracken, R.E., 1991, Aeromagnetic gridded data for a portion of the San Jose 1 x 2 quadrangle, California: U.S. Geological Survey Open-File Report 91-030, 4 p., 1 diskette ([mrdata.usgs.gov/geophysics/surveys/geophysics2CA/CA\\_1140.zip](http://mrdata.usgs.gov/geophysics/surveys/geophysics2CA/CA_1140.zip)), <http://pubs.usgs.gov/of/1991/0030/report.pdf> (last accessed July 5, 2016).
- Almgren, A.A., 1984, Timing of Tertiary submarine canyons and marine cycles of deposition in the southern Sacramento Valley, *in* Almgren, A.A., and Hacker, P.D., eds., Paleogene submarine canyons of the Sacramento Valley, California: Pacific Section, American Association of Petroleum Geologists, S.V. 1, p. 1-16.
- Atwater, B.F., 1982, Geologic maps of the Sacramento-San Joaquin Delta, California: U.S. Geological Survey Miscellaneous Field Studies Map MF-1401, 15 p., 21 sheets, scale 1:24,000.
- Atwater, T., 1970, Implications of plate tectonics for the Cenozoic tectonic evolution of western North America: Geological Society of America Bulletin, v. 81, p. 3513–3535, doi: 10.1130/0016-7606(1970)81[3513:IOPTFT]2.0.CO;2.
- Atwater, T. M., and P. Molnar (1973), Relative motions of the Pacific and North American plates deduced from seafloor spreading in the Atlantic, Indian, and South Pacific Oceans, *in* Proceedings of the Conference on Tectonic Problems of the San Andreas Fault System, edited by R. L. Kovach and A. Nur, Stanford University publications. Geological sciences, 13, 136 – 148.
- Atwater, Tanya, and Stock, Joann, 1998, Pacific-North America plate tectonics of the Neogene southwestern United States; an update: International Geology Review, v. 40, p. 375-402.
- Bailey, E.H., M.C. Blake, Jr., and D.L. Jones, 1970, On-land Mesozoic oceanic crust in California Coast Ranges, U.S. Geol. Surv. Prof. Pap., 700-C, C70-C81.
- Bailey, E.H., Irwin, W.P., and Jones, D.L., 1964, Franciscan and related rocks and their significance in the geology of western California: California Division of Mines and Geology Bulletin 183, 177 p.
- Baranov, V.I., 1957, A new method for interpretation of aeromagnetic maps Pseudo-gravimetric anomalies: Geophysics, v. 22, p. 359–383.
- Barlock, V.E., 1989, Sedimentology of the Livermore Gravels (Miocene-Pleistocene), southern Livermore Valley, California: U.S. Geological Survey Open-File Report 89-131, 102 p., 1 plate, scale 1:48,000.
- Bartow, J.A., 1991, The Cenozoic evolution of the San Joaquin Valley, California: U.S. Geological Survey Professional Paper 1501, 40 p., 2 plates.
- Bartow, J.A., Lettis W.R., Sonneman, H.S., and Switzer, J.R., 1985, Geologic map of the east flank of the Diablo Range from Hospital Creek to Poverty Flat, San Joaquin, Stanislaus, and Merced Counties, California: U.S. Geological Survey Miscellaneous Investigations Series Map 1-1656, scale 1:62,500.
- Bartow, J.A., and Nilsen, T.H., 1990, Review of the Great Valley sequence, eastern Diablo Range and northern San Joaquin Valley, central California: U.S. Geological Survey Open-File Report 90-226. 25 p.
- Bedrossian, T.L., and Saucedo, G.J., 1981, Location map of rock samples dated by radiometric methods, Sacramento Quadrangle, California, *in* Wagner, D.L., Jennings, C.W., Bedrossian, T.L., and Bortugno, E.J., Geologic map of the Sacramento Quadrangle, California: California Division of Mines and Geology Regional Geologic Map Series, Map No. 1A, sheet 4, scale 1:250,000.
- Berkland, J.O., 1973, Rice Valley outlier – New sequence of Cretaceous-Paleocene strata in the northern Coast Ranges, California: Geological Society of America Bulletin, v. 84, p. 2389-2406.
- Bishop, C.C., and Davis, J.F., coordinators, 1984, Correlation of Stratigraphic Units in North America-Northern California Province Correlation Chart: American Association of Petroleum Geologists Correlation Chart Series.



- Blake, M.C., Jr., Bartow, J.A., Frizzell, V.A., Jr., Sorg, D., Schlocker, J., Wentworth, C.M., and Wright, R.H., 1974, Preliminary geologic map of Marin, San Francisco, and parts of adjacent Counties, California: U.S. Geological Survey Miscellaneous Field Studies Map MF-574.
- Blake, M.C., Jr., Graymer, R.W., and Stamski, R.E., 2002, Geologic map and map database of western Sonoma, northernmost Marin, and southernmost Mendocino counties, California: U.S. Geological Survey Miscellaneous Field Studies Map MF-2402, 45 p, 1 plate, scale 1:100,000.
- Blake, M.C., Jr., Harwood, D.S., Helley, E.J., Irwin, W.P., Jayko, A.S., and Jones, D.L., 1999, Geologic map of the Red Bluff 30' x 60' quadrangle, California: U.S. Geological Survey Geologic Investigations Series Map I-2542, 1 sheet, scale 1:100,000, pamphlet 15 p., and database, available at <https://pubs.usgs.gov/imap/2542/>.
- Blake, M.C., Jr., Howell, D.G., and Jayko, A.S., 1984, Tectonostratigraphic terranes of the San Francisco Bay Region *in* Blake, M.C., Jr., ed., Franciscan geology of Northern California: Pacific Section Society of Economic Paleontologists and Mineralogists, v. 43, p. 5-22.
- Blake, M.C., Jr., Jayko, A.S., Murchey, B.L., and Jones, D.L., 1992, Formation and deformation of the Coast Range Ophiolite and related rocks near Paskenta, California: American Association of Petroleum Geologists Bulletin, v. 76, p. 417.
- Blake, M. C., and Jones, D. L. 1981. The Franciscan assemblage and related rocks in northern California: a reinterpretation. *in* Ernst, W. G., ed. The geotectonic development of California. Englewood Cliffs, New Jersey, Prentice-Hall, p. 307-328.
- Blake, M.C. Jr., and Wentworth, C.M., 1999, Structure and metamorphism of the Franciscan Complex, Mt. Hamilton area, northern California: International Geology Review, v. 41, p. 417-424.
- Blakely, R.J., 1995, Potential theory in gravity and magnetic applications: Cambridge, England, Cambridge University Press, 441 p.
- Bonilla, M.G., Lienkaemper, J.J., and Tinsley, J.C., 1980, Surface faulting near Livermore, California associated with the January 1980 earthquakes: U.S. Geological Survey Open-File Report 80-523, 32 p., 1 plate, scale 1:24:000, available at <http://pubs.usgs.gov/of/1980/0523/>.
- Brabb, E.E., 2011, Location and age of foraminifer samples examined by Chevron paleontologists from more than 2,500 oil test wells in California: U.S. Geological Survey Open-File Report 2011-1262.
- Brabb, E.E., Graymer, R.W., Knudsen, K.L., and Wentworth, C.M., 2001, Preliminary Geologic Map of the Stockton 30 x 60 Minute Quadrangle, California: U.S. Geological Survey, unpublished draft plot and digital GIS database, scale 1:100,000.
- Brabb, E.E., Sonneman, H.S., and Switzer, J.R., Jr., 1971, Preliminary geologic map of the Mt. Diablo - Byron area, Contra Costa, Alameda, and San Joaquin Counties, California: U.S. Geological Survey Open-File Map, scale 1:62,500.
- Briggs, L.I., Jr., 1953, Geology of the Ortigalita Peak quadrangle, California: California Division of Mines Bulletin 167, 61 p., 1 map, scale 1:62,500.
- Brocher, T.M., Ruebel, A.L., and Brabb, E.E., 1997, Compilation of 59 sonic and density logs from 51 oil test wells, San Francisco Bay area, California: U.S. Geological Survey Open-File Report 97-687, 75 p.
- Bryant, W.A. (compiler), 2005, Digital Database of Quaternary and Younger Faults from the Fault Activity Map of California, version 2.0: California Geological Survey Web Page: [http://www.consrv.ca.gov/CGS/information/publications/QuaternaryFaults\\_ver2.ht](http://www.consrv.ca.gov/CGS/information/publications/QuaternaryFaults_ver2.ht).
- Cady, J.W., 1972, Magnetic and gravity anomalies in the California Great Valley and western Sierra Nevada metamorphic belt: Unpublished Ph.D. thesis, Stanford University, 104 p.
- Cady, J.W., 1975, Magnetic and gravity anomalies in the Great Valley and western Sierra Nevada metamorphic belt, California: Geological Society of America Special Paper 168, p. 1-56.
- California Division of Mines and Geology, 1980, Niles quadrangle, Special Studies Zones maps of California [Alquist-Priolo]: Sacramento, Calif., California Division of Mines and Geology, scale 1:24,000.

- California Division of Mines and Geology, 1982a, Altamont quadrangle, Special Studies Zones maps of California [Alquist- Priolo]: Sacramento, Calif., California Division of Mines and Geology, scale 1:24,000.
- California Division of Mines and Geology, 1982b, Byron Hot Springs quadrangle, Special Studies Zones maps of California [Alquist- Priolo]: Sacramento, Calif., California Division of Mines and Geology, scale 1:24,000.
- California Division of Mines and Geology, 1982c, Dublin quadrangle, Special Studies Zones maps of California [Alquist-Priolo]: Sacramento, Calif., California Division of Mines and Geology, scale 1:24,000.
- California Division of Mines and Geology, 1982d, Livermore quadrangle, Special Studies Zones maps of California [Alquist- Priolo]: Sacramento, Calif., California Division of Mines and Geology, scale 1:24,000.
- Case, J.E., 1968, Upper Cretaceous and lower Tertiary rocks, Berkeley and San Leandro Hills, California: U.S. Geological Survey Bulletin 1251-J, p. J1-J29.
- Cloos, M., 1982, Flow mélanges; numerical modeling and geologic constraints on their origin in the Franciscan subduction complex, California: Geological Society of America Bulletin, v. 93, p. 330–345.
- Conduit, C., 1938, The San Pablo flora of west central California: Carnegie Inst. Washington Publ. Contr. Paleontology, v. 476, p. 217-268.
- Colburn, R., and Mooney W.D., 1986, Two-dimensional velocity structure along the synclinal axis of the Great Valley, California, Bulletin of Seismological Society of America, 76, pp. 1305-1322.
- Coney, P.J., 1976, Plate tectonics and the Laramide orogeny, *in* Woodward, L.A., and Northrop, S.A., eds., Tectonics and mineral resources of southwestern North America: New Mexico Geological Society Special Publication, no. 6, p.5–10.
- Coney, P. J., and Reynolds, S. J., 1977, Cordilleran Benioff zones: Nature, v. 270, p. 403–406.
- Cordell, Lindrith, and Grauch, V.J.S., 1985, Mapping basement magnetization zones from aeromagnetic data in the San Juan Basin, New Mexico, *in* Hinze, W.J., ed., The utility of regional gravity and magnetic anomaly maps: Society of Exploration Geophysicists, p. 181– 192.
- Crane, R.C., 1995, Geology of Mount Diablo Region and East Bay Hills, *in* Sangines, E.M., Andersen, D.W., and Buising, A.B., eds., Recent Geologic Studies in the San Francisco Bay Area: Pacific Section Society of Economic Paleontologists and Mineralogists, v. 76, p. 87-114.
- Crawford, K.E., 1976, Reconnaissance geologic map of the Eylar Mountain quadrangle, Santa Clara and Alameda Counties, California: U.S. Geological Survey Miscellaneous Field Studies Map MF-764, scale 1:24,000.
- Dawson, T.E., and R.J. Weldon, II, 2013, Appendix B—Geologic-Slip-Rate Data and Geologic Deformation Model; Uniform California Earthquake Rupture Forecast, Version 3 (UCERF3)—The Time-Independent Model: U.S. Geological Survey Open-File Report 2013-1165.
- Dibblee, T.W., Jr., 1974, Geologic map of the Shandon and Orchard Peak quadrangles, San Luis Obispo and Kern counties, California: U.S. Geological Survey Miscellaneous Investigations Series Map I-788, scale 1:62,500.
- Dibblee, T.W., Jr., 1980a, Preliminary geologic map of the Altamont quadrangle, Alameda County, California: U.S. Geological Survey Open-File Report 80-538, scale 1:24,000.
- \_\_\_ 1980b, Preliminary geologic map of the Byron Hot Springs quadrangle, Alameda and Contra Costa Counties, California: U.S. Geological Survey Open-File Report 80-534, scale 1:24,000.
- \_\_\_ 1980c, Preliminary geologic map of the Cedar Mountain quadrangle, Alameda and San Joaquin Counties, California: U.S. Geological Survey Open-File Report 80-850, scale 1:24,000.
- \_\_\_ 1980d, Preliminary geologic map of the Dublin quadrangle, Alameda and Contra Costa Counties, California: U.S. Geological Survey Open-File Report 80-537, scale 1:24,000.

- \_\_\_ 1980e, Preliminary geologic map of the La Costa Valley quadrangle, Alameda County, California: U.S. Geological Survey Open-File Report 80-533-A, scale 1:24,000.
- \_\_\_ 1980f, Preliminary geologic map of the Livermore quadrangle, Alameda and Contra Costa Counties, California: U.S. Geological Survey Open-File Report 80-533-B, scale 1:24,000.
- \_\_\_ 1980g, Preliminary geologic map of the Midway quadrangle, Alameda and Contra Costa Counties, California: U.S. Geological Survey Open-File Report 80-535, scale 1:24,000.
- \_\_\_ 1980h, Preliminary geologic map of the Niles quadrangle, Alameda County, California: U.S. Geological Survey Open-File Report 80-533-C, scale 1:24,000.
- \_\_\_ 1980i, Preliminary geologic map of the Tassajara quadrangle, Contra Costa and Alameda Counties, California: U.S. Geological Survey Open-File Report 80-544, scale 1:24,000.
- \_\_\_ 1981a, Preliminary geologic map of the Lone Tree Creek quadrangle, San Joaquin and Stanislaus Counties, California: U.S. Geological Survey Open-File Report 81-466, scale 1:24,000.
- \_\_\_ 1981b, Preliminary geologic map of the Mendenhall Springs quadrangle, Alameda County, California: U.S. Geological Survey Open-File Report 81-235, scale 1:24,000.
- \_\_\_ 1981c, Preliminary geologic map of the Solyo quadrangle, San Joaquin and Stanislaus Counties, California: U.S. Geological Survey Open-File Report 81-465, scale 1:24,000.
- Dibblee, T.W., Jr., and Minch, J.A., 2005, Geologic map of the Diablo quadrangle, Contra Costa and Alameda Counties, California: Dibblee Geological Foundation, Dibblee Foundation Map DF-162, scale 1:24,000.
- Dibblee, T.W., Jr., and Minch, J.A., 2006a, Geologic map of the Cedar Mountain quadrangle, Alameda & San Joaquin Counties, California: Dibblee Geological Foundation, Dibblee Foundation Map DF-241, scale 1:24,000.
- \_\_\_ 2006b, Geologic map of the Eylar Mountain quadrangle, Santa Clara & Alameda Counties, California: Dibblee Geological Foundation, Dibblee Foundation Map DF-239, scale 1:24,000.
- \_\_\_ 2006c, Geologic map of the Livermore quadrangle, Contra Costa & Alameda Counties, California: Dibblee Geological Foundation, Dibblee Foundation Map DF-196, scale 1:24,000.
- \_\_\_ 2006d, Geologic map of the Lone Tree Creek quadrangle, Alameda, San Joaquin, and Stanislaus Counties, California: Dibblee Geological Foundation, Dibblee Foundation Map DF-242, scale 1:24,000.
- \_\_\_ 2006e, Geologic map of the Midway & Tracy quadrangles, Alameda & San Joaquin Counties, California: Dibblee Geological Foundation, Dibblee Foundation Map DF-243, scale 1:24,000.
- \_\_\_ 2007, Geologic map of the Solyo and Westerley quadrangles, San Joaquin and Stanislaus Counties [California]: Dibblee Geological Foundation, Dibblee Foundation Map DF-340, scale 1:24,000.
- Dickinson, W. R., 1996, Kinematics of transrotational tectonism in the California Transverse Ranges and its contribution to cumulative slip along the San Andreas transform fault system: *Geol. Soc. Am.*, Special Paper 305, 46 pp.
- Dickinson, W. R., 1997, Tectonic implications of Cenozoic volcanism in coastal California, *Geol. Soc. Am. Bull.*, 109, 936 – 954.
- Dickinson, W.R., 2008, Accretionary Mesozoic-Cenozoic expansion of the Cordilleran continental margin in California and adjacent Oregon: *Geosphere*, v. 4, p. 329-353.
- Dickinson, W.R., Hopson, C.A., Saleeby, J.B., Schweickert, R.A., Ingersoll, R.V., Pessagno, E.A., Jr., Mattinson, J.M., Luyendyk, B.P., Beebe, Ward, Hull, D.M., Munoz, I.M., and Blome, C.D., 1996, Alternate origins of the Coast Range Ophiolite (California); introduction and implications: *GSA Today*, v. 6, no. 2, p. 1–10.
- Dickinson, W.R., Ingersoll, R.V., and Graham, S.A., 1979, Paleogene sediment dispersal and paleotectonics in northern California: *Geological Society of America Bulletin*, v. 90, pt. I, p. 897–898; pt. II, p. 1458–1528.

- Dickinson, W.R., and Rich, E.I., 1972, Petrologic intervals and petrofacies in the Great Valley Sequence, Sacramento Valley, California: *Geological Society of America Bulletin*, v. 83, p. 3007–3024, doi: 10.1130/0016-7606(1972)83[3007:PIAPIT]2.0.CO;2.
- Dickinson, W.R., and Seely, D.R., 1979, Structure and stratigraphy of forearc regions: *American Association of Petroleum Geologists Bulletin*, v. 63, p. 2–31.
- Dresen, M.D., 1979, Geology and slope stability of part of Pleasanton Ridge, Alameda County, California: Hayward, Calif., California State University, M.S. thesis.
- Dumitru, T.A., Hourigan, J.K., Elder, W.P., Ernst, W.G., and Joesten, R., 2018, New, much younger ages for the Yolla Bolly terrane and a revised time line for accretion in the Franciscan subduction complex, California, *in* Ingersoll, R.V., Lawton, T.F., and Graham, S.A., eds., *Tectonics, Sedimentary Basins, and Provenance; A Celebration of William R. Dickinson's Career: Geological Society of America Special Paper 540*, p. 339–366, [https://doi.org/10.1130/2018.2540\(15\)](https://doi.org/10.1130/2018.2540(15)).
- Edwards, S.W., 1982, A new species of Hipparion (Mammalia-Equidae) from the Clarendonian (Miocene) of California: *Journal of Vertebrate Paleontology*, v. 2, no. 2, p. 173-183.
- Elder, W.P., n.d., Geology of the Golden Gate Headlands: National Park Service, retrieved from <https://www.nps.gov/goga/learn/education/upload/Geology%20of%20the%20Golden%20Gate%20Headlands%20Field%20Guide.pdf>.
- Elder, W. P., and Miller, J. W., 1992, Map and checklists of U.S. Geological Survey Jurassic and Cretaceous macrofossil localities, northernmost Diablo Range, California: U.S. Geological Survey Open-File Report OFR 92–278, 13 p., <https://doi.org/10.3133/ofr92278>
- Ellsworth, W.L., 1990, Earthquake history, 1769-1989, *in* Wallace, R.E., ed., *The San Andreas Fault System, California: U.S. Geological Survey Professional Paper 1515*, p. 153-188.
- Ellsworth, W.L., and Marks, S.M., 1980, Seismicity of the Livermore Valley, California region 1969-1979: U.S. Geological Survey Open-File Report 80-515, 42 p.
- Erickson, Rolfe, 2011, Petrology of a Franciscan olistostrome with a massive sandstone matrix; the King Ridge Road mélange at Cazadero, California, *in* Wakabayashi, J., and Dilek, Y., eds., *Mélanges; processes of formation and societal significance: Geological Society of America Special Paper 480*, p. 171–188.
- Ernst, W.G., 2011, Accretion of the Franciscan Complex attending Jurassic-Cretaceous geotectonic development of Northern and Central California, *Geological Society of America Bulletin* v. 123 (9-10): p. 1667-1678.
- Ernst, W. G., Martens, U., and Valencia, V., 2009, U-Pb ages of detrital zircons in Pacheco Pass metagraywackes—Sierran-Klamath source of mid- and Late Cretaceous Franciscan deposition and underplating: *Tectonics*, v. 28, TC6011, doi:10.1029/2008TC002352.
- Evarts, R.C., Sharp, W.D., and Phelps, D.W., 1992, The Del Puerto Canyon remnant of the Great Valley Ophiolite—Geochemical and age constraints on its formation and evolution [abs.]: *American Association of Petroleum Geologists*, v. 76, no. 3, p. 418.
- Fay, R.P., and Fleck, R.J., 2014, New age constraints on the late Miocene Orinda Formation in the southern Contra Costa basin: *Geological Society of America Abstracts with Programs*, v. 46, no 6, p. 551.
- Fischer, P.J., 1984, An early Paleogene submarine canyon and fan system—The Meganos Formation, southern Sacramento Basin California: *in* Almgren, A.A., and Hacker, P.D., eds., *Paleogene submarine canyons of the Sacramento Valley, California: Pacific Section, American Association of Petroleum Geologists*, S.V. 1, p. 174-187.
- Fox, K.F., Jr., Fleck, R.J., Curtis, G.H., and Meyer, C.E., 1985, implications of the northwestwardly younger age of the volcanic rocks of west-central California: *Geological Society of America Bulletin*, v. 96, no. 5, p. 647-654.

- Godfrey, N.J., Beaudoin, B.C., and Klemperer, S.L., 1997, Ophiolitic basement to the Great Valley forearc basin, California, from seismic and gravity data—Implications for crustal growth at the North American continental margin: *Geological Society of America Bulletin*, v. 108, p. 1536-1562.
- Grauch, V.J.S., and Cordell, Lindrith, 1987, Limitations of determining density or magnetic boundaries from the horizontal gradient of gravity or pseudogravity data: *Geophysics*, v. 52, no. 1, p. 118–121.
- Graymer, R.W., 2002, Geologic map and map database of the Oakland metropolitan area, Alameda, Contra Costa, and San Francisco Counties, California: U.S. Geological Survey Miscellaneous Field Studies Map MF-2342, <http://pubs.usgs.gov/mf/2000/2342>.
- Graymer, R.W., 2005, Jurassic-Cretaceous assembly of central California, *in* Stevens, Calvin, and Cooper, John, eds., *Mesozoic tectonic assembly of California: Pacific Section, Society of Economic Paleontologists and Mineralogists Book 96*, p. 21-64.
- Graymer, R.W., 2018, Geologic history of San Francisco, *in* Johnson, K.A., and Bartow, G.W., eds., *Geology of San Francisco, California, United States of America: Association of Engineering Geologists, Geology of Cities of the World Series*, p. 61-67.
- Graymer, R.W., and Jones, D.L., 1994, Tectonic implications of radiolarian cherts from the Placerville Belt, Sierra Nevada Foothills, California—Nevadan-age continental growth by accretion of multiple terranes: *Geological Society of America Bulletin*, v. 106, p. 531-540.
- Graymer, R.W., Jones, D.L., and Brabb, E.E., 1994a, Preliminary geologic map emphasizing bedrock formations in Contra Costa County, California: A digital database: U.S. Geological Survey Open-File Report 94-622.
- Graymer, R.W., Jones, D.L., Brabb, E.E., and Helley, E.J., 1994b, Preliminary geologic map of the Niles 7.5- minute quadrangle, Alameda County, California: U.S. Geological Survey Open-File Report 94-132, 3 sheets, scale 1:24,000.
- Graymer, R.W., Jones, D.L., and Brabb, E.E., 1995, Geologic map of the Hayward fault zone, Contra Costa, Alameda, and Santa Clara Counties, California: A digital database: U.S. Geological Survey Open-File Report 95-597.
- Graymer, R.W., Jones, D.L., and Brabb, E.E., 1996, Preliminary geologic map emphasizing bedrock formations in Alameda County, California: A digital database: U.S. Geological Survey Open-File Report 96-252.
- Graymer, R.W., Jones, D.L. and Brabb, E.E., 2002, Geologic map and map database of northeastern San Francisco Bay Region, California: U.S. Geological Survey Miscellaneous Field Studies Map MF-2403, <http://pubs.usgs.gov/mf/2002/2403>.
- Graymer, R.W., Jones, D.L., and Brabb, E.E., 1994a, Preliminary geologic map emphasizing bedrock formations in Contra Costa County, California: A digital database: U.S. Geological Survey Open-File Report 94-622.
- Graymer, R.W., Jones, D.L., Brabb, E.E., and Helley, E.J., 1994b, Preliminary geologic map of the Niles 7.5 minute quadrangle, Alameda County, California: U.S. Geological Survey Open-File Report 94-132, 3 sheets, scale 1:24,000.
- Graymer, R.W., and Langenheim, V.E., 2021, Geologic framework of Mount Diablo, California, *in* Sullivan, R., Sloan, D., Unruh, J.R., and Schwartz, D.P., eds., *Regional Geology of Mount Diablo, California: Its Tectonic Evolution on the North America Plate Boundary: Geological Society of America Memoir 217*, p. 1–34, [https://doi.org/10.1130/2021.1217\(01\)](https://doi.org/10.1130/2021.1217(01)).
- Graymer, R.W., Stanley, R.G., Ponce, D.A., Jachens, R.C., Simpson, R.W., and Wentworth, C.M., 2015, Structural superposition in fault systems bounding Santa Clara Valley, California: *Geosphere*, v. 11, p. 63-75.
- Graymer, R.W., Sarna-Wojcicki, AM., Walker, J.P., and McLaughlin, R.J., 2002, Controls on timing and amount of right-lateral offset on the East Bay fault system, San Francisco Bay region, California: *Geological Society of America Bulletin*, v. 114, p. 1471-1479.

- Griscom, Andrew, Roberts, C.W., and Holden, K.D., 1979, Gravity data and interpretation of detailed gravity profiles in the Livermore Valley area, California: U.S. Geological Survey Open-File Report 79-0549, 17 p., 4 plates.
- Haggart, J.W., 1984, Upper Cretaceous (Santonian-Campanian) ammonite and inoceramid biostratigraphy of the Chico Formation, California: *Cretaceous Research*, v. 5, p. 225-241.
- Hagstrum, J.T., 1997, Paleomagnetism, paleogeographic origins, and remagnetization of the Coast Range Ophiolite and Great Valley Sequence, Alta and Baja California: *American Association of Petroleum Geologists Bulletin*, v. 81, p. 686-687.
- Hagstrum, J.T., and Jones, D.L., 1998, Paleomagnetism, paleogeographic origins, and uplift history of the Coast Range ophiolite at Mount Diablo: *Journal of Geophysical Research*, v. 103, p. 597-603.
- Hagstrum, J.T., and Murchey, B.L., 1993, Deposition of Franciscan Complex cherts along the paleoequator and accretion to the American margin at tropical paleolatitudes: *Geological Society of America Bulletin*, v. 105, p. 766-778.
- Hall, C.A., 1958, Geology and paleontology of the Pleasanton area, Alameda and Contra Costa Counties, California: *University of California Publications in Geological Sciences*, v. 34, no. 1, 90 p., 3 sheets.
- Hall, C.A., Jr., 1991, Geology of the Point Sur-Lopez Point region, Coast Ranges, California—A part of the Southern California allochthon: *Geological Society of America Special Paper* 266, 40 p., 2 plates.
- Harms, T.A., Jayko, A.S., and Blake, M.C., Jr., 1992, Kinematic evidence of extensional unroofing of the Franciscan Complex along the Coast Range fault, Northern Diablo Range, California: *Tectonics*, v. 11, p. 228-241.
- Harwood, D.S., and Helley, E.J., 1987, Late Cenozoic Tectonism of the Sacramento Valley, California: U.S. Geological Survey Professional Paper 1359, 46 p., 1 plate.
- Heiskanen, W.A., and Vening-Meinesz, F.A., 1958, *The Earth and its gravity field*: New York, McGraw-Hill Book Company, Inc., 470 p.
- Herd, D.G., 1977a, Geologic map of the Las Positas, Greenville, and Verona faults, eastern Alameda County, California: U.S. Geological Survey Open-File Report 77-689, scale 1:24,000.
- \_\_\_\_\_, 1977b, Map of Quaternary faulting along the Hayward and Calaveras fault zones; Niles and Milpitas 7 1/2 ' quadrangles, California: U.S. Geological Survey Open-File Report 77-645, 2 sheets, scale 1:24,000.
- Hillhouse, J.W., and Jachens, R.C., 2005, Highly magnetic upper Miocene sandstones of the San Francisco Bay area, California: *Geochemistry, Geophysics, Geosystems*, v. 6, Q05005, doi:10.1029/2004GC000876.
- Hilton, R. P. and Antuzzi, P. J. 1997. Chico Formation yields clues to Late Cretaceous paleoenvironment in California: *California Geology*, v. 50, p. 136-144.
- Hinds, N.E.A., 1934, The Jurassic age of the last granitoid intrusives in the Klamath Mountains and Sierra Nevada, California: *American Journal of Science*, v. 227, p. 182-192.
- Hopson, C.A., Mattinson, J.M., Luyendyk, B.P., Beebe, W.J., Pessagno, E.A., Jr., Hull, D.M., Munoz, I.M., and Blome, C.D., 1997, Coast Range Ophiolite; paleoequatorial ocean-ridge lithosphere: *American Association of Petroleum Geologists Bulletin*, v. 81, p. 687.
- Huey, A.S., 1948, Geology of the Tesla quadrangle, California: *California Division of Mines and Geology Bulletin* 140, 75 p., map, scale 1:62,500.
- Imperato, D., 1992, Structure and tectonics of the Stockton fault zone (abstract), in *Structural Geology of the Sacramento Basin*: Association of American Petroleum Geologists (Annual Meeting, Pacific Section, Sacramento, California, April 27, 1992-May 2, 1992), Miscellaneous Publication 41, p. 157.

- Ingersoll, R.V., 1990, Nomenclature of upper Mesozoic strata of the Sacramento Valley of California, Review and recommendations *in* Ingersoll, R.V. and Nilsen, T., editors, Sacramento Valley Symposium and Guidebook, Society of Economic Paleontologists and Mineralogists, v. 65, p. 1-3.
- Irwin, W.P., 1964, Late Mesozoic orogenies in the ultramafic belts of northwestern California and southwestern Oregon, U.S. Geological Survey Prof. Pap., 501-C, C 1 – C9.
- Irwin, W.P., and Wooden, J.L., 2001, Map showing plutons with accreted terranes of the Sierra Nevada, California, with a tabulation of U/Pb isotopic ages: U.S. Geological Survey Open-File Report 01-229, 1 plate, scale 1:1,000,000.
- Isaacson, K.A., and Andersen, D.W., 1992, Neogene synorogenic sedimentation in the northern Livermore basin, California, *in* Borchardt, G., Hirschfeld, S.E., Lienkaemper, J.J., McClellan, P., Williams, P.L., and Wong, I.G., eds., Proceedings of the Second Conference on Earthquake Hazards in the Eastern San Francisco Bay Area: California Division of Mines and Geology Special Publication 113, p. 339-344.
- Jachens, R.C., and Griscom, Andrew, 1985, An isostatic residual gravity map of California—A residual map for interpretation of anomalies from intracrustal sources, *in* Hinze, W.J., ed., The utility of regional gravity and magnetic maps: Society of Exploration Geophysicists, p. 347–360.
- Jachens, R.C., Griscom, Andrew, and Roberts, C.W., 1995, Regional extent of Great Valley basement west of the Great Valley, California: Implications for extensive tectonic wedging in the California Coast Ranges: *Journal of Geophysical Research*, v. 100, p. 12769-12790.
- Jachens, R.C., Wentworth, C.M., Graymer, R.W., Williams, R.A., Ponce, D.A., Mankinen, E.A., Stephenson, W.J., and Langenheim, V.E., 2017, The Evergreen basin and the role of the Silver Creek Fault in the San Andreas Fault System, San Francisco Bay region, California: *Geosphere*, v. 13, p. 269-286, doi.10.1130/GES01385.1.
- Jennings, C.W., and Bryant, W.A., 2010, Fault activity map of California: Department of Conservation, California Geological Survey, Geologic Data Map No. 6, scale 1:750,000.
- Joesten, R., Wooden, J.L., Silver, L.T., Ernst, W.G., and McWilliams, M.O., 2004, Depositional age and provenance of jadeite-grade metagraywacke from the Franciscan accretionary prism, Diablo Range, central California—SHRIMP Pb-isotope dating of detrital zircon: *Geological Society of America Abstracts with Programs*, v. 36, no. 5, p. 120.
- Jones, D.L., and Curtis, G.H., 1991, Guide to the geology of the Berkeley Hills, central Coast Ranges, California *in* Sloan, D., and Wagner, D.L., eds., *Geologic Excursions in Northern California: San Francisco to the Sierra Nevada*, California Division of Mines and Geology Special Publication 109, p. 63-74.
- Kelson, K.J., and Simpson, G.D., 1995, Late Quaternary deformation of the southern East Bay Hills, Alameda County, CA: *American Association of Petroleum Geologists Bulletin*, v. 79, p. 590.
- Knudsen, K.L., and Lettis, W.R., 1997, Preliminary maps showing Quaternary geology of twenty 7.5-minute quadrangles, eastern Stockton, California, 1:100,000 quadrangle: National Earthquake Hazards Reduction Program, U.S. Geological Survey, Final Technical Report, Award #1434-94-G-2499.
- Knudsen, K.L., Sowers, J.M., Witter, R.C., Wentworth, C.M. and Helley, E.J., 2000, Preliminary maps of Quaternary deposits and liquefaction susceptibility, nine-county San Francisco Bay Region, California: A Digital Database: U.S. Geological Survey Open-File Report 00-444: <http://pubs.usgs.gov/of/2000/of00-444/> (last accessed 2001/10/01).
- Krug, E.H., Cherven, V.B., Hatten, C.W., and Roth, J.C., 1992, Subsurface structure in the Montezuma Hills, southwestern Sacramento basin, *in* Cherven, V.B., and Edmondson, W.F., eds., *Structural Geology of the Sacramento Basin: Volume MP-41*, Annual Meeting, Pacific Section, Society of Economic Paleontologists and Mineralogists, p. 41-60.

- Langenheim, V.E., 2015, Aeromagnetic survey map of Sacramento Valley, California: U.S. Geological Survey Open-File Report 2015-1186, scale 1:250,000, available at [pubs.usgs.gov/publication/ofr20151186](https://pubs.usgs.gov/publication/ofr20151186).
- Langenheim, V.E., Jachens, R.C., Wentworth, C.M., and McLaughlin, R.J., 2012, Aeromagnetic and Aeromagnetic-based Geologic maps of the Coastal Belt, Franciscan Complex, northern California: U.S. Geological Survey Scientific Investigations Map 3188, pamphlet 20 p., 3 sheets, various scales, and database, available at <http://pubs.usgs.gov/sim/3188/>.
- Langenheim, V.E., Brocher, T.M., McPhee, D.K., Earney, T.E., McPherson-Krutzky, Carson, Morgan, K.S., Matson, Gabriel, and McFaul, R.S., 2018, Digitized sonic velocity log data of the Sacramento Delta region, California: U.S. Geological Survey data release, <https://doi.org/10.5066/P9PYUFI7>.
- Langenheim, V.E., Roberts, M.A., Earney, T.E., and Ritzinger, B.T., 2022, Gravity data and geophysical gradient data of the Stockton 30 x 60 minute quadrangle, California: U.S. Geological Survey Data Release, <https://doi.org/10.5066/P92D15J8>.
- Lindquist, T.A., and Morgenthaler, J.D., 1991, Radiometric ages of rocks in the San Francisco-San Jose quadrangles, California: Calif. Div. of Mines and Geol. Map No. 5, scale 1:250,000.
- Maddock, M.E., 1964, Geology of the Mt. Boardman quadrangle, Santa Clara and Stanislaus counties, California: California Division of Mines and Geology Map Sheet 3, scale 1: 62,500.
- Mankinen, E.A., Gromme, C.S., and Williams, K.M., 1991, Concordant paleolatitudes from ophiolite sequences in the northern California Coast Ranges, U.S.A.: *Tectonophysics*, v. 198, p. 1-21.
- Marchand, D.E., and Allwardt, A., 1981, Late Cenozoic stratigraphic units, northeastern San Joaquin Valley, California: U.S. Geological Survey Bulletin 1 470, 70 p.
- Marchand, D.E., and Bartow, J.A., 1979, Preliminary geologic map of Cenozoic deposits of the Bellota quadrangle, California: U.S. Geological Survey, Open-File Report OF-79-664, scale 1:62,500.
- Marchand, D.E., and Harden, J.W., 1978, Preliminary geologic map showing Quaternary deposits on the lower Tuolumne and Stanislaus alluvial fans and along the lower San Joaquin River, Stanislaus County, California: U.S. Geological Survey, Open-File Report 78-656, scale 1:24,000.
- Marchand, D.E., Bartow, J.A., and Shipley, S., 1981, Preliminary geologic maps showing Cenozoic deposits of the Farmington and Bachelor Valley quadrangles, San Joaquin, Stanislaus and Calaveras counties, California: U.S. Geological Survey Open-File Report 81-1050, scale 1:24,000.
- McClay, Ken, and Bonora, Massimo, 2001, Analog models of restraining stepovers in strike-slip fault systems: *American Association of Petroleum Geologists Bulletin*, v. 85, p. 233-260.
- McDougall, Kristin, and Block, Debra, 2014, Digital database of microfossil localities in Alameda and Contra Costa Counties, California: U.S. Geological Survey Scientific Investigations Report 2014-5120, 108 p, 1 plate.
- McElhiney, M.A., 1992, Soil survey of San Joaquin County, California: U.S. Department of Agriculture, Soil Conservation Service, 479 p., plus plates, 1 :24, 000.
- McLaughlin, J.C., and Huntington, G.L., 1968, Soils of westside Stanislaus area California: Department of Soils and Plant Nutrition, University of California, Davis, 85 p., plus plates, 1:24,000.
- McLaughlin, R.J., Sliter, W.V., Sorg, D.H., Russell, P.C., and Sarna-Wojcicki, A.M., 1996, Large-scale right-slip displacement on the East San Francisco Bay fault system—Implications for location of late Miocene to Pliocene Pacific plate boundary: *Tectonics*, v. 15, p. 1-18.
- Meltzer, A.S., Levander, A.R., and Mooney, W.D., 1987, Upper crustal structure, Livermore Valley and vicinity, California Coast Ranges: *Bulletin of the Seismological Society of America*, v. 77, p. 1655-1673.
- Meuschke, J.L., Pitkin, J.A., and Smith, W.C., 1966, Aeromagnetic map of Sacramento and vicinity, California: U.S. Geological Survey Geophysical Investigations Map GP-574, scale 1:250,000.



- Mitchell, C, Graham, S.A., and David, D.H., 2010, Subduction complex uplift and exhumation and its influence on Maastrichtian forearc stratigraphy in the Great Valley Basin, northern San Joaquin Valley, California: *GSA Bulletin*, v. 122, no. 11/12; p. 2063–2078; doi: 10.1130/B30180..
- Montgomery, D.R., and Jones, D.L., 1992, How wide is the Calaveras fault zone? - Evidence for distributed shear along a major fault in central California: *Geology*, v. 20, p. 55-58.
- Morris, W.J., 1971, A review of Pacific Coast Hadrosaurs: *Journal of Paleontology*, v. 47, p. 551-561.
- Murchev, B.L., and Jones, D.L., 1984, Age and significance of chert in the Franciscan Complex, in the San Francisco Bay region, *in* Blake, M.C., Jr., ed., *Franciscan Geology of Northern California: Pacific Section*, Society of Economic Paleontologists and Mineralogists, v. 43, p. 23-30.
- Murphy, Lin, Fleck, Robert, and Wooden, Joseph, 2002, Northbrae rhyolite in the Berkeley Hills, CA—A rock well-misunderstood: *Geological Society of America Abstracts with Programs*, Paper No. 162-15.
- Murphy, M.A., 1956, Lower Cretaceous stratigraphic units of northern California: *American Association of Petroleum Geologists Bulletin*, v. 40, p. 2098-2119.
- Norris, R.M., and Webb, R.W., 1976, *Geology of California*: New York, John Wiley & Sons, Inc., 341 p.
- Oliver, H.W., and Hanna, W.F., 1970, Structural significance of gravity and magnetic meganomalies in central California: *Geological Society of America Abstracts with Programs*, v. 2, no. 2, p. 126-127.
- Page, B.M., 1978, Franciscan mélanges compared with olistostromes of Taiwan and Italy: *Tectonophysics*, v. 47, p. 223-246.
- Pampeyan, E.H., 1993, Geologic map of the Palo Alto and part of the Redwood Point 1-1/2 degree quadrangles, San Mateo and Santa Clara Counties, California: U.S. Geological Survey Miscellaneous Investigations Series Map I-2371, 26 p., scale 1:24,000.
- Pan-American Center for Earth and Environmental Studies, 2015, Gravity database, accessed April, 10, 2010 at <http://irpsvgis00.utep.edu/repositorywebsite> (Accessed July 15, 2013 at <http://research.utep.edu/default.aspx?tabid=37229>).
- Parsons, T., and 12 others, 2013, Appendix C; Deformation models for UCERF3. The Uniform California earthquake rupture forecast, version 3 (UCERF3)—The time-independent model: U.S. Geological Survey Open File Report 2013–1165.
- Pelletier, W.J., 1951, Paleontology and stratigraphy of the Clarendonian continental beds west of Tracy, California: University of California at Berkeley, M.S. thesis, 57 p.
- Perkins, M.G., 1974, Geology and petrology of the East Bay outlier of the late Mesozoic Great Valley sequence, Alameda County, California: University of California at Berkeley, M.S. thesis.
- Phipps, S.P., 1984, Ophiolitic olistostromes in the basal Great Valley sequence, Napa County, northern California Coast Ranges, *in* Raymond, L.A., ed., *Mélanges—Their nature, origin, and significance*: Geological Society of America Special Paper 198, p. 103-125.
- Platt, J.P., 1986, Dynamics of orogenic wedges and the uplift of high-pressure metamorphic rocks: *Geological Society of America Bulletin*, v. 97, p. 1037–105.
- Plouff, Donald, 1977, Preliminary documentation for a FORTRAN program to compute gravity terrain corrections based on topography digitized on a geographic grid: U.S. Geological Survey Open-File Report 77–535, 45 p.
- Ponce, D.A., 2001, Principal facts for gravity data along the Hayward Fault and vicinity, San Francisco Bay area, northern California: U.S. Geological Survey Open-File Report 01-124, 29 pp., <http://pubs.usgs.gov/of/2001/0124> (last accessed July 5, 2016).
- Prothero, D.R., and Tedford, R.H., 2000, Magnetic stratigraphy of the type Montediablan Stage (Late Miocene), Black Hawk Ranch, Contra Costa County, California; Implications for regional correlations: *PaleoBios*, v. 20, no. 3, p. 1-10.
- Radbruch, D.H., 1967, Approximate location of fault traces and historic surface ruptures within the Hayward fault zone between San Pablo and Warm Springs, California: U.S. Geological Survey, Miscellaneous Geologic Investigations Map I-522, scale 1:62,500.

- Raymond, L.A., 1969, The stratigraphic and structural geology of the northern Lone Tree Creek and southern Tracy quadrangles: San Jose State University, M.S. thesis, 143p., plate 1, scale 1:24,000.
- Raymond, L.A., 1973a, Franciscan Geology of the Mt. Oso Area, Central California [Ph.D. dissertation]: Davis, University of California, 185p, plate 1, scale 1:24,000.
- Raymond, L.A., 1973b, Tesla-Ortugalita fault, Coast Range thrust fault, and Franciscan metamorphism, northeastern Diablo Range, California: Geological Society of America Bulletin, v. 84, p. 3547-3562.
- Raymond, L.A., 2014, Designating tectonostratigraphic terranes versus mapping rock units in subduction complexes: perspectives from the Franciscan Complex of California, USA: International Geology Review, DOI:10.1080/00206814.2014.911124, 22p.
- Raymond, L.A., unpublished field maps and personal communications regarding work in the eastern Diablo Range, with latest notes 2015.
- Retzer, J.L., Glassey, T.W., Goff, A.M., and Harradine, F.F., 1951, Soil Survey of the Stockton area: U.S. Department of Agriculture, 121 p., plates 1:31,680.
- Robbins, S.L., Oliver, H.W., Holden, K.D., and Farewell, R.C., 1974, Principal facts for 3046 gravity stations on the San Jose 1 x 2 quadrangle map, California: U. S. Geological Survey Report, 106 p.; available from National Technical Information Service, U.S. Department of Commerce, Springfield, VA, NTIS-PB-232-728/AS.
- Robbins, S.L., Oliver, H.W., and Holden, K.D., 1976, San Jose sheet-Bouguer gravity map of California: California Division of Mines and Geology, 10 p., scale 1:250,000.
- Roberts, C.W., Jachens, R.C., and Oliver, H.W., 1990, Isostatic residual gravity map of California and offshore southern California: California Division of Mines and Geology, Geologic data map no. 7, scale 1:750,000.
- Sarna-Wojcicki, A.M., 1976, Correlation of late Cenozoic tuffs in the Central California Coast Ranges by means of trace and minor element chemistry: U.S. Geological Survey Professional Paper 972, 30 p.
- Sarna-Wojcicki, A.M., Bowman, H.W., and Russell, P.C., 1979, Chemical correlation of some late Cenozoic tuffs of northern and central California by neutron activation analyses of glass and comparison with X-ray fluorescence analysis: U.S. Geological Survey Professional Paper 1147, 15 p.
- Sarna-Wojcicki, A.M., Deino, A.L., Fleck, R.J., McLaughlin, R.J., Wagner, D.L., Wan, E., Wahl, D., Hillhouse, J.W., and Perkins, M., 2011, Age, composition, and areal distribution of the Pliocene Lawlor Tuff, and three younger Pliocene tuffs, California and Nevada: Geosphere, v. 7, p. 599-628.
- Savage, D.E., 1951, Late Cenozoic vertebrates of the San Francisco Bay region: University of California Publications Bulletin of the Department of Geological Sciences, v. 28, p. 215-314.
- Sawyer, T.L., 2015, Characterizing rates of contractional deformation on the Mt. Diablo Thrust Fault, Eastern San Francisco Bay Region, Northern California: U.S. Geological Survey NEHRP Final Technical Report 00HQGR0004, 33 p.
- Sawyer, T.L. and Unruh, J.R., 2012, Refining the Holocene slip rate on the Greenville fault zone, eastern San Francisco Bay area, California: Final Technical Report submitted to the U.S. Geological Survey National Earthquake Hazards Reduction Program, Award No. 03HQGR0108., p. 19, 2 tables, 6 figures, 1 plate.
- Shervais, J.W., Kimbrough, D.L., Renne, P., Murchey, B., Snow, C.A., Schaman, R.M.Z., Beaman, J., 2004, Multi-stage origin of the Coast Range ophiolite, California: implication for the life cycle of supra-subduction zone ophiolites: Int. Geol. Rev. Vol. 46, 289–315.

- Shervais, J.W., Kimbrough, D.L., Renne, P., Hanan, B.B., Murchey, B., Snow, C.A., Zoglman, S., Schuman, M.M., Beaman, J., 2006, Multi-stage origin of the Coast Range ophiolite, California; implications for the life cycle of supra-subduction zone ophiolites: in Liou, J.G., and Cloos, M., eds., *Phase relations, high-pressure terranes, P-T-ometry, and plate pushing; a tribute to W. G. Ernst*, GSA International Book Series, Vol. 9, 570-596.
- Snow, Cameron, Wakabayashi, John, Ernst, W., and Wooden, Joseph, 2010, Detrital zircon evidence for progressive underthrusting in Franciscan metagraywackes, west-central California: *Geological Society of America, Bull.* 122, p. 282-291. Doi: 10.1130/B26399.1.
- Sowers, J.M., Noller, J.S., and Lettis, W.R.: 1993, Preliminary Quaternary geology of the Tracy and Midway 7.5-minute quadrangles, California: U. S. Geological Survey Open-File Report 93-225.
- Sterling, R.H. Jr., 1992, Intersection of the Stockton and Vernalis Faults, southern Sacramento Valley, California, in Cheveron, V.B., and Edmondson, W.F., eds., *Structural Geology of the Sacramento Basin*, AAPG Pacific Section annual convention, p. 143-151.
- Stewart, Ralph, 1949, Lower Tertiary stratigraphy of Mount Diablo, Marysville Buttes, and west border of lower Central Valley of California: U.S. Geological Survey Oil and Gas Investigations Chart OC-34, 2 plates.
- Stock, C., 1941, Duckbill dinosaur from the Moreno Cretaceous, California [abs.]: *Geological Society of America Bulletin*, v. 52, no. 12, Pt. 2, p. 1956.
- Sullivan, M., Raymond, L.A., Edwards, S.W., Sarna-Wojcicki, A., Hackworth, R.A., and Deino, A., in press, The mid-Cenozoic succession on the northeast limb of Mount Diablo Anticline, California—A stratigraphic record of tectonic events in the forearc basin, in Sullivan, Raymond, and others, eds., *Regional Geology of Mount Diablo [working title]*: Geological Society of America Memoir.
- Surpless, K.D., Graham, S.A., Jacob, A.C., and Wooden, J.L., 2006, Does the Great Valley Group contain Jurassic strata? Reevaluation of the age and early evolution of a classic forearc basin: *Geology*, v. 34, no. 1, p. 21–24, doi: 10.1130/G21940..
- Sweeney, J.J., 1982, Magnitudes of slip along the Greenville fault in the Diablo Range and Corral Hollow areas in *Proceedings, Conference on earthquake hazards in the eastern San Francisco Bay area*, California Division of Mines and Geology Special Publication 62, p. 137-146.
- Telford, W.M., Geldart, L.O., Sheriff, R.E., and Keyes, D.A., 1976, *Applied Geophysics*: New York, Cambridge University Press, 960 p.
- Throckmorton, C.K., 1988, Geology and paleontology of the Tesla formation, Alameda and San Joaquin Counties, central California: U.S. Geological Survey Open-File Report 88-59, 104 p., 2 pls.
- Thurber, Clifford, Zhang, Haijiang, Brocher, Thomas, and Langenheim, Victoria, 2009, Regional three-dimensional seismic velocity model of the crust and uppermost mantle of northern California: *Journal of Geophysical Research*, v. 114, DOI: 10.1029/2008JB005766.
- Tiballi, C.A., and Brocher, T.M., 1998, Compilation of 71 additional sonic and density logs from 5 oil test wells in the San Francisco Bay area, California: U.S. Geological Survey Open-File Report 98-615, 131 p.
- Topozada, T. R., Real, C.R., and Parke, D.L., 1981. Preparation of isoseismal maps and summaries of reported effects for pre-1900 California earthquakes: California Division of Mines and Geology Open-File Report 81-11, 182 p.
- Trask, P.D. 1950, Geologic description of the manganese deposits of California: California Division of Mines, *Bulletin*, v. 152, 378p, plate 4.
- Tripathy, A., Housh, T.B., Morisani, A.M., and Cloos, M., 2005, Detrital zircon geochronology of coherent jadeitic pyroxene-bearing rocks of the Franciscan Complex, Pacheco Pass, California: Implications for unroofing: *Geological Society of America Abstracts with Programs*, v. 37, no. 7, p. 18.

- Ukar, Estibalitz, Cloos, Mark, and Vasconcelos, Paulo, 2012, First  $^{40}\text{Ar}$ - $^{39}\text{Ar}$  ages from low-T mafic blueschist blocks in a Franciscan mélangé near San Simeon—Implications for initiation of subduction: *The Journal of Geology*, v. 120, p. 543-556.
- Unruh, J.R., 2000, Characterization of blind seismic sources in the Mt. Diablo-Livermore region, San Francisco Bay Area, California: final technical report to the National Earthquake Hazards Reduction Program, U.S. Geological Survey, contract number 99-HQ-GR-0069, 30 p.
- Unruh, J.R., Dumitru, T.A., and Sawyer, T.L., 2007, Coupling of early Tertiary extension in the Great Valley forearc basin with blueschist exhumation in the underlying Franciscan accretionary wedge at Mt. Diablo, California: *Geological Society of America Bulletin*, v. 119, no., 11/12, p. 1347-1367; doi: 10.1130/B26057.
- Unruh, J.R., and Hitchcock, C.S., 2009, Characterization of Potential Seismic Sources in the Sacramento-San Joaquin Delta, California: Final Technical Report submitted to the U.S. Geological Survey National Earthquake Hazard Reduction Program, Award Number 08HQGR0055, 45 p.
- Unruh, J.R., and Hitchcock, C.S., 2015, Detailed mapping and analysis of fold deformation above the West Tracy Fault, southern San Joaquin-Sacramento Delta, northern California: Final Technical Report submitted to the U.S. Geological Survey National Earthquake Hazard Reduction Program, Award Number G14AP00069, 46 p.
- Unruh, J.R., and Krug, Kate, 2007, Assessment and Documentation of Transpressional Structures, Northeastern Diablo Range, for the Quaternary Fault Map Database: Final Technical Report submitted to the U.S. Geological Survey National Earthquake Hazard Reduction Program, Award Number 06HQGR0139, 45 p.
- Unruh, J.R., and Lettis, W.R., 1998, Kinematics of transpressional deformation in the eastern San Francisco Bay region, California: *Geology*, v. 26, p. 19-22.
- Unruh, J.R. and Sawyer, T.L., 1995, Late Cenozoic growth of the Mt. Diablo fold and thrust belt, central Contra Costa County, California and implications for transpressional deformation of the northern Diablo Range: Pacific Section Convention, American Association of Petroleum Geologists and Society of Economic Paleontologists and Mineralogists, p. 47.
- Unruh, J.R., and Sundermann, S., 2006, Digital compilation of thrust and reverse fault data for the Northern California Map Database: Collaborative research with William Lettis & Associates, Inc., and the U.S. Geologic Survey: Final Technical Report submitted to the U.S. Geological Survey, National Hazards Reduction Program, Award No. 05-HQ-GR-0054, 20 p.
- Unruh, J.R., Dumitru, T.A., and Sawyer, T.L., 2007, Coupling of early Tertiary extension in the Great Valley forearc basin with blueschist exhumation in the underlying Franciscan accretionary wedge at Mount Diablo, California: *Geological Society of America Bulletin*, v. 119, no. 11/12, p. 1347-1367, 17 figures; Data Respository item 2007140.
- U.S. Geological Survey, 1992, Aeromagnetic map of the Livermore area, Central California: U.S. Geological Survey Open-File Report, 92-531, scale 1:250,000.
- Wagner, D.L., Saucedo, G.J., Clahan, K.B., Fleck, R.J., Langenheim, V.E., McLaughlin, R.J., Sarna-Wojcicki, A.M., Allen, J.R., and Deino, A.L., 2011, Geology, geochronology, and paleogeography of the southern Sonoma volcanic field and adjacent areas, northern San Francisco Bay region, California: *Geosphere*, v. 7, p. 658-683.
- Wagner, J.R., 1978, Late Cenozoic history of the Coast Ranges east of San Francisco Bay: Univ. of Calif., Berkeley, Ph.D. thesis, 160 p., 12 plates.
- Wakabayashi, John, 2011, Mélanges of the Franciscan Complex, California; diverse structural settings, evidence for sedimentary mixing, and their connection to subduction processes, *in* Wakabayashi, J., and Dilek, Y., eds., *Mélanges; processes of formation and societal significance*: Geological Society of America Special Paper 480, p. 117–141.
- Walker, J.P., and Graymer, R.W., 2003, Absence of late Neogene offset on the Northern Calaveras Fault [abs.]: American Geophysical Union Fall Meeting.

- Wentworth, C.M., Blake, M.C., Jr., McLaughlin, R.J., and Graymer, R. W., 1999a, Preliminary geologic map of the San Jose 30 x 60-Minute Quadrangle, California: US Geological Survey Open File Report 98-795, Part 7, scale 1:100000, 1 sheet.
- Wentworth, C.M., Blake, M.C., Jr., McLaughlin, R.J., and Graymer, R.W., 1999b, Preliminary geologic description of the San Jose 30 x 60 minute quadrangle, California: US Geological Survey Open File Report 98-795, Part 3, 52p.
- Wentworth, C.M., Fisher, G.R., Levine, Paia, and Jachens, R.C., 1995, revised 2012, The surface of crystalline basement, Great Valley and Sierra Nevada, California: U.S. Geological Survey Open-File Report 95-96, v. 1.11, 18 p. and database (Available at <http://pubs.usgs.gov/of/1995/96/>).
- Wilson, D.S., McCrory, P.A., and Stanley, R.G., 2005, Implications of volcanism in coastal California for the Neogene deformation history of western North America: *Tectonics*, v. 24, TC3008, 22 p.
- Witter, R.C., Knudsen, K.L., Sowers, J.M., Wentworth, C.M., Koehler, R.D. and Randolph, C.E., 2006, Maps of Quaternary deposits and liquefaction susceptibility in the central San Francisco Bay Region, California: U.S. Geological Survey Open-File Report 2006-1037: <http://pubs.usgs.gov/of/2006/1037/>.
- Wood, L.C., 1964, A gravity survey of the Mount Diablo area, California, *in* Guidebook to the Mount Diablo field trip: Geological Society of Sacramento, p. 33-36.
- Wright, J.E., and Wyld, S.J., 2007, Alternative tectonic model for Late Jurassic through Early Cretaceous evolution of the Great Valley sequence, California, *in* Cloos, M., Carlson, W.D., Gilbert, M.C., Liou, J.G., and Sorensen, S.S., eds., *Convergent Margin Terranes and Associated Regions—A Tribute to W.G. Ernst*: Geological Society of America Special Paper 419, p. 81-95.

**AUTHORSHIP DOCUMENTATION AND PRODUCT LIMITATIONS**

**PUBLICATION TITLE:** Geologic and Geophysical Maps of the Stockton 30'x60' Quadrangle, California  
Regional Geologic Map No. 5

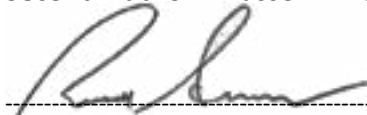
**LIMITATIONS:** The California Department of Conservation makes no warranties as to the suitability of this product for any given purpose. This map should not be considered as an authoritative or comprehensive source for landslide and seismic hazard data. For landslide data, please visit the California Geological Survey Landslides web page at: <https://www.conservation.ca.gov/cgs/landslides>. For seismic hazards data and Zones of Required Investigation, please visit the California Geological Survey Seismic Hazards Program web page at: <https://www.conservation.ca.gov/cgs/sh/program>.

**First Author** – Marc P. Delattre, PG 5230 CEG 1819

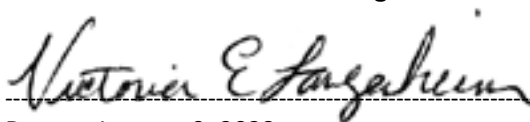
  
-----  
Date: January 11, 2023



**Second Author** – Russell W. Graymer

  
-----  
Date: January 9, 2023

**Third Author** – Victoria E. Langenheim

  
-----  
Date: January 9, 2023

**Fourth Author** – Keith L. Knudsen, PG 6202 CEG 2042

  
-----  
Date: January 9, 2023



**Fifth Author** – Timothy E. Dawson, PG 8502 CEG 2618



Date: January 9, 2023



**Sixth Author** – Earl E. Brabb

Deceased

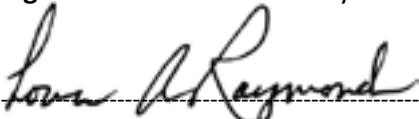
Date: January 9, 2023

**Seventh Author** – Carl M. Wentworth



Date: January 10, 2023

**Eighth Author** – Loren A Raymond



Date: January 9, 2023

This authorship document accompanies the publication with the following citation:

Delattre, M.P., Graymer, R.W., Langenheim, V.E., Knudsen, K.L., Dawson, T.E., Brabb, E.E.,  
Wentworth, C.M., and Raymond, L.A., 2023, Geologic and geophysical maps of the Stockton 30'  
x 60' quadrangle, California: California Geological Survey Regional Geologic Map No. 5, scale  
1:100,000